Cooperation and cognition in wireless communication systems for spectrum efficiency enhancement

Yang, Han

2011

Yang, H. (2011). Cooperation and cognition in wireless communication systems for spectrum efficiency enhancement. Doctoral thesis, Nanyang Technological University, Singapore.

https://hdl.handle.net/10356/42832

https://doi.org/10.32657/10356/42832

COOPERATION AND COGNITION IN WIRELESS COMMUNICATION SYSTEMS FOR SPECTRUM EFFICIENCY ENHANCEMENT

Yang Han

School of Electrical & Electronic Engineering

A thesis submitted to the Nanyang Technological University in partial fulfillment
of the requirement for the degree of
Doctor of Philosophy

2011

Acknowledgments

Without a doubt, what I have learnt and experienced in the past four years at NTU is one of the most precious treasures in my life. I owe my Ph.D. to many wonderful people around me who gave me much encouragement, support, and guidance to achieve this goal, and the least I can do is to thank them.

I considered myself blessed to be a student of Professor Ting See Ho. His depth of knowledge, dedication to work, and passion in research never cease to amaze me. Along all the way of my Ph.D., he has always been my source of inspiration and support. He read and advised on every draft of this dissertation at every stage with thoroughness, and it was his judicious guidance that made this work possible. I learned from Professor Ting not only professional knowledge but also positive attitudes towards life. When I was having difficult moments, he has never lost faith in me but instead always led me back on the right track with his patient help and inspiring encouragement. I would like to express my deepest gratitude to Professor Ting for everything he has done for me. Thank you!

I am deeply indebted to Dr. Ashish Pandharipande, my supervisor in Philips Research-Eindhoven where I spent nine months for my overseas research attachment. During the period in Philips, I have been working under the close supervision of Dr. Pandharipande and we have together came up several initial ideas for the work presented in Chapter 3-5 of this dissertation. His guidance to me does not end after I came back to Singapore, and I would like to thank him for all the constructive advice and valuable discussions. I am also grateful to his hospitality which made me feel at home in Eindhoven. I will always remember the dinners and table tennis games that we enjoyed together.

I would also like to thank Professor Guan Yong Liang, the director of Positioning and Wireless Technology Centre, who has provided many useful suggestions to my research topics on space-time block coding and cognitive radios. As an expert on coding theory, Professor Guan was always ready to share his wealth of knowledge and insightful perspectives with all students–not just those who are under his direct supervision. His wisdom, kindness, and generosity definitely set a role model for my future life and career.

Of course, I will not leave out the good friends in NTU like Li Qiang, Liu Liang, Vivek Ashok Bohara, Harya Wicaksana, Tan Chin Hock, Zhang Feng, Yu Xiaojun, Xiao Shi, Wang Guohua, Fan Rongli, Zhao Zhi, Che Yueling, Zhao Chenxi, Fu Kai, Zhang Xiaojuan, Zhang Jiliang, Li Qian, and so many other nice fellows who I have to skip here. These days would not be as memorable without the fraternity among them. I would also like to express my appreciation to Mr. Joseph Lim, Ms. Chai Ooy Mei, Ms. Hannah Lim, and Ms. Than Thida for their administrative assistance and support.

Finally, I cannot thank enough my parents Han Jiangshui and Fu Mei as well as my fiancee Zhou Na for their unconditional love, endless support, and undying belief in me. It was them who brought me to where I am today, and for that I am deeply grateful. Here, I humbly dedicate this dissertation to them.

Dedication

To my family, for always being there at the end of the day.

Table of Contents

List of Figures

List of Tables

List of Symbols

$\boldsymbol{A}$	matrix
$\boldsymbol{I}_l$	$l \times l$ identity matrix
$\boldsymbol{a}$	vector
$(\cdot)^*$	conjugation
$(\cdot)^{\mathrm{T}}$	transpose
$(\cdot)^{\mathrm{H}}$	Hermitian transpose
$E\{\cdot\}$	expectation
$Ei(\cdot)$	exponential integral
$\lfloor \cdot \rfloor$	floor operator
$\lvert \cdot \rvert$	norm or cardinality
$U(x)$	unit-step function
$\mathcal{E}(\mu)$	exponential random variable with mean μ
$\mathcal{CN}(\mu, \sigma^2)$	complex Gaussian random variable with mean μ and variance σ^2
$\mathcal{G}(\alpha, \beta)$	Gamma random variable with shape parameter α and scale parameter β
$\mathcal{X}^2_\Omega$	chi-square random variable with Ω degrees of freedom
$\mathcal{X}^2_\Omega(\lambda)$	non-central chi-square random variable with Ω degrees of freedom and non-centrality parameter λ
${}_2F_1(\cdot,\cdot;\cdot;\cdot)$	Gauss' hypergeometric function
${}_1F_1(\cdot,\cdot,\cdot)$	confluent hypergeometric function

$H(\cdot,\cdot)$	harmonic mean
$B(\cdot,\cdot)$	Beta function
$\Gamma(a,b)$	incomplete Gamma function
$Q_\Lambda(a,b)$	generalized Marcum-Q function
P_{fa}	probability of false alarm
P_d	probability of detection
P_{out}	outage probability
max	maximization operator
min	minimization operator
$\mathcal{H}_0$	null hypothesis
$\mathcal{H}_1$	alternative hypothesis
$I_{(\cdot)}(\cdot)$	modified Bessel function of the first kind
$\Psi(\cdot,\cdot,\cdot)$	confluent hypergeometric function
$\emptyset$	empty set
$\binom{\cdot}{\cdot}$	binomial coefficient

List of Abbreviations

ACT	average collision time
AF	amplify-and-forward
AUT	average utilization time
AWGN	additive white Gaussian noise
BER	bit error rate
BLER	block error rate
CAM	cooperation acknowledge message
CCM	cooperation confirm message
CF	compress-and-forward
CR	cognitive radio
CRM	cooperation request message
CSI	channel state information
CTS	clear-to-send
DF	decode-and-forward
DPC	dirty paper coding
DSTC	distributed space time coding
FSDF	fixed selective decode-and-forward
MAC	media access control
MIMO	multiple-input multiple-output

MRC	maximal ratio combining
MVUE	minimum variance unbiased estimation
OSTBC	orthogonal space time block code
OSUT	overall system utilization time
PCAM	primary cooperation acknowledged message
PCCM	primary cooperation confirmation message
PCRM	primary cooperation request message
PEP	pairwise error probability
QAM	quadrature amplitude modulation
QoS	quality of service
RTS	ready-to-send
SCAM	secondary cooperation acknowledged message
SCCM	secondary cooperation confirmation message
SIC	self interference cancelation
SIMO	single-input multiple-output
SINR	signal-to-interference-and-noise ratio
SNR	signal-to-noise ratio
SUSW	secondary user selection window
UWB	ultra-wide band

Abstract

The explosive growth of wireless applications and steadily increasing demands for higher quality of service have led to a perceived dearth of available radio bandwidth, which necessitates a more efficient utilization of spectrum resources. Both cooperation and cognition in wireless networks have individually been shown to be powerful tools to achieve such a purpose. The objective of this dissertation is to jointly investigate these two techniques and propose practical protocols for spectrum efficiency enhancement in wireless networks.

We first analyze the performance of two-way amplify-and-forward (AF) half-duplex relaying protocol. We analytically prove that two-way relaying can significantly recover the spectrum efficiency loss of conventional one-way relaying. In addition, we show that spectrum efficiency can be further improved by applying multiple antennas and OSTBC at the relay terminal. We then combine cooperative relay transmission with interweave cognitive radios (CR), and consider the scenario where the secondary system is a dual-hop relay system. A spectrally efficient sensing protocol is proposed for such a system.

Furthermore, we also combine the cooperative relaying transmission with an overlay CR and propose a two-phase communication protocol for secondary spectrum access, where both cooperative AF and decode-and-forward (DF) relaying are considered. With the proposed protocols, the secondary system is able to access the spectrum band while ensuring that the performance of the primary system is maintained or improved by a certain margin.

Finally, a general multi-user scenario is considered. We present a cooperative spectrum sharing protocol with a two-step distributed secondary user selection scheme. In the proposed protocol, the primary system is able to achieve the same multi-user diversity gain as a conventional selective relaying scheme, and we show that the outage performance for both the primary and secondary systems improves as the number of secondary transmitters increases.

Chapter 1

Introduction

1.1 Overview

The dramatic growth of wireless applications and steadily increasing demands for higher quality of service have led to a perceived dearth of available radio bandwidth [1], which necessitates the search for more efficient utilization of spectrum resources. In the past decade, two important paradigms in wireless networks, namely cooperation and cognition, have individually been shown to be effective and efficient tools in achieving such a purpose.

1.1.1 Cooperation in Wireless Network

Future wireless networks are expected to be able to offer ubiquitous high-throughput services over large areas. However, due to the random (fading) nature of wireless channels, there are many obstacles in realizing such an ambitious target. Fundamental changes in the system infrastructure and protocol stacks, as well as incorporation of advanced signal processing techniques, are required to meet various demands in spectrum efficiency, power efficiency, and transmission coverage [2, 3].

Multiple-input multiple-output (MIMO) techniques have been proposed and investigated [4, 5, 6] to exploit both multiplexing and diversity gains for wireless systems. Although MIMO techniques have been shown to achieve promising performance, the practical application of such systems is restricted by several implementation difficulties. First of all, the small physical size of wireless devices

limits the spatial separation of the antennas which is critical for MIMO systems to achieve their optimal performance. Furthermore, the complex MIMO signal processing involved presents great challenges to the power usage and processing capabilities of wireless devices, which are expected to be lightweight and cheap. Therefore, deployment of a small number of antennas at wireless devices is a more feasible choice. For example, in IEEE standards 802.16 and 802.16e for MIMO WiMAX [7, 8], systems with up to 4 transmit/receive antennas are specified, and practical implementations with only 1 receive antenna is considered in [9]. Obviously, the benefit that can be exploited from a MIMO system is limited by the small number of transmit/receive antennas.

In view of this problem, cooperation in wireless networks is considered as an alternative technique to enable wireless terminals to achieve the benefits of a MIMO system. By definition, cooperative communications refers to a communication network where terminals *collaborate*, rather than *compete*, to transmit data for themselves and others. Specifically, in a wireless network, terminals can take advantage of the broadcast nature of wireless channels by overhearing and relaying the signals of other terminals such that the inherent spatial diversity in the channel can be exploited.

1.1.1.1 History of Cooperative Relaying

The wireless relay channel was first introduced by Van der Meulen in [10], way before the birth of MIMO techinques. Later, Cover and El-Gamal [11] derived the capacity of the degraded relay channel and the capacity bounds of a general relay channel. In [2], Sendonaris, Erkip, and Aazhang proposed a two-user cooperative relaying scheme for code division multiple access (CDMA) systems. Instead of the decode-and-forward (DF) relaying scheme proposed in [11], Laneman, Tse, and Wornell investigated the amplify-and-forward (AF) relaying protocol in [3] with an outage probability analysis. They showed that a cooperative relay system can achieve full spatial diversity corresponding to the number of cooperating terminals. It is worth mentioning that AF relaying is a special case of compress-and-forward relaying protocol (CF) which was first proposed in [11]. However, AF relaying attracts more research attention due to its simplicity. Coded cooperation was introduced by Hunter, Sanayei, and Nosratinia in [12], where additional parity

check bits are added at the relay such that a more powerful code is achieved at the destination. Coded cooperation can be understood as a practical coding scheme for the information theoretical results presented in [10, 11].

Multi-hop relay systems were studied in [13, 14], where closed-form expressions for bit error rate (BER) of multi-hop relay system with parallel and serial relays are derived. User cooperation based on distributed space time coding (DSTC) was introduced in [15, 16, 17], and the performance comparison of DSTC with orthogonal and quasi-orthogonal space-time codes are presented in [18]. DSTC has been shown to be able to bring about significant spatial diversity gain to the wireless network [18], which can be translated into an improvement in spectrum efficiency. However, its application requires symbol-level synchronization of the relays, which is especially tough to achieve in practice with distributed relays. In order to avoid this synchronization requirement in DSTC, asynchronous DSTC was considered in [19, 20].

On the other hand, relay selection protocols were proposed in [21, 22] where only one relay is selected from multiple candidates for cooperation. It was shown that relay selection is able to achieve the same diversity order as DSTC with much less complexity. Recently, the idea of relay selecton is extended to the scenario where multiple relays are selected to cooperate [23], and the performance is shown to be superior to single relay selection schemes in [21, 22]. A distributed relay selection protocol is proposed in [24] where the optimal relay is selected in a distributed manner.

1.1.1.2 Full-duplex and Half-duplex Relaying

When Cover and El-Gamal derived the capacity bounds of cooperative relay channel in [11], they assumed a full-duplex operation at the relay, i.e., the relaying terminal receives and transmits simultaneously in the same frequency band. Although full-duplex relaying achieves higher spectrum efficiency, the large difference in power levels of the receive and transmit signals makes it practically difficult to implement [25]. Thus, most of the practical relaying protocols (including the works discussed above) assume a half-duplex operation at the relay, i.e., reception and transmission at relay are performed in time-orthogonal channels[1]. However, due to

[1] Or frequency-orthogonal channels.

the extra time slot required for listening, half-duplex relaying suffers from a spectrum efficiency loss reflected by the pre-log factor of $\frac{1}{2}$ in the sum rate expressions [26].

1.1.1.3 One-way and Two-way Relaying

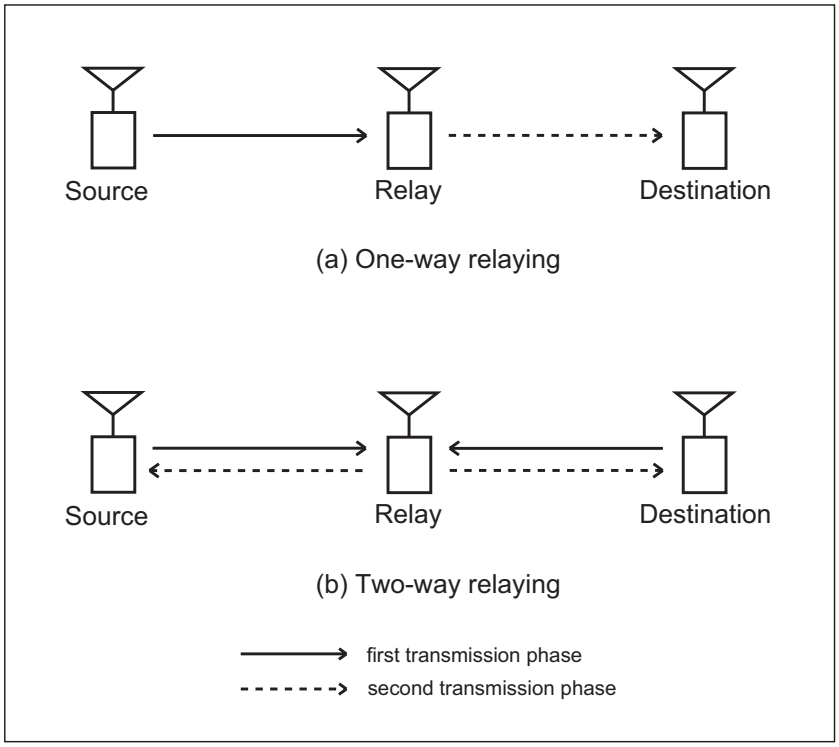

Figure 1.1. Illustration of (a) one-way and (b) two-way cooperative relaying protocols.

In view of the spectral efficiency loss of half-duplex protocols, two-way relaying protocol[2] was proposed in [25, 27]. The idea of two-way communication was first studied by Shannon in [28]. An illustration of conventional one-way relaying and two-way relaying is shown in Figure 1.1. In [25], both AF and DF relaying are considered. Specifically, in the two-way AF relaying scheme the source and destination transmit to the relay simultaneously in the first transmission phase. In the second transmission phase, the relay normalizes the signal received based on

[2]In two-way relaying protocols, the source and destination terminals are in symmetric positions, i.e., both of them transmit data to and receive data from each other. However, for consistency, we follow the notations in one-way relaying protocols and denote them as "source" and "destination" respectively.

its transmit power constraint and then broadcast to both source and destination. For two-way DF relaying, the only difference is that after the relay had received the signals from source and destination in the first transmission phase, it has to decode the respective codewords and then generate a new one (or a superposition of the original codewords) which is then broadcasted in the second transmission phase[3]. It is clear that for two-way relaying, both the source to destination link and the destination to source link still suffer from the spectrum efficiency loss, as two transmission phases, instead of one, are required. However, since the two links utilize the same time and frequency resources, this loss is expected to be recovered by proper signal processing.

Two-way DF relaying has been studied from a network coding perspective in [25, 29, 30, 31, 32] and the bounds for achievable sum rates of several variants of this DF protocol were derived in [31]. On the other hand, although two-way AF relaying is more practically attractive than DF relaying due to the very simple processing at the relay terminal, it has not received much attention in the works cited above. The lack of a closed-form solution for the achievable rate of two-way AF relaying in fading channels motivated the work in Chapter 2 of this dissertation.

1.1.2 Cognition in Wireless Network

In spite of all the above mentioned advancements of new technologies aimed at improving the spectrum efficiency, the traditional way by which the spectrum is being regulated and utilized has increasingly showed its incapability in accommodating the rapid growth of wireless services. Therefore, fundamental changes in the regulation bodies are required to enable a more flexible and efficient utilization of the spectrum band, leading to the development of cognition in wireless networks.

1.1.2.1 Limitations of Conventional Spectrum Regulation

Under the conventional spectrum regulatory framework, the national government authorities, e.g., Federal Communications Commission (FCC) in the USA, allocates spectrum resources to different wireless systems exclusively, and only the

[3]In two-way DF relaying, the overall transmission could also be accomplished over three phases, where the source, destination, and relay transmit in the first, second, and third phases respectively.

licensed system is allowed to operate in a certain spectrum band with limited transmit power. In general, this allocation of spectrum will be effective in the long term (e.g., a couple of years) and over a large geographical region (e.g., a country).

This spectrum regulation based on exclusive allocation has the advantage of simple interference management, and thus has been widely adopted globally. However, as expected, the spectrum band gradually becomes very crowded due to the exclusive allocation. Taking a glance at the National Telecommunications and Information Administrations frequency allocation chart [1], it is evident that almost all useful frequency bands for wireless transmission from 3 kHz to 5 GHz have been assigned, and there is very little new bandwidth available for emerging wireless products and services.

On the other hand, field measurements of frequency occupancy in the licensed bands revealed that a significant portion of the assigned spectrum is severely underutilized [33, 34, 35, 36]. In other words, at any given time and location, the licensed user of a certain spectrum band is not always in operation. However, according to the conventional spectrum regulations, these underutilized spectrum bands cannot accommodate other unlicensed systems which are desperate for the spectrum access. Clearly, an artificial "spectrum scarcity" is created by the rigid spectrum allocation mechanism.

On the contrary, the unlicensed bands in the 2.4 GHz range have seen more innovative applications such as wireless mesh networks (WMNs), wireless local area networks (WLANs), wireless sensor networks (WSNs) for a variety of military, environmental monitoring and commercial purposes. The success of this sharing-based spectrum utilization model led the regulatory authorities to re-evaluate the philosophy of exclusive spectrum allocation and eventually shifted their focus towards the more flexible dynamic spectrum sharing policies. For example, IEEE 802.22 [37, 38] has been proposed as the first standard to support the secondary usage of TV broadcasting bands.

1.1.2.2 Definitions of Cognitive Radio

Cognitive radio (CR) is recognized as a promising technique to facilitate dynamic spectrum utilization. The term "cognitive radio" was first coined by Miltola in 1999 to describe a radio platform which achieves a high flexibility in personal

wireless connections [39, 40]. FCC then followed up and defined a CR as "a radio that can change its transmitter parameters based on interactions with the environment in which it operates" [41]. Later on, Haykin gave the widely known definition for CR in his landmark paper [42]: "Cognitive radio is an intelligent wireless communication system that is aware of its surrounding environment (i.e., outside world), and uses the methodology of understanding-by-building to learn from the environment and adapt its internal states to statistical variations in the incoming RF stimuli by making corresponding changes in certain operating parameters (e.g., transmit-power, carrier-frequency, and modulation strategy) in real-time, with two primary objectives in mind: i) highly reliable communications whenever and wherever needed, and ii) efficient utilization of the radio spectrum".

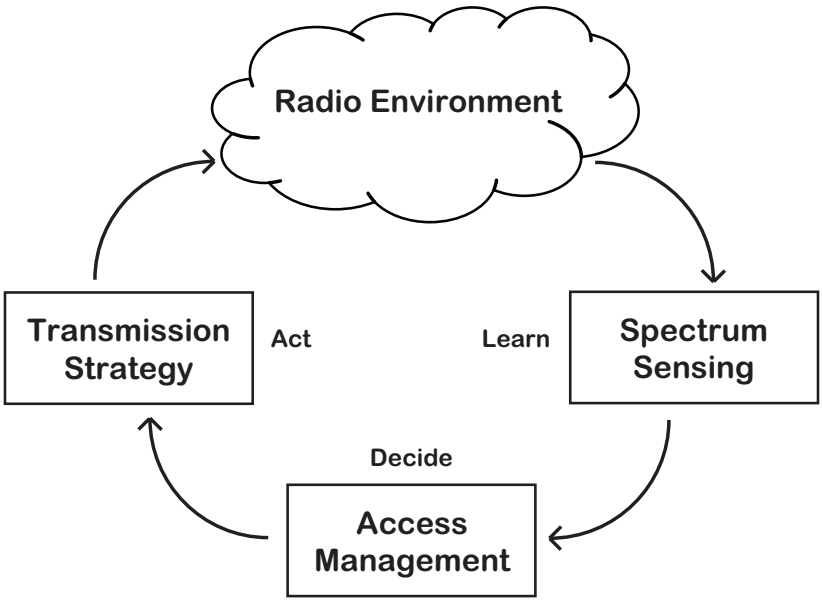

Figure 1.2. Illustration of the cognition cycle.

As shown in Figure 1.2, a CR system is in general composed of three major functional components, namely "learn", "decide", and "act", which together bring about cognition to the system. By introducing cognition (intelligence) to the wireless terminals, CR has been shown to be able to significantly improve the performance of wireless communications in various aspects [36, 37, 42, 43, 44, 45]. It is worth mentioning that dynamic spectrum sharing is an important application of CR, but by no means the only one. However, in this dissertation, we only concentrate on CR protocols and schemes for spectrum efficiency enhancement purposes

through dynamic spectrum sharing. Thus, hereafter by "CR" we will only refer to "CR for dynamic spectrum sharing". A definition for CR by Goldsmith [45] fits our context perfectly: "A cognitive radio is a wireless communication system that intelligently utilizes any available side information about the a) activity, b) channel conditions, c) codebooks, or d) messages of other nodes with which it shares the spectrum".

1.1.2.3 Categories of Cognitive Radio

In the CR system model, the licensed system, also known as primary system, is assumed to be implemented with conventional radio techniques and thus does not possess any cognition. On the other hand, the unlicensed system, also known as secondary system, is assumed to be intelligent and capable of sophisticated signal processing. By monitoring the radio environment and adjusting its transmission parameters adaptively, the secondary system attempts to exploit access to the licensed spectrum bands, while guaranteeing that the impact to the primary system is minimized. It is worth emphasizing that the primary system is assumed to be oblivious to the operations of secondary system, and it is the onus of the secondary system to facilitate the spectrum sharing and ensure that primary performance is not affected. Based on this secondary access model, CR schemes can be roughly categorized into the following three schemes [45].

♦ Underlay Scheme

Secondary spectrum access is allowed if the interference caused to the primary system is below a predefined threshold. Achievable rate regions for underlay CR with different system configurations were investigated in [46, 47, 48, 49]. For practical implementation, the interference constraint can be met by deploying multiple antennas at the secondary transmitter and directing the interference away from the primary receiver through beamforming [50]. However, obtaining the channel coefficients of the interfering channel is a major challenge for this method. Alternatively, ultra-wide band (UWB) technique can be used at the secondary transmitter to spread the interference below the noise floor [51]. As can be observed from Figure 1.3, the secondary signal is spread across a very wide bandwidth, and thus the

in-band interference to the primary system can be considered as negligible. In spite of its simplicity, due to the inherent power constraints of UWB systems, underlay CR with UWB is typically restricted to only short range communications.

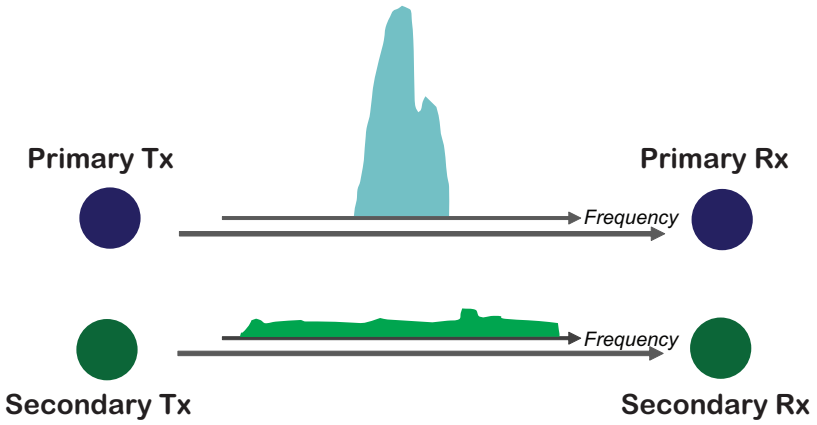

Figure 1.3. Underlay CR with UWB.

♦ Interweave Scheme

Secondary system detects the space-time-frequency vacancies in the spectrum band and transmits only in these "spectrum holes" – for this reason, the interweave scheme is also known as the "detect-and-avoid" scheme. Under this scheme, theoretically, the transmissions of primary and secondary systems will be orthogonal in at least one domain among the triplets of space, time, and frequency, and thus no harmful interference is caused to the primary system. As an illustration, in the interweave CR system shown in Figure 1.4, the secondary system monitors the channel and attempts to identify the spectrum holes in the time domain where it is able to access the spectrum band.

It is obvious that detection of spectrum holes is the key task in the interweave CR, and the technique for obtaining the awareness of such spectrum holes is commonly known as spectrum sensing. Since the distribution of spectrum holes changes with time, location, as well as traffic of the primary system, spectrum sensing has to be actively performed to identify a spectrum hole in real time. Furthermore, in order to minimize any possible interference to the primary system, spectrum sensing should also be accomplished promptly and reliably. To this end, much research attention has been drawn to this area in recent years, such as [42, 52] and

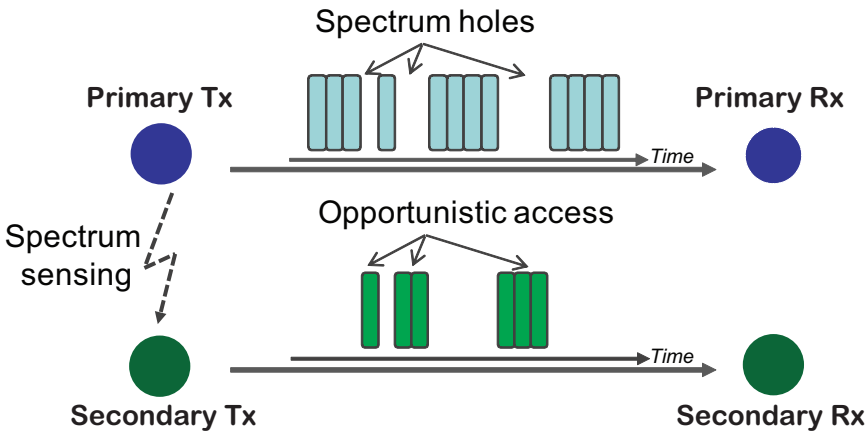

Figure 1.4. Interweave CR exploiting spectrum holes in time domain.

the references therein.

In the case where a secondary terminal is performing spectrum sensing, [53] studied the optimal sensing parameters which balances the tradeoff between sensing speed and reliability. In [54], multiple antennas are applied at the sensing terminal, and it was shown that the detection probability can be improved compared to the single antenna case. In [55], sensing algorithms based on time-domain symbol cross-correlation are proposed for detecting primary OFDM signals. The proposed scheme is shown to be superior to conventional schemes based on cyclic prefix detection in terms of probability of detection.

Spectrum sensing at a single secondary terminal is susceptible to fading and shadowing [56], which are inevitable due to the random nature of wireless channels. In addition, the geographical distance between primary transmitter and receiver also leads to the "hidden node" problem [42]. In view of these challenges, cooperative spectrum sensing is proposed in [57], and it is shown that the probability of detection for primary signal can be improved by allowing multiple secondary sensing terminals to share their local detection results. In [58], the authors showed that the sensing sensitivity requirement can be greatly reduced through hard-decision based cooperation. In [59], a suboptimal data fusion rule for combining correlated observations of multiple secondary sensing terminals is proposed. It outperforms the simple counting fusion rule, which ignores the correlation, in terms of probability of detection.

All the above works focused on enhancing the sensing capabilities of secondary

system through cooperation among secondary spectrum sensing terminals. However, analysis of the spectrum efficiency for the secondary system, i.e., how much time the secondary system is able to access the spectrum band for actual data transmission in the respective sensing protocols, is not provided. This motivates the work in Chapter 3 of this dissertation, where we focus on the spectrum efficiency of a secondary dual-hop relaying system, and propose a sensing protocol which is shown to be able to significantly improve secondary spectrum utilization while satisfying the interference constraint for the primary system.

♦ Overlay Scheme

The paradigm of overlay CR was first introduced by Devroye *et al.* [43] and also in [44, 45] to study the achievable rate bounds of CR systems from an information theoretical perspective. One of the most important enabling assumption for this approach is that the secondary transmitter is aware of the codebook and messages of the primary transmitter non-causally, i.e., before the primary transmission actually starts. Furthermore, the secondary system is also assumed to have obtained global channel state information (CSI).

With all the information above, the secondary transmitter can then adopt two strategies to either cancel off or mitigate the interference caused to the primary system. On one hand, the secondary transmitter is able to apply sophisticated coding techniques, e.g., dirty paper coding (DPC), to eliminate all the interference at the primary receiver. On the other hand, it could also split and use some of its transmit power to assist the primary transmission such that the decrease in the signal-to-interference-and-noise ratio (SINR) of the primary system due to the interference from the secondary system is exactly (or over) compensated by this assistance. This guarantees that the achievable rate of the primary system remains unchanged or even be improved by a certain margin, while the secondary system accesses the spectrum band with its remaining transmission power. An illustration of overlay CR with non-causal primary information at the secondary transmitter is shown in Figure 1.5.

Regarding the non-causal primary information required at the secondary transmitter, one can argue that the secondary transmitter is able to decode the primary message prior to the primary receiver if it is located closer to the primary trans-

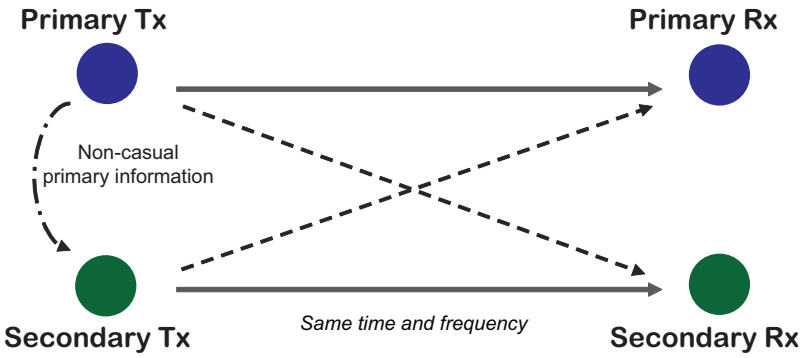

Figure 1.5. Overlay CR with non-causal primary information at the secondary transmitter.

mitter [45]. However, in general, this assumption is not practical in most cases. Furthermore, obtaining the global CSI at the secondary transmitter is a major challenge, which is especially true in a CR context, because no assistance for channel estimation can be expected from the primary system. Finally, the high computational complexity involved in DPC also prevents the implementation of such an overlay CR.

The above limitations of overlay CR scheme based on non-causal primary information motivated the work in Chapter 4 and Chapter 5 of this dissertation, where we propose practical spectrum sharing protocols based on cooperative AF and DF relaying techniques respectively. In order to obtain protocols which are feasible for practical implementations, we bear in mind the following design criterions:

1. No explicit communication between the primary and secondary system is required, and modification to primary legacy protocols is minimized. In other words, the primary system should be oblivious (as far as possible) to the operations of the secondary system.

2. CSI is only available at the respective receivers but not at the transmitters.

3. Signal processing at the secondary system should be as simple as possible.

In the proposed protocols, primary and secondary systems transmit simultaneously in the same frequency band and the secondary system attempts to compensate for the interference caused by its transmissions. Thus our proposed protocols fall into the category of overlay CR. Secondary access is achieved by the secondary

transmitter as it partially performs as a cooperative relay for the primary system and transmits a superimposed signal[4] in the relaying phase. We show that with the proposed protocols, the secondary system is able to access the spectrum band while the performance of the primary system is maintained or improved by a desired margin.

We also consider a more general multi-user scenario in Chapter 6 where multiple secondary transmitters desire to access the spectrum band by providing cooperation to the primary system. We propose a spectrum sharing protocol along with a two-step distributed secondary user selection scheme for such a CR network. Specifically, one secondary transmitter is first selected to serve as a cooperative relay for the primary system, and another secondary transmitter which optimizes the rate of the secondary system is then selected to access the spectrum band along with the primary system. We show that with the proposed protocol, secondary spectrum access is achieved without degrading the performance of the primary system or causing any additional overheads to the primary system.

1.2 Contributions and Outline of Dissertation

This dissertation investigates the roles of cooperation and cognition for spectrum efficiency enhancement in wireless communication systems. The main contributions are listed as following.

Chapter 2

In Chapter 2, we will first derive the moments of the harmonic mean of two independent gamma distributed random variables which have the same shape parameter but different scale parameters. We will then apply these results to analyze the average sum rate of two-way AF half duplex relaying systems. By deriving tight upper and lower bounds for the average sum rate of two-way relaying, we will show that the spectrum efficiency loss caused by the half-duplex constraint in an one-way relaying system can be significantly recovered by its two-way counterpart. The analysis and derivations had been presented in [60]

[4]Which contains both primary and secondary signals.

Y. Han, S. H. Ting, C. K. Ho, W. H. Chin, "Moments of harmonic mean and rate analysis for two-way amplify-and-forward relaying," in *Proceedings of IEEE International Conference on Communications, Workshop on Cooperative Communications and Networking, Theory, Practice, and Applications*, Beijing, PRC China, pp. 365-369, May 2008.

We also extend the two-way AF half-duplex relaying to the case where source and destination terminals both transmit Alamouti's orthogonal space time block code (OSTBC) utilizing two antennas and the relay has only one antenna. The spectrum efficiency is shown to be further improved compared to the single antenna case. These results had been presented in [61]

Y. Han, S. H. Ting, C. K. Ho, W. H. Chin, "High rate two-way amplify-and-forward half-duplex relaying with OSTBC," in *Proceedings of IEEE Vehicular Technology Conference 2008 Spring*, Singapore, pp. 2426-2430, May 2008.

Finally, a tight upper bound for the pair-wise error probability (PEP) for the above proposed OSTBC two-way relaying scheme is published in [62]

Y. Han, S. H. Ting, C. K. Ho, W. H. Chin, "Performance bounds for two-way amplify-and-forward relaying," *IEEE Transactions on Wireless Communications*, vol. 8, no. 1, pp. 432-439, Jan. 2009.

This PEP upper bound proved that a spatial diversity gain of 2 is achieved by the proposed scheme. Optimal power allocations under a global power constraint for two-way relaying with single antenna and the proposed two-way OSTBC scheme will also be derived.

Chapter 3

Instead of the pure cooperative system discussed in Chapter 2, we will combine cooperative relaying transmission with interweave CR in Chapter 3 and consider the scenario where the secondary system is a dual-hop relay system. Two different spectrum sensing protocols, namely dedicated and simultaneous sensing protocols, are then considered. The dedicated sensing protocol is a straightforward extension of the sensing protocols in a non-relaying CR system and is used as a benchmark

for performance comparison. We will analyze the average collision time (ACT), average utilization time (AUT), and an overall system utilization time (OSUT) for both protocols. The protocol descriptions and analysis had been presented and submitted respectively in [63, 64]

> Y. Han, A. Pandharipande, S. H. Ting, "Spectrally efficient sensing protocol for cognitive relay systems," in *Proceedings of 1st International Conference on COMmunication Systems and NETworkS (COMSNETS), WIreless Systems: Advanced Research and Development (WISARD)*, Bangalore, India, pp. 1-6, Jan. 2009.

> Y. Han, S. H. Ting, and A. Pandharipande, "Spectrally efficient sensing protocol in cognitive relay systems," to appear in *IET Communications*, 2010.

We will show that by removing the dedicated sensing periods, the simultaneous sensing protocol significantly improves the spectrum efficiency for the secondary system and also achieves a higher overall spectrum utilization compared to the dedicated sensing protocol.

Chapter 4

In Chapter 4, we will combine AF cooperative relaying transmission with overlay CR and propose an opportunistic spectrum sharing protocol with a corresponding handshake mechanism. The secondary system exploits the scenario where the link between primary transmitter and receiver is weak and gains access to the spectrum band by assisting the primary system in achieving a request target rate. We will show that the proposed protocol benefit both the primary and secondary system, and the main results had been been presented in [65]

> Y. Han, A. Pandharipande, and S. H. Ting, "Cooperative spectrum sharing via controlled amplify-and-forward relaying," in *Proceedings of IEEE PIMRC 2008, Workshop on Wireless Distributed Networks*, Cannes, France, pp.1-5, Sept. 2008.

Chapter 5

Spectrum sharing protocol based on DF cooperative relaying will be presented in Chapter 5. A critical radius from the primary transmitter will be derived, within which the secondary transmitter is able to achieve spectrum access without degrading the outage performance of the primary system by properly choosing the transmission power for relaying the primary signal. The derivations had been published in [66]

> Y. Han, A. Pandharipande, and S. H. Ting, "Cooperative decode-and-forward relaying for secondary spectrum access," *IEEE Transactions on Wireless Communications*, vol. 8, no. 10, pp. 4945-4950, Oct. 2009.

We will also present a distributed secondary user selection scheme with statistical channel information which optimizes the performance for primary system. The contents had been presented in [67]

> Y. Han, S. H. Ting, and A. Pandharipande, "Cooperative spectrum sharing with distributed secondary user selection," in *Proceedings of IEEE ICC 2010*, Cape Town, South Africa, pp.1-5, May 2010.

Chapter 6

In Chapter 6, we will shift our focus to a more general multi-user scenario for the secondary system and present a cooperative spectrum sharing protocol with a two-step distributed secondary user selection scheme. The system configuration, protocol descriptions, and performance analysis had been published in [68]

> Y. Han, S. H. Ting, and A. Pandharipande, "Cooperative spectrum sharing protocol with secondary user selection" *IEEE Transactions on Wireless Communications*, vol. 9, no. 9, pp. 2914-2923, Sept. 2010.

We will show that with the proposed protocol, secondary spectrum access is achieved without degrading the performance of the primary system or causing any additional overheads to the primary system.

Chapter 7

Conclusions for this dissertation will be drawn in Chapter 7, where the protocols and schemes proposed in this dissertation will be summarized, and future research directions on cooperation and cognition in wireless networks will be discussed.

Chapter 2

Two-way Amplify-and-Forward Half-duplex Relaying with Orthogonal Space Time Block Code

2.1 Introduction

Cooperative relaying transmission has been shown to be a practical technique to achieve spectrum efficiency enhancement [69], communication range extension [70], and spatial diversity gain [15], by allowing user terminals to share their antennas and transmit cooperatively. Cooperative relaying transmission can be classified into two main categories, namely full-duplex relaying and half-duplex relaying. Full-duplex relaying allows the user terminals to receive and transmit at the same time in the same frequency band, whereas reception and transmission for half-duplex relaying are usually performed in time-orthogonal channels. Although full-duplex relaying achieves higher spectral efficiency [71], the large difference in power levels of the receive and transmit signals makes it practically difficult to implement [15]. On the other hand, although half-duplex relaying protocols are relatively easier for implementation, they have lower spectral efficiency than full-duplex relaying due to the pre-log factor of $\frac{1}{2}$ in the sum rate expressions [3].

In consideration of the practical concerns mentioned above, in this dissertation we assume all the terminals in a relaying network are operated in a half-duplex

fashion. In view of the spectral efficiency loss of half-duplex protocols, two-way relaying protocol was proposed in [25, 27]. Based on different processing at the relay (R), Rankov *et al.* proposed two bidirectional transmission schemes, known as two-way AF relaying and two-way decode-and-forward (DF) relaying. Specifically, in the two-way AF relaying scheme the source terminal (S) and destination terminal (D) transmit to R simultaneously in the first transmission phase, and in the second transmission phase R normalizes the signal received based on its transmit power constraint and then broadcast to both S and D. For two-way DF relaying, the only difference is that after R received the signals from S and D in the first transmission phase, it has to decode the respective codewords and then generate a new one (or a superposition of the original codewords) which is then broadcasted in the second transmission phase. Obviously, for two-way relaying, both the source to destination (S $\rightarrow$ D) link and the destination to source (D $\rightarrow$ S) link still suffer from the spectral efficiency loss, as two transmission phases, instead of one, are required. However, since the S $\rightarrow$ D link and D $\rightarrow$ S link utilize the same time and frequency resources, this loss is expected to be recovered by proper signal processing.

Two-way DF relaying has been studied from a network coding perspective in [25, 29, 30, 31, 32] and the bounds for achievable sum rates of several variants of this DF protocol were derived in [31]. On the other hand, although two-way AF relaying is more practically attractive than DF relaying due to the very simple processing at the relay terminal, it was less addressed in previous works. The received signal-to-noise ratio (SNR) of two-way AF relaying was given in [32] and the achievable sum rate was derived in [25]. However, to the best of our knowledge, published results for the achievable rate of two-way AF relaying in fading channels are not closed-form expressions and need to be evaluated by numerical methods.

It has been shown in [72, 73] that the equivalent end-to-end SNR of a two-hop one-way relaying[1] system is well approximated by the harmonic mean of the SNR of S $\rightarrow$ R and R $\rightarrow$ D links. Closed-form expressions for the probability density function of harmonic mean of two independent and identically distributed exponential and gamma random variables were derived in [72] and [73], respectively.

[1]In this chapter, hereafter, by "relaying" we only refer to "amplify-and-forward half-duplex relaying".

The authors applied these results to analyze the one-way relaying transmission where the S $\rightarrow$ R and R $\rightarrow$ D links are independent and identical Rayleigh or Nakagami fading channels, i.e., the means and variances are equal. In [61], we showed that the average sum rate of two-way relaying can be approximated by a function of the harmonic mean of the channel gains of S $\rightarrow$ R and R $\rightarrow$ D links. This allowed us to apply the results in [73] to study the average sum rate of two-way relaying under the assumption that the channel coefficients of S $\rightarrow$ R and R $\rightarrow$ D links have equal average channel gains. However, the above assumption of equal average channel gains in [61, 72, 73] is generally not true in a practical scenario, especially when path loss is taken into consideration.

In order to relax the constraint of equal average channel gains in [61, 72, 73], in this chapter, we first derive all the moments of the harmonic mean of two independent gamma distributed random variables which have the same shape parameter but different scale parameters. Note that the scale parameter here corresponds to the average channel gain. Then we use these results to study both the one-way and two-way relaying under a more practical assumption where the channels of S $\rightarrow$ R and R $\rightarrow$ D links experience independent Rayleigh fading with different average channel gains. Specifically, we analyze the average sum rate of two-way relaying by deriving an analytical upper and lower bound in the high SNR regime. We also extend the work in [25] by assuming that S and D each has two antennas and transmits an Alamouti's OSTBC [74], whereas the relay has only one antenna. We derive both upper and lower bounds of average sum rate, and an upper bound of the PEP for the proposed two-way OSTBC scheme. Furthermore, we also analytically derive the optimal power allocation between S, D and R that maximizes the average sum rate for both two-way relaying schemes with single antenna and OSTBC. Our analytical results show that two-way relaying can significantly recover the spectral efficiency loss of conventional one-way relaying and the proposed two-way OSTBC scheme achieves higher average sum rate compared to the single antenna case. In addition, both S and D are able to achieve a diversity order of two.

2.2 Moments of the Harmonic Mean of Two Gamma Random Variables

Throughout this chapter, a gamma distributed random variable x with shape parameter α and scale parameter β is denoted as $x \sim \mathcal{G}(\alpha, \beta)$ and the probability density function is given as

$$p_X(x) = \frac{x^{\alpha-1}e^{-\frac{x}{\beta}}}{\beta^{\alpha}\Gamma(\alpha)}U(x)$$

where $\Gamma(\cdot)$ is the gamma function and $U(x)$ is the unit-step function.

We first present the results on the moments of the harmonic mean of two independent gamma distributed random variables. The harmonic mean of X and Y, $H(X,Y)$ is given as [73]

$$H(X,Y) = \frac{2}{\frac{1}{X}+\frac{1}{Y}} = \frac{2XY}{X+Y} \tag{2.1}$$

Theorem 2.2.1. *Suppose X and Y are two independent gamma distributed random variables, where $X \sim \mathcal{G}(\alpha, \beta_1)$ and $Y \sim \mathcal{G}(\alpha, \beta_2)$. Then the nth moment of $H(X,Y)$ is given as*

$$\begin{aligned} E\{H(X,Y)^n\} &= 2^n \frac{\Gamma(2\alpha+n)B(\alpha+n,\alpha+n)}{\Gamma(\alpha)^2} \\ &\quad \times \frac{\beta_{\min}^{\alpha+n}}{\beta_{\max}^{\alpha}} {}_2F_1\left(2\alpha+n, \alpha+n; 2\alpha+2n; 1-\frac{\beta_{\min}}{\beta_{\max}}\right) \end{aligned} \tag{2.2}$$

where $B(\cdot,\cdot)$ is the Beta function [75, Eq.(8.380.1)], ${}_2F_1(\cdot,\cdot;\cdot;\cdot)$ is the Gauss' hypergeometric function [75, Eq.(9.100.1)], $\beta_{\min} = \min(\beta_1, \beta_2)$, and $\beta_{\max} = \max(\beta_1, \beta_2)$.

Proof: See Appendix A.

Corollary 2.2.1. *Suppose X and Y are two independent and identically distributed (i.i.d.) gamma random variables, where $X \sim \mathcal{G}(\alpha, \beta)$ and $Y \sim \mathcal{G}(\alpha, \beta)$. Then the nth moment of $H(X,Y)$ is given as*

$$E\{H(X,Y)^n\} = (2\beta)^n \frac{\Gamma(2\alpha+n)B(\alpha+n,\alpha+n)}{\Gamma(\alpha)^2}$$

$$= \left(\frac{\beta}{2}\right)^n \frac{(\alpha)_n(2\alpha)_n}{(\alpha+\frac{1}{2})_n} \tag{2.3}$$

where $(c)_q = \frac{\Gamma(c+q)}{\Gamma(c)}$. *Note that the result in (2.3) coincides with that in [73, Eq.(7)], which is a special case of (2.2).*

Proof: Substituting $\beta_{\min} = \beta_{\max} = \beta$ into (2.2) and using the identity ${}_2F_1(\cdot,\cdot;\cdot;0) = 1$, we have

$$\begin{aligned} E\{H(X,Y)^n\} &= (2\beta)^n \frac{\Gamma(2\alpha+n)B(\alpha+n,\alpha+n)}{\Gamma(\alpha)^2} \\ &= (2\beta)^n \frac{\Gamma(2\alpha+n)\Gamma(\alpha+n)^2\Gamma(\alpha+n+\frac{1}{2})\Gamma(\alpha+\frac{1}{2})}{\Gamma(\alpha)^2\Gamma(2\alpha+2n)\Gamma(\alpha+n+\frac{1}{2})\Gamma(\alpha+\frac{1}{2})} \end{aligned} \tag{2.4}$$

Applying the relationship $\Gamma(x)\Gamma(x+\frac{1}{2}) = 2^{1-2(x)}\sqrt{x}\,\Gamma(2x)$, (2.4) can be simplified as

$$\begin{aligned} E\{H(X,Y)^n\} &= \left(\frac{\beta}{2}\right)^n \frac{\Gamma(\alpha+n)\Gamma(2\alpha+n)\Gamma(\alpha+\frac{1}{2})}{\Gamma(\alpha)\Gamma(2\alpha)\Gamma(\alpha+n+\frac{1}{2})} \\ &= \left(\frac{\beta}{2}\right)^n \frac{(\alpha)_n(2\alpha)_n}{(\alpha+\frac{1}{2})_n} \end{aligned} \tag{2.5}$$

and hence concludes the proof.

■

2.3 Two-way Relaying with Single Antenna

2.3.1 Average Rate of One-way Relaying

We denote the transmit powers at S and R as P_1^s and P_1^r respectively. For simplicity of derivation we presume $P_1^s = P_1^r = P_1$ and we consider Rayleigh flat fading channels[2]. Let $h_{s,r} \sim \mathcal{CN}(0, d_1^{-\nu})$ and $h_{r,d} \sim \mathcal{CN}(0, d_2^{-\nu})$ denote the channel coefficients of S $\rightarrow$ R link and R $\rightarrow$ D link respectively, where d_1 and d_2 are the normalized distances from S to R and from R to D respectively, and ν is the path loss exponent.

[2]Since Theorem 2.2.1 applies to all values of α, the extension to Nakagami fading channels is straightforward and thus we shall omit the detailed derivations here.

Then the rate of one-way relaying can be expressed as [25]

$$R_1 = \frac{1}{2}\log_2\left(1 + \frac{g_1^2\gamma_{r,d}\gamma_{s,r}P_1}{g_1^2\gamma_{r,d}\sigma_r^2 + \sigma_d^2}\right) \tag{2.6}$$

where $\gamma_{s,r} = |h_{s,r}|^2 \sim \mathcal{G}(1, d_1^{-\nu})$, $\gamma_{r,d} = |h_{r,d}|^2 \sim \mathcal{G}(1, d_2^{-\nu})$, σ_r^2 and σ_d^2 denote the variances of additive white Gaussian noise (AWGN) at R and D respectively. We presume $\sigma_r^2 = \sigma_d^2 = \sigma^2$ and $P_1 \gg \sigma^2$, then the power normalization factor g_1 can be approximated as

$$g_1 = \sqrt{\frac{P_1}{P_1\gamma_{s,r} + \sigma^2}} \approx \sqrt{\frac{1}{\gamma_{s,r}}}. \tag{2.7}$$

Substituting (2.7) into (2.6), we have the following approximation when $P_1 \gg \sigma^2$,

$$\begin{aligned} R_1 &= \frac{1}{2}\log_2\left(1 + \frac{g_1^2\gamma_{r,d}\gamma_{s,r}P_1}{g_1^2\gamma_{r,d}\sigma^2 + \sigma^2}\right) \\ &\approx \frac{1}{2}\log_2(\theta_1) + \frac{1}{2}\log_2\left(\frac{P_1}{\sigma^2}\right) \end{aligned} \tag{2.8}$$

where $\theta_1 = \frac{1}{2}H(\gamma_{s,r}, \gamma_{r,d})$. Thus the average rate

$$E\{R_1\} \approx \frac{1}{2}E\{f(\theta_1)\} + \frac{1}{2}\log_2\left(\frac{P_1}{\sigma^2}\right) \tag{2.9}$$

where $f(\theta_1) = \log_2(\theta_1)$.

Since $f(\theta_1)$ is analytic on any open set of its domain, we can write $f(\theta_1)$ as its Taylor's series expansion [76] around μ_1, where $\mu_1 = E\{\theta_1\}$ to obtain

$$\begin{aligned} E\{f(\theta_1)\} &= \int_0^\infty f(\theta_1)p_{\theta_1}(\theta_1)d\theta_1 \\ &= \int_0^\infty \sum_{n=0}^{\infty} \frac{f^{(n)}(\mu_1)}{n!}(\theta_1 - \mu_1)^n p_{\theta_1}(\theta_1)d\theta_1 \end{aligned} \tag{2.10}$$

Note that $E\{\theta_1^n\}, n = 1, 2, \cdots, \infty$, are given by Theorem 2.2.1, thus (2.10) is a closed-form expression. However, here we apply the second order Taylor's series

approximation[3] as follows,

$$\begin{aligned} E\{f(\theta_1)\} &= \int_0^\infty \left(\sum_{n=0}^{2} \frac{f^{(n)}(\mu_1)}{n!}(\theta_1-\mu_1)^n + T_2(\theta_1) \right) p_{\theta_1}(\theta_1) d\theta_1 \\ &\approx \int_0^\infty \sum_{n=0}^{2} \frac{f^{(n)}(\mu_1)}{n!}(\theta_1-\mu_1)^n p_{\theta_1}(\theta_1) d\theta_1 \\ &= f(\mu_1) + \int_0^\infty (\theta_1-\mu_1)\, f'(\mu_1)\, p_{\theta_1}(\theta_1)\, d\theta_1 \\ &\quad + \frac{1}{2}\int_0^\infty (\theta_1-\mu_1)^2 f''(\mu_1)\, p_{\theta_1}(\theta_1)\, d\theta_1 \\ &= f(\mu_1) + \frac{f''(\mu_1)}{2}\left(E\{(\theta_1)^2\} - (\mu_1)^2 \right) \\ &= f(\mu_1) - \frac{1}{2\ln 2}\left(\frac{E\{(\theta_1)^2\} - (\mu_1)^2}{(\mu_1)^2} \right) \end{aligned} \tag{2.11}$$

where $T_2(\theta_1)$ denotes the remainder term of the second order Taylor's series expansion. The approximation error is given by $\varepsilon = \int_0^\infty |T_2(\theta_1)| p_{\theta_1}(\theta_1) d\theta_1$. It can be derived that in the interval $\theta_1 \in (\mu_1-\kappa,\ \mu_1+\kappa)$, where $0 < \kappa < \mu_1$, $|T_2(\theta_1)|$ is upper bounded by $|T_2(\theta_1)| \le \frac{1}{3\ln 2}\left(\frac{\kappa}{\mu_1-\kappa}\right)^3$. Thus the estimation error is upper bounded by $\varepsilon < \varepsilon_1 = \frac{1}{3\ln 2}\left(\frac{\kappa}{\mu_1-\kappa}\right)^3$. On the other hand, in the interval $\theta_1 \in (\mu_1+\kappa,\ \infty)$, ε is upper bounded by $\varepsilon < \varepsilon_2 = \frac{1}{3\kappa\ln 2}\sum_{k=0}^{3}\binom{3}{k}\mu_1^k E\{\theta_1^{3-k}\}$, where $E\{\theta_1^{3-k}\}$ can be obtained by using Theorem 2.2.1. Therefore, the approximation error in (2.11) is upper bounded by $\varepsilon < \max(\varepsilon_1, \varepsilon_2)$.

Without loss of generality, we assume $d_1 \le d_2$. When $d_1 > d_2$, the following results still apply by simply interchanging d_1 and d_2. By applying Theorem 2.2.1 and substituting (2.11) into (2.9), we can easily obtain

$$E\{R_1\} \approx \frac{1}{2}\log_2\left(\frac{P_1 d_1^\nu \Upsilon_1}{3 d_2^{2\nu}\sigma^2}\right) - \frac{1}{4\ln 2}\left(\frac{9}{5}\frac{d_2^\nu}{d_1^\nu}\frac{\Upsilon_2}{\Upsilon_1^2} - 1\right) \tag{2.12}$$

where $\Upsilon_1 = {}_2F_1\left(3,2;4;\frac{d_2^\nu-d_1^\nu}{d_2^\nu}\right)$, $\Upsilon_2 = {}_2F_1\left(4,3;6;\frac{d_2^\nu-d_1^\nu}{d_2^\nu}\right)$. Note that (2.12) is a closed-form expression and is applicable for arbitrary d_1, d_2, and ν.

[3]Due to the Runge's phenomenon [77], the higher order Taylor's series expansions actually provide worse approximations.

2.3.2 Average Sum Rate of Two-way Relaying

When considering the two-way relaying scheme, we let P_2^s, P_2^r and P_2^d denote the transmit powers at S, R and D respectively, and for simplicity of derivation we presume $P_2^s = P_2^d = P_2$. We also let $h_{d,r} \sim \mathcal{CN}(0, d_2^{-\nu})$ and $h_{r,s} \sim \mathcal{CN}(0, d_1^{-\nu})$ denote channel coefficients for destination to relay link (D $\rightarrow$ R) link and relay to source (R $\rightarrow$ S) link, respectively. Further, we presume that all the channels are static in an interval of two symbol periods[4].

Signals x_s and x_d are transmitted from S and D respectively in the first symbol period, where $E\{x_s^* x_s\} = E\{x_d^* x_d\} = 1$. In the second symbol period, the relay normalizes the signal it received in the first symbol period based on its transmit power constraint and then broadcast to S and D. The signal received at D in the second symbol period is given as

$$y_2^d = g_2 h_{r,d} h_{s,r} \sqrt{P_2} x_s + g_2 h_{r,d} h_{d,r} \sqrt{P_2} x_d + g_2 h_{r,d} n_r + n_d \tag{2.13}$$

where $n_r \sim \mathcal{CN}(0, \sigma_r^2)$ and $n_d \sim \mathcal{CN}(0, \sigma_d^2)$ denote the AWGN at R and D. Presuming $\sigma_r^2 = \sigma_d^2 = \sigma^2$ and $P_2 \gg \sigma^2$, the power normalization factor g_2 at R can be approximated as

$$g_2 = \sqrt{\frac{P_2^r}{P_2^s \gamma_{s,r} + P_2^d \gamma_{d,r} + \sigma_r^2}} \approx \sqrt{\frac{P_2^r}{P_2} \frac{1}{\gamma_{s,r} + \gamma_{d,r}}} \tag{2.14}$$

where $\gamma_{d,r} = |h_{d,r}|^2$.

We presume perfect knowledge of the corresponding channel coefficients at D, thus the self-interference component $g_2 h_{r,d} h_{d,r} \sqrt{P_2} x_d$ can be subtracted[5] from y_2^d to obtain

$$\widetilde{y}_2^d = g_2 h_{r,d} h_{s,r} \sqrt{P_2} x_s + g_2 h_{r,d} n_r + n_d. \tag{2.15}$$

Then the rate for the S $\rightarrow$ R $\rightarrow$ D link is given by

$$R_2^{s \rightarrow d} = \frac{1}{2} \log_2 \left(1 + \frac{g_2^2 \gamma_{r,d} \gamma_{s,r} P_2}{g_2^2 \gamma_{r,d} \sigma_r^2 + \sigma_d^2} \right). \tag{2.16}$$

[4]We assume each transmission phase occurs over one symbol period

[5]Note that only the product $g_2 h_{r,d} h_{d,r} \sqrt{P_2}$ is needed and it can be obtained in practice through the use of training symbols. Knowledge of the individual channel coefficients $h_{r,d}$ and $h_{d,r}$ is not required.

Substituting (2.14) into (2.16) and presuming that the channels are reciprocal in their gains, i.e., $\gamma_{r,s} = \gamma_{s,r}$ and $\gamma_{d,r} = \gamma_{r,d}$, we have the following approximation when $P_2 \gg \sigma^2$,

$$R_2^{s\to d} \approx \frac{1}{2}\log_2\left(\frac{\gamma_{r,d}\gamma_{s,r}}{\lambda\gamma_{r,d}+\gamma_{s,r}}\frac{P_2^r}{\sigma^2}\right) \tag{2.17}$$

where $\lambda = \frac{P_2+P_2^r}{P_2}$. Similarly, the rate for D $\to$ R $\to$ S link is given by

$$R_2^{d\to s} \approx \frac{1}{2}\log_2\left(\frac{\gamma_{r,d}\gamma_{s,r}}{\lambda\gamma_{s,r}+\gamma_{r,d}}\frac{P_2^r}{\sigma^2}\right). \tag{2.18}$$

Thus the sum rate of two-way relaying is given as

$$\begin{aligned} R_2 &= R_2^{s\to d} + R_2^{d\to s} \\ &\approx \frac{1}{2}\log_2\left(\frac{(\gamma_{r,d}\gamma_{s,r})^2}{(\lambda\gamma_{r,d}+\gamma_{s,r})(\lambda\gamma_{s,r}+\gamma_{r,d})}\left(\frac{P_2^r}{\sigma^2}\right)^2\right) \\ &= \log_2(\theta_1) + \log_2\left(\frac{P_2^r}{\sigma^2}\right) + \frac{1}{2}\log_2(\Lambda) \end{aligned} \tag{2.19}$$

where $\Lambda = \frac{(\gamma_{r,d}+\gamma_{s,r})^2}{(\lambda\gamma_{r,d}+\gamma_{s,r})(\lambda\gamma_{s,r}+\gamma_{r,d})}$. We can bound Λ on both sides and derive upper and lower bounds for R_2 as follows.

Theorem 2.3.1. *Λ is bounded as $\frac{2}{\lambda^2+1} < \Lambda < \frac{1}{\lambda}$ and thus R_2 has an upper bound R_2^{ub} and lower bound R_2^{lb} given by*

$$R_2^{\text{ub}} = \log_2(\theta_1) + \frac{1}{2}\log_2(\Phi_1), \tag{2.20}$$

$$R_2^{\text{lb}} = \log_2(\theta_1) + \frac{1}{2}\log_2(\Phi_2), \tag{2.21}$$

where $\Phi_1 = \frac{P_2(P_2^r)^2}{(P_2+P_2^r)(\sigma^2)^2}$ and $\Phi_2 = \frac{2(P_2P_2^r)^2}{((P_2+P_2^r)^2+P_2^2)(\sigma^2)^2}$.

Proof: Let

$$\begin{aligned} t &= (\lambda\gamma_{r,d}+\gamma_{s,r})(\lambda\gamma_{s,r}+\gamma_{r,d}) \\ &= \lambda(\gamma_{r,d}^2+\gamma_{s,r}^2) + (\lambda^2+1)\gamma_{r,d}\gamma_{s,r}. \end{aligned}$$

It is obvious that $(\lambda^2+1) > 2\lambda$. Thus we have

$$\lambda(\gamma_{r,d}+\gamma_{s,r})^2 < t < \frac{\lambda^2+1}{2}(\gamma_{r,d}+\gamma_{s,r})^2$$

and since $\Lambda = \frac{(\gamma_{r,d}+\gamma_{s,r})^2}{t}$, we obtain

$$\frac{2}{\lambda^2+1} < \Lambda < \frac{1}{\lambda}. \tag{2.22}$$

Substituting (2.22) into (2.19), we can easily obtain (2.20) and (2.21).

■

Applying (2.20), (2.21) and Theorem 2.2.1 we can easily obtain

$$E\{R_2^{\text{ub}}\} \approx \log_2\left(\frac{d_1^{\nu}\Upsilon_1\sqrt{\Phi_1}}{3d_2^{2\nu}}\right) - \frac{1}{2\ln 2}\left(\frac{9d_2^{\nu}\Upsilon_2}{5d_1^{\nu}\Upsilon_1^2}-1\right) \tag{2.23}$$

$$E\{R_2^{\text{lb}}\} \approx \log_2\left(\frac{d_1^{\nu}\Upsilon_1\sqrt{\Phi_2}}{3d_2^{2\nu}}\right) - \frac{1}{2\ln 2}\left(\frac{9d_2^{\nu}\Upsilon_2}{5d_1^{\nu}\Upsilon_1^2}-1\right) \tag{2.24}$$

We consider the problem of optimizing the power allocation between P_2 and P_2^r (note that the optimality is under the assumption $P_2^s = P_2^d = P_2$). For simplicity of derivation, we only make use of $E\{R_2^{\text{ub}}\}$ to derive the optimal power allocation, which maximizes Φ_1. For a fair comparison between one-way and two-way relaying, we assume the total transmit power P_T for the whole relaying system is fixed for both schemes, i.e., $2P_1 = 2P_2 + P_2^r = P_T$. From (2.20), it is easy to obtain that $E\{R_2^{\text{ub}}\}$ is maximized when $P_2^r = \frac{\sqrt{5}-1}{2}P_T \approx 0.618P_T$ and $P_2 = \frac{3-\sqrt{5}}{4}P_T \approx 0.191P_T$. Note that the derived optimal power allocation is independent of d_1, d_2, and ν, which is an important and useful result when we consider practical implementations.

With the above power allocation, $E\{R_2^{\text{ub}} - R_2^{\text{lb}}\} = \log_2\left(\sqrt{\frac{\Phi_1}{\Phi_2}}\right) \approx 0.58$ bit/s/Hz. We can observe that $E\{R_2^{\text{ub}} - R_2^{\text{lb}}\}$ is small and also independent of d_1, d_2, ν, and P_T which indicates that both the upper and lower bounds are tight under different channel conditions and total transmit powers. We can also obtain $E\{R_2^{\text{ub}}\} = 2E\{R_1\} - 0.74$ bit/s/Hz, which verifies that two-way relaying is able to recover almost all the spectral efficiency loss of one-way relaying due to the pre-log factor of $\frac{1}{2}$.

2.4 Two-way Relaying with OSTBC

From results of the previous section, although the sum rate of two-way relaying is almost doubled compared to one-way relaying, due to the absence of a direct S $\rightarrow$ D link no diversity gain is achieved. In this section, we extend the conventional two-way relaying to the case where Alamouti's OSTBC [74] is applied at S and D utilizing two antennas each and R has only one antenna. We show that with our proposed scheme, besides a higher average sum rate, a diversity order of two can also be achieved at both S and D.

2.4.1 Average Sum Rate of Two-way Relaying with OSTBC

Since the relay has only one antenna, we consider the transmit power per transmit antenna instead of per terminal. The transmit power *per antenna* at S, D and R are denoted as $P_2^{A,s}$, $P_2^{A,d}$, and $P_2^{A,r}$ respectively, where the superscript A denotes that Alamouti's OSTBC [74] is applied. We also presume $P_2^{A,s} = P_2^{A,d} = P_2^A$, and all the channels are static in an interval of four symbol periods.

For the first transmission from S to R and D to R, the received signal $\boldsymbol{y}_2^{A,r}$ at R over two symbol periods is given by (after some manipulations)

$$\boldsymbol{y}_2^{A,r} = \begin{bmatrix} y_{2,1}^{A,r} \\ y_{2,2}^{A,r} \end{bmatrix} = \sqrt{P_2^A}\boldsymbol{H}_{s,r}\boldsymbol{x}_s + \sqrt{P_2^A}\boldsymbol{H}_{d,r}\boldsymbol{x}_d + \boldsymbol{n}_r \tag{2.25}$$

where $y_{2,i}^{A,r}$, $i \in \{1,2\}$ is the signal received at R in the ith symbol period, and

$$\boldsymbol{H}_{l,r} = \begin{bmatrix} h_{l,r,1} & h_{l,r,2} \\ h_{l,r,2}^* & -h_{l,r,1}^* \end{bmatrix} \tag{2.26}$$

are the equivalent channel matrices for Alamouti's OSTBC where $l \in \{s,d\}$, $h_{s,r,m} \sim \mathcal{CN}(0, d_1^{-\nu})$ and $h_{d,r,m} \sim \mathcal{CN}(0, d_2^{-\nu})$, $m \in \{1,2\}$, are the channel coefficients from the respective antennas ($m = 1, 2$) at S and D to R. Signal vectors transmitted from S and D are denoted as $\boldsymbol{x}_s = [x_{s,1}, x_{s,2}]^{\mathrm{T}}$ and $\boldsymbol{x}_d$ respectively, where $E\{\boldsymbol{x}_s\boldsymbol{x}_s^{\mathrm{H}}\} = \boldsymbol{I}_2$ and $E\{\boldsymbol{x}_d\boldsymbol{x}_d^{\mathrm{H}}\} = \boldsymbol{I}_2$. Here, $\boldsymbol{n}_r \sim \mathcal{CN}(\boldsymbol{0}_2, \sigma^2\boldsymbol{I}_2)$ is the AWGN vector at R. Presuming $P_2^A \gg \sigma^2$, the power normalization factor at R can

be approximated as

$$g_2^A = \sqrt{\frac{P_2^{A,r}}{P_2^A \gamma_{s,r}^A + P_2^A \gamma_{d,r}^A + \sigma^2}} \approx \sqrt{\frac{P_2^{A,r}}{P_2^A} \frac{1}{\gamma_{s,r}^A + \gamma_{d,r}^A}} \tag{2.27}$$

where $\gamma_{l,r}^A = |h_{l,r,1}|^2 + |h_{l,r,2}|^2$, $l \in \{s, d\}$.

After power scaling, $g_2^A y_{2,1}^{A,r}$ and $g_2^A y_{2,2}^{A,r}$ are broadcasted to S and D over two consecutive symbol periods. The signal received at D in the ith (i=1, 2) symbol period during this broadcast phase is given by

$$\boldsymbol{y}_{2,i}^{A,d} = \boldsymbol{h}_{r,d} g_2^A y_{2,i}^{A,r} + \boldsymbol{n}_{d,i} \tag{2.28}$$

where $\boldsymbol{h}_{r,d} = [h_{r,d,1}, h_{r,d,2}]^{\mathrm{T}}$ is the channel coefficient vector from R to the two antennas at D. Here, $h_{r,d,m} \sim \mathcal{CN}(0, d_2^{-\nu})$ and $m \in \{1, 2\}$. Vector $\boldsymbol{n}_{d,i} \sim \mathcal{CN}(\boldsymbol{0}_2, \sigma^2 \boldsymbol{I}_2)$ denotes the AWGN at D in the ith symbol period. Interchanging the first element in $\boldsymbol{y}_{2,1}^{A,d}$ with the second element in $\boldsymbol{y}_{2,2}^{A,d}$, we rewrite (2.28) as

$$\widetilde{\boldsymbol{y}}_{2,1}^{A,d} = g_2^A h_{r,d,1} \boldsymbol{y}_2^{A,r} + \widetilde{\boldsymbol{n}}_{d,1}, \tag{2.29}$$

$$\widetilde{\boldsymbol{y}}_{2,2}^{A,d} = g_2^A h_{r,d,2} \boldsymbol{y}_2^{A,r} + \widetilde{\boldsymbol{n}}_{d,2}. \tag{2.30}$$

Similarly to the single antenna case, we presume perfect knowledge of the corresponding channel coefficients at D, thus the self-interference component

$$g_2^A h_{r,d,m} \sqrt{P_2^A} \boldsymbol{H}_{d,r} \boldsymbol{x}_d$$

can be subtracted[6] from (2.29) and (2.30) to obtain

$$\widehat{\boldsymbol{y}}_{2,1}^{A,d} = g_2^A h_{r,d,1} \boldsymbol{H}_{s,r} \sqrt{P_2^A} \boldsymbol{x}_s + g_2^A h_{r,d,1} \boldsymbol{n}_r + \widetilde{\boldsymbol{n}}_{d,1}, \tag{2.31}$$

$$\widehat{\boldsymbol{y}}_{2,2}^{A,d} = g_2^A h_{r,d,2} \boldsymbol{H}_{s,r} \sqrt{P_2^A} \boldsymbol{x}_s + g_2^A h_{r,d,2} \boldsymbol{n}_r + \widetilde{\boldsymbol{n}}_{d,2}. \tag{2.32}$$

We presume that the channels are reciprocal in their gains, i.e. $\gamma_{r,s}^A = \gamma_{s,r}^A$ and $\gamma_{d,r}^A = \gamma_{r,d}^A$. We perform matched filtering followed by maximal ratio combining

[6] Again, only the product $g_2^A h_{r,d,m} \sqrt{P_2^A} \boldsymbol{H}_{d,r}$ is required, not the individual channel coefficients.

(MRC) to $\widehat{\boldsymbol{y}}_{2,1}^{A,d}$ and $\widehat{\boldsymbol{y}}_{2,2}^{A,d}$ in (2.31) and (2.32), then by applying the same derivations as for the single antenna case, we obtain the sum rate of two-way relaying with OSTBC[7] as

$$\begin{aligned} R_2^A &= R_2^{A,s\to d} + R_2^{A,d\to s} \\ &\approx \frac{1}{2}\log_2\left[\left(\frac{\gamma_{r,d}^A\gamma_{s,r}^A P_2^{A,r}}{(\lambda^A\gamma_{r,d}^A+\gamma_{s,r}^A)\sigma^2}\right)\left(\frac{\gamma_{r,d}^A\gamma_{s,r}^A P_2^{A,r}}{(\lambda^A\gamma_{s,r}^A+\gamma_{r,d}^A)\sigma^2}\right)\right] \\ &= \frac{1}{2}\log_2\left(\frac{(\gamma_{r,d}^A\gamma_{s,r}^A)^2\left(P_2^{A,r}\right)^2}{(\lambda^A\gamma_{r,d}^A+\gamma_{s,r}^A)(\lambda^A\gamma_{s,r}^A+\gamma_{r,d}^A)(\sigma^2)^2}\right) \end{aligned} \tag{2.33}$$

where $\lambda^A = \frac{P_2^A+P_2^{A,r}}{P_2^A}$. We can find upper and lower bounds for R_2^A by using Theorem 2.3.1. In the following, we only consider the upper bound, as an extension to the lower bound is straightforward. The upper bound for R_2^A is given as

$$R_2^{A,\mathrm{ub}} = \log_2(\theta_2) + \log_2\left(\frac{P_2^{A,r}}{\sigma^2}\right) - \frac{1}{2}\log_2(\lambda^A) \tag{2.34}$$

where $\theta_2 = \frac{1}{2}H(\gamma_{s,r}^A, \gamma_{r,d}^A)$. Assuming $d_1 \le d_2$, by applying Theorem 2.2.1 and second order Taylor's approximation (the approximation error can be analyzed similarly to that in (2.11)), we have

$$E\{R_2^{A,\mathrm{ub}}\} \approx \log_2\left(\frac{4P_2^{A,r}(P_2^A)^{\frac{1}{2}}d_1^{2\nu}\Upsilon_3}{5\sigma^2 d_2^{3\nu}(P_2^A+P_2^{A,r})^{\frac{1}{2}}}\right) - \frac{1}{2\ln 2}\left(\frac{1.34 d_2^{2\nu}\Upsilon_4}{d_1^{2\nu}\Upsilon_3^2} - 1\right) \tag{2.35}$$

where $\Upsilon_3 = {}_2F_1(5,3;6;\frac{d_2^\nu - d_1^\nu}{d_2^\nu})$ and $\Upsilon_4 = {}_2F_1(6,4;8;\frac{d_2^\nu - d_1^\nu}{d_2^\nu})$. We again assume the total transmit power is P_T, i.e., $4P_2^A + P_2^{A,r} = P_T$. From (2.34), it is easy to show that $E\{R_2^{A,\mathrm{ub}}\}$ in (2.35) is maximized when $P_2^A = \frac{3-\sqrt{3}}{12}P_T \approx 0.1057P_T$ and $P_2^{A,r} = \frac{\sqrt{3}}{3}P_T \approx 0.5774P_T$. Again, we notice that the derived optimal power allocation is independent of d_1,d_2, and ν.

From (2.20) and (2.34), it follows that the improvement of the proposed two-way OSTBC scheme over conventional two-way relaying with single antenna is

[7]The derivation for $R_2^{A,d\to s}$ is omitted here as it is similar to that for $R_2^{A,s\to d}$.

given as

$$\begin{aligned} &E\{R_2^{A,\mathrm{ub}} - R_2^{\mathrm{ub}}\} \\ &= E\{\log_2(\theta_2) - \log_2(\theta_1)\} + \frac{1}{2}\log_2\left(\left(\frac{P_2^{A,r}}{P_2^r}\right)^2\left(\frac{P_2^A(P_2+P_2^r)}{P_2(P_2^{A,r}+P_2^A)}\right)\right). \end{aligned} \tag{2.36}$$

By applying Theorem 2.2.1, we can easily evaluate (2.36) for arbitrary d_1, d_2, and ν. Specifically, for $d_1^{-\nu} = d_2^{-\nu} = 1$ and applying the corresponding optimal power allocations derived above and in Section 2.3, we have

$$E\{R_2^{A,\mathrm{ub}} - R_2^{\mathrm{ub}}\} \approx 1.19 \text{ bit/s/Hz}. \tag{2.37}$$

which indicates that with the same total transmit power P_T, higher average sum rate can be achieved by the proposed two-way OSTBC scheme compared to conventional two-way relaying with single antenna.

2.4.2 PEP Upper Bound and Diversity Gain

With some manipulations, we can rewrite (2.31) and (2.32) in the equivalent STBC transmission form as

$$\boldsymbol{Y} = g_2^A\sqrt{P_2^A}\boldsymbol{X}\widetilde{\boldsymbol{h}} + \boldsymbol{N} \tag{2.38}$$

where

$$\boldsymbol{X} = \begin{bmatrix} x_{s,1} & x_{s,2} & 0 & 0 \\ -x_{s,2}^* & x_{s,1}^* & 0 & 0 \\ 0 & 0 & x_{s,1} & x_{s,2} \\ 0 & 0 & -x_{s,2}^* & x_{s,1}^* \end{bmatrix},$$

and $\boldsymbol{N} = [\tilde{\boldsymbol{n}}_{d,1}^{\mathrm{T}}, \tilde{\boldsymbol{n}}_{d,2}^{\mathrm{T}}]^{\mathrm{T}}$. The channel coefficient vector $\widetilde{\boldsymbol{h}} = \boldsymbol{v}\boldsymbol{h}$, where

$$\boldsymbol{v} = \begin{bmatrix} h_{r,d,1} & 0 & h_{r,d,2} & 0 \\ 0 & h_{r,d,1} & 0 & h_{r,d,2} \end{bmatrix}^{\mathrm{T}} \tag{2.39}$$

and $\boldsymbol{h} = [h_{s,r,1}, h_{s,r,2}]^{\mathrm{T}}$.

Let $\mathbf{\Sigma} = E\{\boldsymbol{N}\boldsymbol{N}^{\mathrm{H}}\}$ and it is easy to verify that

$$\mathbf{\Sigma} = \sigma^2 \begin{bmatrix} \mathbf{\Sigma}_1 & \mathbf{\Pi}_1 \\ \mathbf{\Pi}_2 & \mathbf{\Sigma}_2 \end{bmatrix} \tag{2.40}$$

where $\mathbf{\Sigma}_m = \left((g_2^A)^2|h_{r,d,m}|^2 + 1\right)\boldsymbol{I}_2$, $m \in \{1,2\}$, $\mathbf{\Pi}_1 = \left((g_2^A)^2 h_{r,d,1}^* h_{r,d,2}\right)\boldsymbol{I}_2$ and $\mathbf{\Pi}_2 = \mathbf{\Pi}_1^{\mathrm{H}}$.

Suppose $\boldsymbol{X}_c$ and $\boldsymbol{X}_e$ are two different codewords in the OSTBC codebook. Thus the PEP of mistaking $\boldsymbol{X}_c$ with $\boldsymbol{X}_e$ is upper bounded as [78]

$$\mathcal{P}_{c\to e} \leq \underset{\boldsymbol{h},\boldsymbol{v}}{E}\left\{e^{-\frac{P_2^A (g_2^A)^2}{4}\boldsymbol{h}^{\mathrm{H}}\boldsymbol{v}^{\mathrm{H}}(\boldsymbol{X}_c-\boldsymbol{X}_e)^{\mathrm{H}}\mathbf{\Sigma}^{-1}(\boldsymbol{X}_c-\boldsymbol{X}_e)\boldsymbol{v}\boldsymbol{h}}\right\} \tag{2.41}$$

where $\underset{\omega}{E}\{\cdot\}$ denotes expectation over ω. It is obvious that the codeword difference matrix $\Delta\boldsymbol{S} = (\boldsymbol{X}_c - \boldsymbol{X}_e)^{\mathrm{H}}(\boldsymbol{X}_c - \boldsymbol{X}_e)$ is a diagonal matrix with four identical elements in its diagonal, which we denote as ϵ. Thus we have

$$\mathcal{P}_{c\to e} \leq \underset{\boldsymbol{h},\boldsymbol{v}}{E}\left\{e^{-\frac{P_2^A (g_2^A)^2 \epsilon}{4}\boldsymbol{h}^{\mathrm{H}}\mathbf{\Omega}\boldsymbol{h}}\right\} \tag{2.42}$$

where

$$\mathbf{\Omega} = \frac{\eta + \gamma_{r,d}^A}{\left((g_2^A)^2\gamma_{r,d}^A + 1\right)\sigma^2}\boldsymbol{I}_2,$$

and

$$\eta = (g_2^A)^2\left[2|h_{r,d,1}|^2|h_{r,d,2}|^2 - (h_{r,d,1}^* h_{r,d,2})^2 - (h_{r,d,2}^* h_{r,d,1})^2\right] \geq 0.$$

We presume $P_2^{A,r} = pP_T$ and $P_2^A = (\frac{1-p}{4})P_T$, where $0 < p < 1$ is the power allocation factor. Note that $(g_2^A)^2$ contains both $h_{s,r,m}$ and $h_{r,d,m}$, thus the exact calculation of (2.42) is difficult. Therefore, we resort to a heuristic argument similar to that in [17] by making a reasonable approximation that $(g_2^A)^2 \approx E\{(g_2^A)^2\} = \frac{2p}{(\beta_1+\beta_2)(1-p)}$, where $\beta_1 = d_1^{-\nu}$ and $\beta_2 = d_2^{-\nu}$. Then by further upper bounding the right hand side of (2.42) through the omission of η, which is strictly non-negative, and taking expectation over $\boldsymbol{h}$ and $\boldsymbol{v}$ successively, we obtain

$$\mathcal{P}_{c\to e} \quad < \quad \underset{\boldsymbol{h},\boldsymbol{v}}{E}\left\{e^{-\boldsymbol{h}^{\mathrm{H}}\left(\frac{P_2^A g\epsilon\gamma_{rd}^A}{4\sigma^2(g\gamma_{rd}^A+1)}\boldsymbol{I}_2\right)\boldsymbol{h}}\right\}$$

$$
\begin{aligned}
&= \underset{\boldsymbol{v}}{E}\left\{\int \frac{1}{\pi^2\beta_1^2} e^{-\boldsymbol{h}^{\mathrm{H}}\left(\frac{P_2^A g\epsilon\gamma_{rd}^A}{4\sigma^2(g\gamma_{rd}^A+1)}\boldsymbol{I}_2\right)\boldsymbol{h}} e^{-\boldsymbol{h}^{\mathrm{H}}\boldsymbol{h}} d\boldsymbol{h}\right\} \\
&= \underset{\gamma_{r,d}^A}{E}\left\{\frac{1}{\beta_1^2}\det{}^{-1}\left[\frac{\boldsymbol{I}_2}{\beta_1}+\frac{\tau g\gamma_{r,d}^A}{g\gamma_{r,d}^A+1}\boldsymbol{I}_2\right]\right\} \\
&= \underset{\gamma_{r,d}^A}{E}\left\{\left(1+\beta_1\tau\frac{g\gamma_{r,d}^A}{g\gamma_{r,d}^A+1}\right)^{-2}\right\} \\
&= \int_0^\infty \frac{\left(g\gamma_{r,d}^A+1\right)^2}{\left((1+\beta_1\tau)g\gamma_{r,d}^A+1\right)^2}\frac{1}{\beta_2^2}\gamma_{r,d}^A e^{-\frac{\gamma_{r,d}^A}{\beta_2}} d\gamma_{r,d}^A \\
&< \int_0^\infty \left(\frac{(\gamma_{r,d}^A)^2g^2+2g\gamma_{r,d}^A}{(1+\beta_1\tau)^2(\gamma_{r,d}^A)^2g^2}+\frac{1}{\left((1+\beta_1\tau)g\gamma_{r,d}^A+1\right)^2}\right)\frac{1}{\beta_2^2}\gamma_{r,d}^A e^{-\frac{\gamma_{r,d}^A}{\beta_2}} d\gamma_{r,d}^A \\
&= \frac{1}{(1+\beta_1\tau)^2}\left(1+\frac{2}{g\beta_2}\right)+\int_0^\infty \frac{1}{\left((1+\beta_1\tau)g\gamma_{r,d}^A+1\right)^2}\frac{1}{\beta_2^2}\gamma_{r,d}^A e^{-\frac{\gamma_{r,d}^A}{\beta_2}} d\gamma_{r,d}^A
\end{aligned}
\tag{2.43}
$$

where $\tau = \frac{P_2^A\epsilon}{4\sigma^2} = \frac{(1-p)P_T\epsilon}{16\sigma^2}$ and $g = \frac{2p}{(\beta_1+\beta_2)(1-p)}$. Let $\frac{\gamma_{r,d}^A}{\beta_2} = x$, we have

$$
\begin{aligned}
\int_0^\infty \frac{\frac{1}{\beta_2^2}\gamma_{r,d}^A e^{-\frac{\gamma_{r,d}^A}{\beta_2}} d\gamma_{r,d}^A}{\left((1+\beta_1\tau)g\gamma_{r,d}^A+1\right)^2} &= \int_0^\infty \frac{x}{\left((1+\beta_1\tau)\beta_2 gx+1\right)^2}e^{-x}dx \\
&< \int_0^\infty \frac{e^{-x}}{\omega^2 x+2\omega}dx
\end{aligned}
\tag{2.44}
$$

where $\omega = (1+\beta_1\tau)\beta_2 g$. Applying the integral in [75, Eq. (3.352.4)], we have

$$
\int_0^\infty \frac{e^{-x}}{\omega^2 x+2\omega}dx = -\frac{1}{\omega^2}e^{\frac{2}{\omega}}Ei\left(\frac{2}{\omega}\right) \tag{2.45}
$$

where $Ei(\cdot)$ is the exponential integral [75, Eq. (8.211.1)]. Substituting (2.45) into (2.43), we will obtain

$$
\mathcal{P}_{c\to e} < \frac{1}{(1+\beta_1\tau)^2}\left(1+\frac{2}{g\beta_2}\right)-\frac{1}{\omega^2}e^{\frac{2}{\omega}}Ei\left(\frac{2}{\omega}\right). \tag{2.46}
$$

Furthermore, since $\epsilon = |x_{s,1}^c - x_{s,1}^e|^2 + |x_{s,2}^c - x_{s,2}^e|^2$, where $x_{s,k}^c$ and $x_{s,k}^e$, $k \in \{1,2\}$ are the symbols in codewords $\boldsymbol{X}_c$ and $\boldsymbol{X}_e$ respectively, it is obvious that the

minimum value of ϵ is given by $\epsilon_{\min} = d_{\min}^2$ where $d_{\min}$ is the minimum distance between two signal points in the constellation. Thus, the upper bound for $\mathcal{P}_{c\to e}$ is given as

$$\begin{aligned}\mathcal{P}_{c\to e}^{\text{ub}} &= \left[1 + \frac{(\beta_1+\beta_2)(1-p)}{\beta_2 p} - \frac{(\beta_1+\beta_2)^2(1-p)^2}{4p^2\beta_2^2} e^{\frac{2}{\omega}} Ei\left(\frac{2}{\omega}\right)\right] \\ &\quad \cdot \left(1 + \beta_1 \frac{(1-p)P_T d_{\min}^2}{16\sigma^2}\right)^{-2}. \end{aligned} \tag{2.47}$$

It is worth emphasizing that due to the approximation $(g_2^A)^2 \approx E\{(g_2^A)^2\}$ used in (2.43), $\mathcal{P}_{c\to e}^{\text{ub}}$ given in (2.47) is an approximation of the actual PEP upper bound given in (2.42). From (2.47) it is clear that a diversity order of two is achieved for the S $\to$ D link. Since the same derivation also applies to D $\to$ S link, diversity order of two is achieved for the whole system.

2.5 Simulation Results and Discussions

It worth emphasizing that due to approximation used in (2.7), (2.14), and (2.35), the theoretical bounds shown in this section are approximations of the actual bounds, and these approximations become more accurate in the high SNR regime. Comparisons of $E\{R_1\}$, $E\{R_2\}$, and $E\{R_2^A\}$ with different average channel gains by varying d_1 are shown in Figure 2.1 where we also plot the derived upper and lower bounds for $E\{R_2\}$ and $E\{R_2^A\}$. We used the respective optimal power allocations derived in Section 2.3 and 2.4 for the two-way relaying schemes with and without OSTBC. We assume $0 < d_1, d_2 < 1$ and $d_1 + d_2 = 1$. The path loss exponent $\nu = 3$. The total transmit power P_T is the same for all schemes and $\frac{P_T}{\sigma^2} = 25$dB. From Figure 2.1, it can be observed that both our derived upper and lower bounds are relatively tight for all values of d_1. We can also observe that the average sum rates of all the three schemes achieve their maximum when $d_1 = d_2 = 0.5$, i.e., when $S \to R$ and $D \to R$ links have the same average channel gains. Furthermore, as mentioned in Section 2.4, it is evident that the gaps between the derived upper and lower bounds, i.e., $E\{R_2^{\text{ub}} - R_2^{\text{lb}}\}$ and $E\{R_2^{A,\text{ub}} - R_2^{A,\text{lb}}\}$, are reasonably small and independent of d_1.

In Figure 2.2, we present the comparison between $E\{R_1\}$, $E\{R_2\}$, and $E\{R_2^A\}$

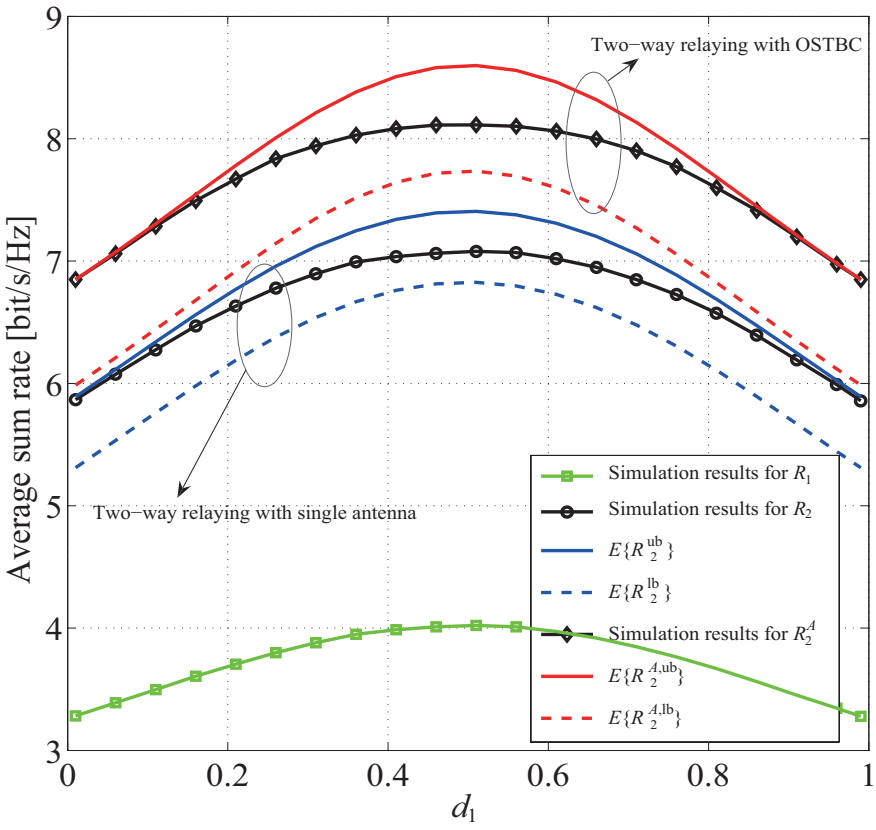

Figure 2.1. Average sum rate comparison with different average channel gains by varying d_1.

with different power allocations. Specifically, we let $p = \frac{P_2^r}{P_T}$ and $p = \frac{P_2^{A,r}}{P_T}$ for two-way relaying with and without OSTBC, respectively. We also presume $d_1 = d_2 = 0.5$, $\nu = 3$, and $\frac{P_T}{\sigma^2} = 25$dB. Note that when p tends to 1, we have $\lambda \gg 1$ and $\lambda^A \gg 1$, where the bounds become loose. However, it is obvious that both the upper and lower bounds are tight in the useful region where the average sum rate is high. This indicates that our derived bounds are useful for finding optimal power allocations. It is worth noting that when p is between 0.3 to 0.7, the sum rate is not very sensitive to the power allocation. This indicates that by simply allocating about half of the total power to the relay terminal, we can more or less achieve the optimal performance. Furthermore, it can be observed from Figure 2.1 and Figure 2.2 that both two-way relaying schemes are capable of significantly recovering the spectral efficiency loss of one-way relaying. Specifically, two-way

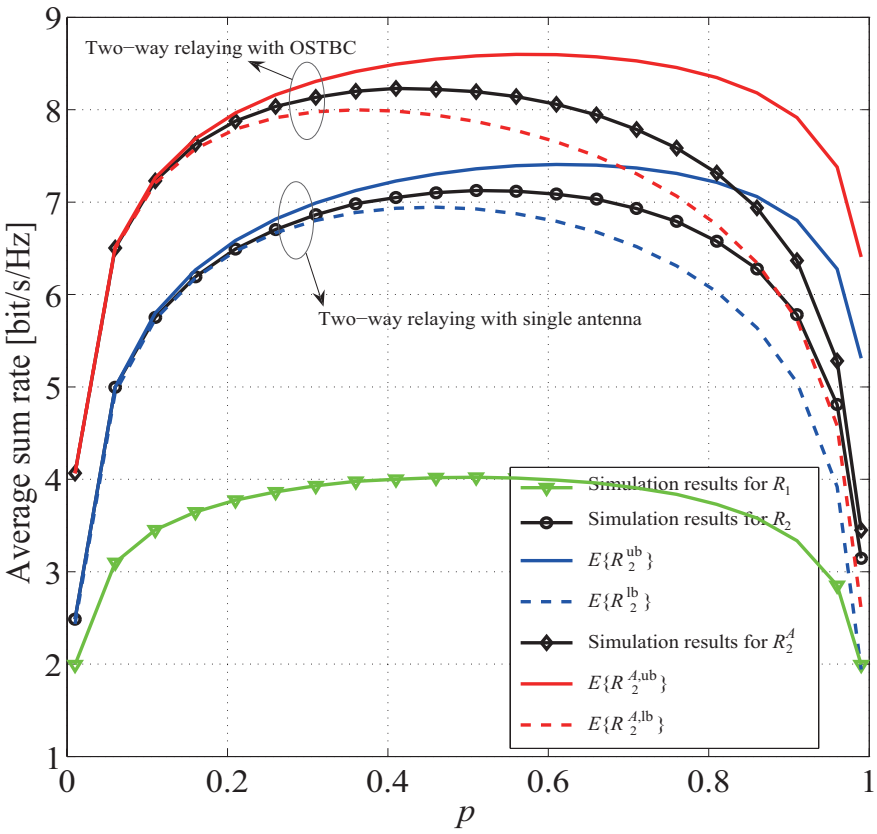

Figure 2.2. Average sum rate comparison with different power allocations by varying p.

relaying with signal antenna achieves slightly less than twice the average sum rate of one-way relaying and our proposed two-way OSTBC scheme achieves higher average sum rate than the single-antenna scheme.

The block error rate[8] (BLER) graphs of two-way relaying with single antenna and the proposed two-way OSTBC scheme are shown in Figure 2.3, where we also plot the PEP upper bound derived in (2.47) for the S $\rightarrow$ D link for the proposed OSTBC scheme. Again, we assume $0 < d_1, d_2 < 1$, $d_1 + d_2 = 1$ and $\nu = 3$. We consider two cases: $d_1 = 0.5$ and $d_1 = 0.9$, which correspond to the scenarios that S $\rightarrow$ R and D $\rightarrow$ R links have identical and different average channel gains, respectively. For both two-way relaying schemes, we use 4QAM and the respective

[8]For a fair comparison, we consider two consecutive complex symbols transmitted by two-way relaying with single antenna as a block.

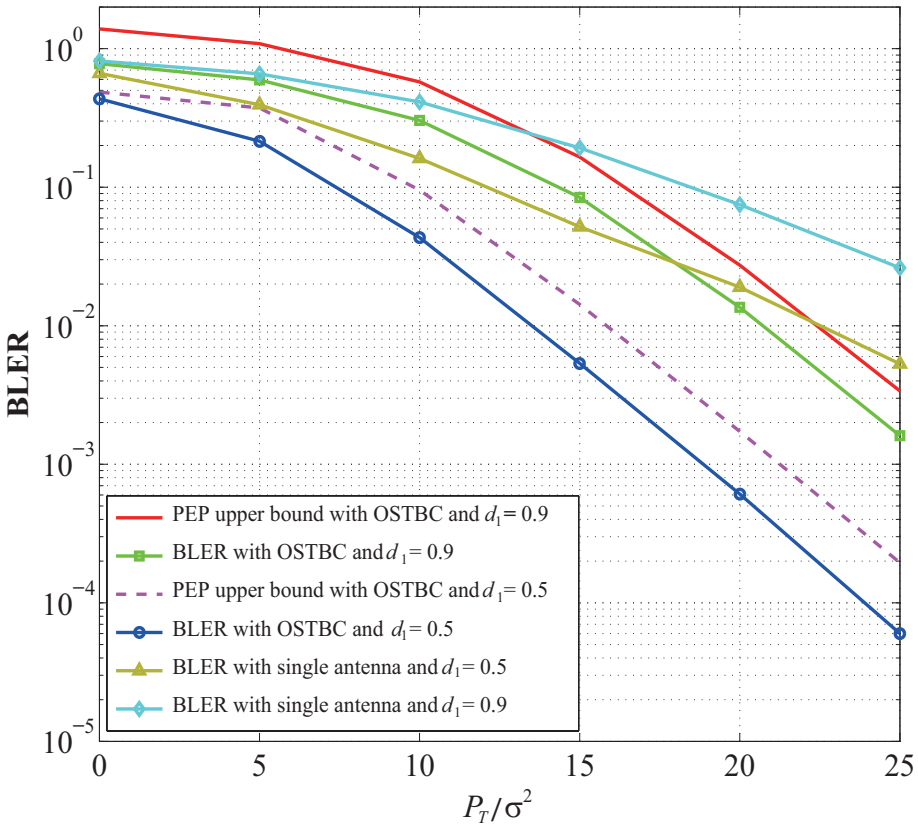

Figure 2.3. BLER performance of two-way relaying with and without OSTBC.

optimal power allocations derived in Section 2.3 and 2.4. From Figure 2.3, it is clear that the derived PEP upper bound is reasonably tight and a diversity order of two is achieved by our proposed two-way OSTBC scheme. Furthermore, we can observe that both two-way relaying schemes perform better when $d_1 = 0.5$ than when $d_1 = 0.9$ which coincides with the fact that maximum average sum rates are achieved when the two hops have equal average channel gains.

2.6 Summary

In this chapter, we derived the moments of the harmonic mean of two independent gamma distributed random variables which have the same shape parameter but different scale parameters. Applying the derived results, we analyzed two-way AF

relaying under a more practical scenario where the channel coefficients of the two hops have different average channel gains. We also extend the conventional two-way AF relaying to the scenario where source and destination terminals utilize two antennas to transmit Alamouti's OSTBC and the relay has only one antenna.

By deriving upper and lower bounds of the average sum rates for the two-way relaying schemes with and without OSTBC in the high SNR regime, we confirm that two-way relaying is capable of significantly recovering the spectrum efficiency loss of one-way relaying. The bounds also showed that the proposed two-way relaying scheme with OSTBC achieves a higher average sum rate than the single antenna scheme without OSTBC. We also used these bounds to analytically derive the optimal power allocations for both two-way relaying schemes. Furthermore, we derived an upper-bound for the PEP of two-way relaying with OSTBC which verified that a diversity order of two is also achieved by the proposed scheme.

In summary, the proposed two-way relaying scheme with OSTBC is able to significantly improve the radio spectrum efficiency with small computational complexity and low cost for practical implementation, thus making itself attractive to the future wireless network.

Chapter 3

Spectrally Efficient Sensing Protocol in Cognitive Relay Systems

3.1 Introduction

The explosion of new wireless technologies and applications makes it essential that the limited spectrum available for radio communications be used more efficiently. Frequency allocation charts [1] showing spectrum license allocations for different wireless services and applications indicate a scarcity of available spectrum. However, spectrum measurements [35, 36] have shown that the prevalent model of dedicated spectrum licensing has led to poor spectrum utilization - primary systems that operate under licensed spectrum are not active all the time in all locations, leaving large portions of spectrum unutilized. Attention has been paid recently to make regulatory changes to move from the current fixed spectrum allocation policies to flexible spectrum usage models [79, 80, 81, 82] which permit secondary access to the licensed spectrum.

One of the most important requirements for operating on a secondary basis is that the secondary system should minimize harmful interference (if any) caused to the primary systems. This requirement can be met by using cognitive radio technologies - spectrum sensing and spectral agility [39, 42]. The secondary system operates on the principle of "detect-and-avoid". Specifically, it monitors the wireless channel and transmits only in spectrum bands where no primary trans-

missions are determined to be present. Once a primary system transmission is detected in the spectrum band where a secondary system transmission is ongoing, the secondary system must switch to other vacant spectrum regions or cease transmission as soon as possible in order to avoid excess interference.

3.1.1 Spectrum Sensing

Due to its essential role in cognitive radio implementation, spectrum sensing has drawn much attention recently. In [57], collaborative spectrum sensing is proposed, and it was shown that the probability of detection for primary signal can be improved by allowing multiple secondary sensing terminals to share their local detection results. In [58], the authors showed that sensing sensitivity requirement can be greatly reduced through hard-decision based cooperation. In [59], a suboptimal data fusion rule for combining correlated observations of multiple secondary sensing terminals is proposed. It outperforms the simple counting fusion rule, which ignores the correlation, in terms of probability of detection. All the above works focused on enhancing the sensing capabilities of secondary system through cooperation among secondary spectrum sensing terminals. However, analysis of the spectrum efficiency for the secondary system, i.e., how much the secondary system is able to access the spectrum band for actual data transmission in the respective sensing protocols, is not provided.

In [83], the authors considered the allocation of sensing and transmission durations for the secondary system and showed that there exists a fundamental tradeoff between sensing capability and throughput performance of the secondary system. An optimal selection of the spectrum sensing duration is then proposed to maximize the achievable throughput for the secondary system under the constraint that the primary system is sufficiently protected with a target probability of detection. It is clearly demonstrated in [83] that a properly designed sensing-transmission protocol will improve the spectrum efficiency of the cognitive radio system.

3.1.2 Cognitive Relay System

The benefits of relaying, and more generally cooperative transmission, in wireless systems are widely recognized [3, 84]. Relaying techniques also form an integral

component of upcoming standards, e.g., IEEE 802.16j. These techniques are known to lead to better system performance and are used for spectrum efficiency enhancement, range extension, spatial diversity gain, etc. In Chapter 2, we discussed the improvement for spectrum efficiency and spatial diversity gain by using two-way cooperative relaying. Relaying in secondary systems is thus a natural extension [85, 86]. Therefore, instead of the point-to-point secondary system investigated in [83], in this chapter we consider a cognitive dual-hop relay system operating on a secondary spectrum sharing basis with a primary system, and propose sensing-transmission protocols for such a system.

In this chapter, we assume that the secondary system is operating in a half-duplex amplify-and-forward relaying mode [3], where the transmission from source S to destination D via relay R is accomplished in two transmission phases. In transmission phase 1, S transmits to D. The signal transmitted by S is also received by R, where it is amplified and forwarded to D in transmission phase 2, while S remains silent. Destination D combines the signals it received in the two transmission phases for decoding.

3.1.3 Cognitive Relay with Spectrum Sensing

3.1.3.1 Our Contributions

We consider two different spectrum sensing protocols for such a dual-hop relay system. A straightforward approach is to allocate a dedicated sensing period before transmission in each phase at S and R, respectively. The transmissions at S and R occur only when the respective sensing confirms the channel vacancy. We name this protocol as dedicated sensing protocol since dedicated sensing periods are required before transmissions. Dedicated sensing protocol is a straightforward extension from the simple periodic sensing protocol for a point-to-point secondary system in [83]. However, it leads to a substantial loss in spectrum efficiency for the secondary system since a fraction of each transmission phase has to be assigned for sensing, hence reducing the effective time for secondary data transmission.

In view of the spectrum efficiency loss in the dedicated sensing protocol, we propose an alternative sensing protocol which is named as simultaneous sensing protocol. First, note that (i) S has prior knowledge of the secondary signal that R

transmits in transmission phase 2, and (ii) S is silent in transmission phase 2 in the relaying protocol. These observations form the basis of our contributions. In the simultaneous sensing protocol, an initial sensing is performed at S to detect the presence of primary signal transmissions. If the channel is determined to be vacant, S transmits the secondary signal to R in transmission phase 1. R amplifies and forwards this signal to D without performing any spectrum sensing in transmission phase 2. While R is relaying the signal in transmission phase 2, S simultaneously performs sensing for the primary signal after canceling out the secondary signal component transmitted by R and known a priori by S. Note that no dedicated sensing period is required in the simultaneous sensing protocol and both S and R use the entire transmission phase for data transmission. Thus the spectrum efficiency loss for the secondary system in the dedicated sensing protocol can be recovered.

An energy detector is employed in the secondary system for detecting primary signal transmissions, with the goal of determining which of the hypotheses - primary signal present ($\mathcal{H}_1$) or absent ($\mathcal{H}_0$) is true. There are two reasons for choosing an energy detector. First, we are interested in the problem on how spectrum sensing and data transmission can be efficiently performed in a cognitive dual-hop relay system, and thus the choice of a specific detector is not critical. Second, an energy detector is easy to implement and it is a good choice for the detection of unknown signals over fading channels [56, 87].

Under $\mathcal{H}_1$, average collision time (ACT) is defined as the average time duration per transmission phase that secondary system transmits due to a miss-detection, thus resulting in a collision with primary system. A lower ACT indicates less interference caused to the primary system due to secondary access. On the other hand, under $\mathcal{H}_0$, average utilization time (AUT) is defined as the average time duration of secondary data transmission per transmission phase due to a correct identification of the channel vacancy. A larger AUT indicates a higher spectrum efficiency for the secondary system. In this chapter, we derive the average probability of detection for both the dedicated and simultaneous sensing protocols, and based on these results we analyze the ACT and AUT for the two sensing protocols. We also define an overall system utilization time (OSUT) which takes into account different priorities for the primary and secondary systems in a cognitive radio network.

We show that while a tradeoff between ACT and AUT exists in the dedicated sensing protocol due to the inherent tradeoff in the allocation of sensing and transmission time in each transmission phase, the simultaneous sensing protocol achieves a good balance between spectrum sensing capability and spectrum efficiency for the secondary system. Specifically, the simultaneous sensing protocol achieves a better performance in terms of both ACT and AUT as compared to the dedicated sensing protocol, when a small fraction of time in each transmission phase is assigned for sensing in the dedicated sensing protocol. On the other hand, when a long sensing time is used, the dedicated sensing protocol outperforms the simultaneous sensing protocol in terms of ACT. However, this is at the expense of a significant loss in AUT. Theoretical and simulation results also confirm that the simultaneous sensing protocol outperforms the dedicated sensing protocol in terms of OSUT.

3.1.3.2 Related Work

In [88, 89], the authors considered a similar system model where the secondary system is a dual-hop relay system which consists of two cognitive transmitters and one receiver. In particular, by allowing the cognitive transmitter (relay) which is located nearer to the primary transmitter to serve as a relay for the other cognitive transmitter (source), the authors showed that the overall sensing performance can be improved compared to the case where the two cognitive transmitters perform spectrum sensing independently. There are several important differences between our work and the one in [88, 89].

First, the objectives are different. In [88, 89], the authors' main aim is to reduce the overall detection time for the primary signal by exploiting cooperative diversity gain. However, the spectrum efficiency for the secondary system is not discussed. On the other hand, in this chapter we consider both detection performance and spectrum efficiency of the cognitive relay system, and analyze the ACT, AUT, and OSUT for both dedicated and simultaneous sensing protocols. Second, the signal processing at the relay terminal is different. In [88, 89], the relay terminal forwards whatever it receives even if the source terminal does not transmit. In the proposed simultaneous protocol, the relay terminal only forwards when the pilot detection is successful. Third, in [88, 89] the forwarded secondary signal component is assumed

to be perfectly canceled out before spectrum sensing is performed at the source terminal. However, in our proposed simultaneous protocol, a more realistic scenario where imperfect cancelation caused by the interference from primary system is considered.

3.2 System Model

The incomplete Gamma function is given by

$$\Gamma(a,b) = \int_b^\infty e^{-t} t^{a-1} dt,$$

and $\Gamma(a,0) = \Gamma(a)$. The generalized Marcum-Q function $Q_\Lambda(a,b)$ is defined as

$$Q_\Lambda(a,b) = \frac{1}{a^{\Lambda-1}} \int_b^\infty x^\Lambda e^{-\frac{x^2+a^2}{2}} I_{\Lambda-1}(ax) dx$$

where $I_{(\cdot)}(\cdot)$ is the modified Bessel function of the first kind. The probability density function of a chi-square distributed random variable $y \sim \mathcal{X}^2_\Omega$ is given by

$$f_Y(y) = \frac{1}{2^{\frac{\Omega}{2}}\Gamma(\frac{\Omega}{2})} y^{\frac{\Omega}{2}-1} e^{-\frac{y}{2}}, \quad y \geq 0.$$

The probability density function of a non-central chi-square distributed random variable $z \sim \mathcal{X}^2_\Omega(\lambda)$ is given by

$$f_Z(z) = \frac{1}{2} e^{-\frac{(z+\lambda)}{2}} \left(\frac{z}{\lambda}\right)^{\frac{\Omega}{4}-\frac{1}{2}} I_{\frac{\Omega}{2}-1}(\sqrt{\lambda z}), \quad z \geq 0.$$

The system configuration is shown in Figure 3.1. We denote the primary transmitter and receiver as PT and PR, respectively. The secondary source S and relay R are within the same sensing environment[1]. The channels over links PT→S, PT→R, S→R, and R→S are modeled to be Rayleigh flat fading with channel coefficients denoted by h_{ps}, h_{pr}, h_{sr}, and h_{rs} respectively. Thus we have $h_{ab} \sim \mathcal{CN}(0, \phi_{ab})$, where

[1]This means that when primary transmission is absent, it applies for both S and R. Likewise, when primary transmission is present, it applies for both S and R. This condition always holds true, regardless of the geographic distances PT→S and PT→R, because electromagnetic wave propagation from PT is continuous and does not stop abruptly.

ab denotes the relevant subscripts and ϕ_{ab} denotes the average channel gains of the corresponding links. Instantaneous channel gains of the respective links are denoted as $\gamma_{ab} = |h_{ab}|^2$. Assuming channel reciprocity, we have $\gamma_{sr} = \gamma_{rs}$. The additive white Gaussian noise (AWGN) at S and R is denoted as $n_s \sim \mathcal{CN}(0, \sigma^2)$ and $n_r \sim \mathcal{CN}(0, \sigma^2)$, respectively.

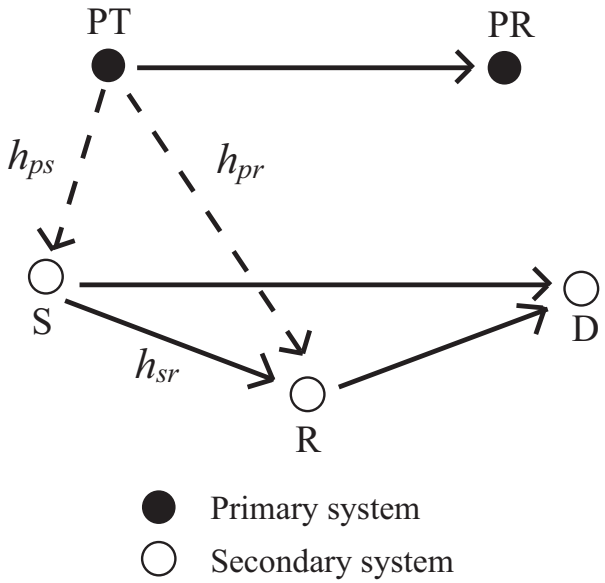

Figure 3.1. Cognitive dual-hop relay system.

For ease of exposition, we divide the continuous time duration under consideration into time slots. Each time slot is equivalent to one transmission phase of the secondary system, which is normalized to unitary without loss of generality. In the following, we shall often use "slot" and "phase" interchangeably and all channel coefficients are assumed to be constant within a time slot. One primary packet is transmitted from PT to PR in one time slot with power P_p when the primary system is active. Similarly, one secondary packet is transmitted from S to R in one time slot with power P_s when the secondary system is active. We also assume that each primary and secondary packet contains K complex symbols.

We focus on two consecutive time slots, i.e., a pair of time slots, which is the time duration required for accomplishing one secondary transmission from S to D via R. We denote the τth symbol of PT in transmission phase ψ as $x_p^{\psi}(\tau)$, where $\psi \in \{1, 2\}$ and $\tau \in \{1, 2, \cdots, K\}$. For simplicity of derivation, we assume that $x_p^{\psi}(\tau)$ is an M-PSK symbol, i.e., $x_p^{\psi}(\tau) = e^{j\frac{2\pi m}{M_1}}$, where $m \in \{0, 1, \cdots, M_1 - 1\}$, and thus

$|x_p^{\psi}(\tau)|^2 = 1$. The τth symbol of S is denoted as $x_s(\tau)$, where $\tau \in \{1, 2, \cdots, K\}$. Similarly, we assume that $x_s(\tau)$ is an M-PSK symbol, i.e., $x_s(\tau) = e^{j\frac{2\pi m}{M_2}}$, where $m \in \{0, 1, \cdots, M_2 - 1\}$, and thus $|x_s(\tau)|^2 = 1$. R amplifies the received signal with power amplification factor g and then forwards it to D in transmission phase 2. Note that the choice of g is arbitrary, and here we let $g = \sqrt{\frac{1}{\gamma_{sr}}}$ without loss of generality[2] [90].

Remark: Note that with modulations having unequal power distribution, e.g. 16QAM and 64QAM, the transmitted primary signal power may vary from symbol to symbol, i.e. $|x_p^1(l)|^2 \neq |x_p^1(k)|^2$, when the lth and kth symbols have different distances to the origin in the constellation. In this case, the specific constellation needs to be taken into consideration for analyzing the detection probability, which will significantly complicate the derivation. Since this issue is not related to the main idea of the proposed spectrum sensing scheme in this chapter, the constellation with equal power distribution (M-PSK) is considered for simplicity and conciseness. However, it is worth emphasizing that this assumption does not restrict application of the proposed scheme to general cases where an arbitrary constellation might be used.

3.3 Dedicated Sensing Protocol

A straightforward sensing protocol for the secondary system can be obtained by periodically incorporating dedicated sensing periods in the two-phase relaying protocol, as depicted in Figure 3.2, where the shaded blocks represent periods during which spectrum sensing is performed at S and R. In transmission phase 1, sensing is first performed at S and if no primary signal transmission is detected, S transmits to R and D. Otherwise, S remains silent. In the meantime, R determines whether a secondary signal is received by detecting the pilot signal of the secondary system[3]. This pilot detection is successful if and only if S transmits in transmission phase 1. If a secondary signal is received by R, the received signal is amplified

[2]The assumptions of M-PSK symbols and $g = \sqrt{\frac{1}{\gamma_{sr}}}$ are made purely for mathematical tractability and do not restrict the application of the sensing protocols under consideration.

[3]We assume that pilot signal detection is robust against fading and interference, and thus pilot detection at R always succeeds if S transmits in transmission phase 1.

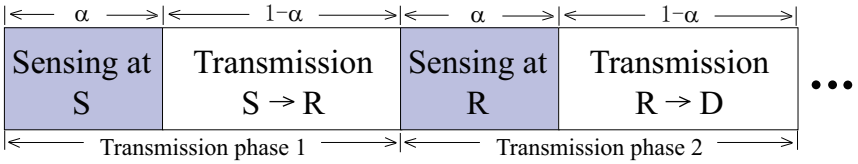

(a)

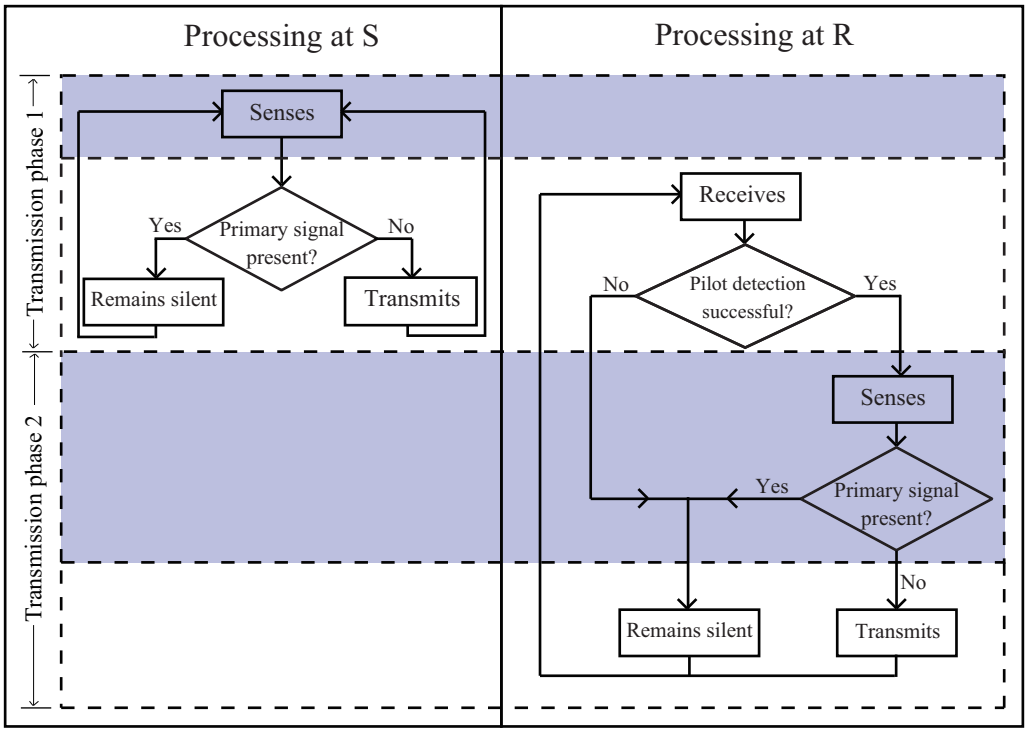

(b)

Figure 3.2. Diagram and flowchart for dedicated sensing protocol.

and stored in the buffer of R, otherwise the buffer remains empty. In transmission phase 2, sensing is first performed at R and if no primary signal transmission is detected, R forwards the secondary signal in its buffer (if any) to D. Otherwise, R remains silent. R empties its buffer at the end of transmission phase 2. Since both S and R transmit only after spectrum sensing confirms a channel vacancy, dedicated sensing periods are needed at both terminals, and this leads to a loss in spectrum efficiency for the secondary system.

For the sensing protocol described above, it is worth mentioning the following

two points.

1) In a practical relay system, performing pilot detection for the secondary signal at R before relaying is a logical and important task. This is especially true in the cognitive radio scenario where we do not want R to relay indiscriminately when S did not transmit in transmission phase 1, and risk causing interference to the primary system without any contribution to the secondary system.

2) Pilot detection at R is assumed to be always successful when S transmits in transmission phase 1. In practical systems, pilot signals are usually well protected by robust modulation and are known a priori by the intended receiver. Thus the detection and identification of the pilot signals at R will be very robust against fading when primary signal does not exist. On the other hand, when primary signal is present as interference, a failure of pilot detection at R will actually provide more protection to the primary system, since R will remain silent in transmission phase 2. Thus the assumption of successful pilot detection as long as S had transmitted is reasonable for evaluating the dedicated sensing protocol since it will lead to a conservative lower bound for the sensing performance and spectrum utilization[4].

3.3.1 Detection Performance

Let $0 < \alpha < 1$ denote the fraction of one time slot that is devoted to sensing. The same sensing duration α is applied at both S and R, and N_d number of samples are collected over this duration. For simplicity of derivation, we assume that the sampling rate is equal to the primary symbol rate, thus $N_d = \lfloor \alpha K \rfloor$ and only one sample is collected from a single primary symbol.We will first analyze the detection performance at S.

Under the hypotheses $\mathcal{H}_0$ and $\mathcal{H}_1$, the lth sample received at S is given by

$$s(l) = \begin{cases} n_s(l) & \mathcal{H}_0 \\ \sqrt{P_p} h_{ps} x_p^1(l) + n_s(l) & \mathcal{H}_1 \end{cases} \tag{3.1}$$

where $n_s(l)$ is the lth sample of n_s, and $l \in \{1, 2, \cdots, N_d\}$.

Remark: It is worth mentioning that (3.1) does not indicate synchronization between the primary and secondary systems. In this chapter, we assume rectangu-

[4]This is also true for the simultaneous sensing protocol.

lar signal pulse, and thus the variation of sampling point due to asynchronization between the primary and secondary systems does not affect the energy of collected samples and hence the detection probability. Therefore, we use $x_p^1(l)$ to denote a sample of of the lth transmitted primary signal pulse (not necessarily at the optimal sampling point) for simplicity of notation.

The energy detector differentiates between hypotheses $\mathcal{H}_0$ and $\mathcal{H}_1$ based on the detection statistic

$$D_d = \frac{1}{\sigma^2} \sum_{l=1}^{N_d} |s(l)|^2.$$

Letting $D'_d = 2D_d$, it is then easy to show that $D'_d \sim \mathcal{X}^2_{2N_d}$ under $\mathcal{H}_0$ [56]. Thus the probability of false alarm is given as

$$P_{fa}^d = \Pr\{D_d > \zeta_d \mid \mathcal{H}_0\} = \Pr\{D'_d > 2\zeta_d \mid \mathcal{H}_0\} = \frac{\Gamma(N_d, \zeta_d)}{\Gamma(N_d)} \tag{3.2}$$

where ζ_d is the detection threshold. Note that P_{fa}^d only depends on the detection threshold ζ_d and the number of samples N_d. It is independent of the channel and primary signal. In practice, given N_d and a target probability of false alarm P_{fa}^d, we can calculate the required ζ_d from (3.2).

We can also easily show that $D'_d \sim \mathcal{X}^2_{2N_d}\left(\frac{2P_pN_d\gamma_{ps}}{\sigma^2}\right)$ under hypothesis $\mathcal{H}_1$ [56]. Therefore, the probability of detection at S, conditioned on γ_{ps}, is given by

$$P_d^{d,s}|_{\gamma_{ps}} = \Pr\{D_d > \zeta_d \mid \mathcal{H}_1, \gamma_{ps}\} = Q_{N_d}\left(\sqrt{\frac{2P_pN_d\gamma_{ps}}{\sigma^2}}, \sqrt{2\zeta_d}\right). \tag{3.3}$$

Note that $\gamma_{ps} \sim \mathcal{E}(\phi_{ps})$, thus averaging across γ_{ps}, the probability of detection at S is given by

$$\begin{aligned} P_d^{d,s} &= \int_0^\infty Q_{N_d}\left(\sqrt{\frac{2P_pN_d\gamma_{ps}}{\sigma^2}}, \sqrt{2\zeta_d}\right) \frac{1}{\phi_{ps}} e^{-\frac{\gamma_{ps}}{\phi_{ps}}} d\gamma_{ps} \\ &= J\left(N_d, \frac{P_pN_d\phi_{ps}}{\sigma^2}, 2\zeta_d\right). \end{aligned} \tag{3.4}$$

The closed-form expression for $J(\Lambda, \rho, \eta)$ is [87]

$$J(\Lambda, \rho, \eta) = e^{-\frac{\eta}{2(\rho+1)}} + \frac{e^{-\frac{\eta}{2}}}{\rho+1} \sum_{n=1}^{\Lambda-1} \frac{\eta^n}{2^n n!} {}_1F_1\left(1; n+1; \frac{\eta\rho}{2(1+\rho)}\right) \quad (3.5)$$

where ${}_1F_1(\cdot,\cdot,\cdot)$ is the confluent hypergeometric function [75, Eq.(9.210.1)].

Relay R also collects N_d samples for sensing and n_r has the same variance as n_s. Fixing the probability of false alarm to be equal to P_{fa}^d given in (3.2) and following the same derivations as above, the probability of detection at R is given by

$$P_d^{d,r} = J\left(N_d, \frac{P_p N_d \phi_{pr}}{\sigma^2}, 2\zeta_d\right). \quad (3.6)$$

In transmission phase 1, if S successfully detects the primary signal and remains silent, R will also remain silent in transmission phase 2 as it is not able to detect the pilot. This means that conditioned on the successful detection at S, the probability of detection at R is 1. On the other hand, if S misdetects, R will detect the pilot from S and decides whether to transmit or not in transmission phase 2 based on its own sensing decision. Thus the average probability of detection across the two transmission phases is given by

$$P_d^d = \frac{1}{2}\left(P_d^{d,s} + P_d^{d,s} + P_d^{d,r}\left(1 - P_d^{d,s}\right)\right) = \frac{1}{2}P_d^{d,r}\left(1 - P_d^{d,s}\right) + P_d^{d,s}. \quad (3.7)$$

3.3.2 Average Collision Time

In the following, we derive the ACT for the dedicated sensing protocol under $\mathcal{H}_1$. Since spectrum sensing and data transmission in different pairs of time slots are performed identically and independently, we only need to focus on one pair of time slots.

In the first time slot, data transmission from S lasting $(1-\alpha)$ of a time slot occurs only when spectrum sensing fails to detect the primary signal, which has a probability of $\left(1 - P_d^{d,s}\right)$. Thus the ACT of the first time slot is given by

$$C_1^d = (1-\alpha)\left(1 - P_d^{d,s}\right).$$

For the second time slot, a collision happens when spectrum sensing at both S and

R fails to detect the primary signal, which has a probability of $\left(1-P_d^{d,s}\right)\left(1-P_d^{d,r}\right)$. Since transmission from R also lasts $(1-\alpha)$ of a time slot, the ACT of the second time slot is given by

$$C_2^d = (1-\alpha)\left(1-P_d^{d,s}\right)\left(1-P_d^{d,r}\right).$$

Averaging across the first and second time slots, the overall ACT of the dedicated sensing protocol is therefore given by

$$C^d = \frac{C_1^d + C_2^d}{2} = \frac{1}{2}(1-\alpha)\left(1-P_d^{d,s}\right)\left(2-P_d^{d,r}\right). \tag{3.8}$$

It is clear from (3.8) that C^d decreases with increasing α, $P_d^{d,s}$, and $P_d^{d,r}$. With a fixed P_{fa}^d, a longer sensing time (i.e., larger α) leads to a higher probability of detection at S and R, and also a reduced possible collision time given by $(1-\alpha)$ of a time slot. Thus with the dedicated sensing protocol, the primary system suffers less interference when a larger α is used at S and R.

3.3.3 Average Utilization Time

In the following, we derive the AUT for the dedicated sensing protocol under $\mathcal{H}_0$. Similarly, we only need to focus on one pair of time slots. In the first time slot, spectrum sensing lasting α of a time slot is first performed at S. Transmission from S to R happens only when the spectrum sensing correctly detects the channel vacancy, which has a probability of $\left(1-P_{fa}^d\right)$. Since only $(1-\alpha)$ of a time slot can be used for data transmission, the AUT in the first time slot is given by

$$U_1^d = (1-\alpha)\left(1-P_{fa}^d\right).$$

For the second time slot, secondary access is possible only if S transmits in the first time slot and spectrum sensing at R also confirms the channel vacancy, which has a probability of $\left(1-P_{fa}^d\right)^2$. Thus the AUT in the second time slot is given by

$$U_2^d = (1-\alpha)\left(1-P_{fa}^d\right)^2.$$

Averaging across the two time slots, the overall AUT of the dedicated sensing protocol is therefore

$$U^d = \frac{U_1^d + U_2^d}{2} = \frac{(1-\alpha)}{2}\left[\left(1 - P_{fa}^d\right) + \left(1 - P_{fa}^d\right)^2\right]. \tag{3.9}$$

It can be observed from (3.9) that given a target probability of false alarm P_{fa}^d, U^d decreases with increasing α.

3.3.4 Overall System Utilization Time

Comparing (3.8) and (3.9), it is clear that although a large α reduces the interference to the primary system, it also leads to a significant spectrum efficiency loss to the secondary system. In the following, we derive an overall system utilization time which takes the performance of both primary and secondary systems, as well as their different priorities in a cognitive radio network, into consideration.

The OSUT of the dedicated sensing protocol is defined as

$$G^d \triangleq w_p\left(1 - C^d\right) + (1 - w_p)U^d, \tag{3.10}$$

where the first and second terms characterize the performance of the primary and secondary systems respectively. Weighting factors for the primary and secondary systems are denoted as w_p and $(1 - w_p)$ respectively, where $0 \leq w_p \leq 1$. By adjusting w_p, different priorities are given to the primary and secondary systems. In a practical cognitive radio system, the primary system has a higher priority, thus in general we have $w_p > \frac{1}{2}$. The actual selection of w_p can be predefined by regulatory bodies, or it can be decided through negotiations between the primary and secondary systems regarding Quality of Service (QoS) requirements, spectrum sharing gains, and the remunerations that the secondary system is willing to pay for accessing the spectrum band [91, 92]. Since both C^d and U^d decrease with increasing α, there is a tradeoff between the primary and secondary systems by varying α. Note that a similar tradeoff was also observed in a point-to-point secondary system scenario [83]. We will show in Section 3.5 by simulations that there exists an optimal value for α such that G^d is maximized.

3.4 Simultaneous Sensing Protocol

The illustrative diagram and flowchart for the simultaneous sensing protocol are shown in Figure 3.3 (a) and (b) respectively, where the shaded blocks represent transmission phase 2 during which spectrum sensing is performed at S.

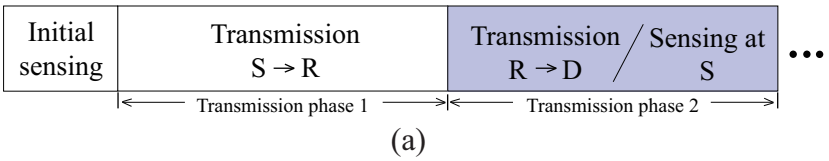

(a)

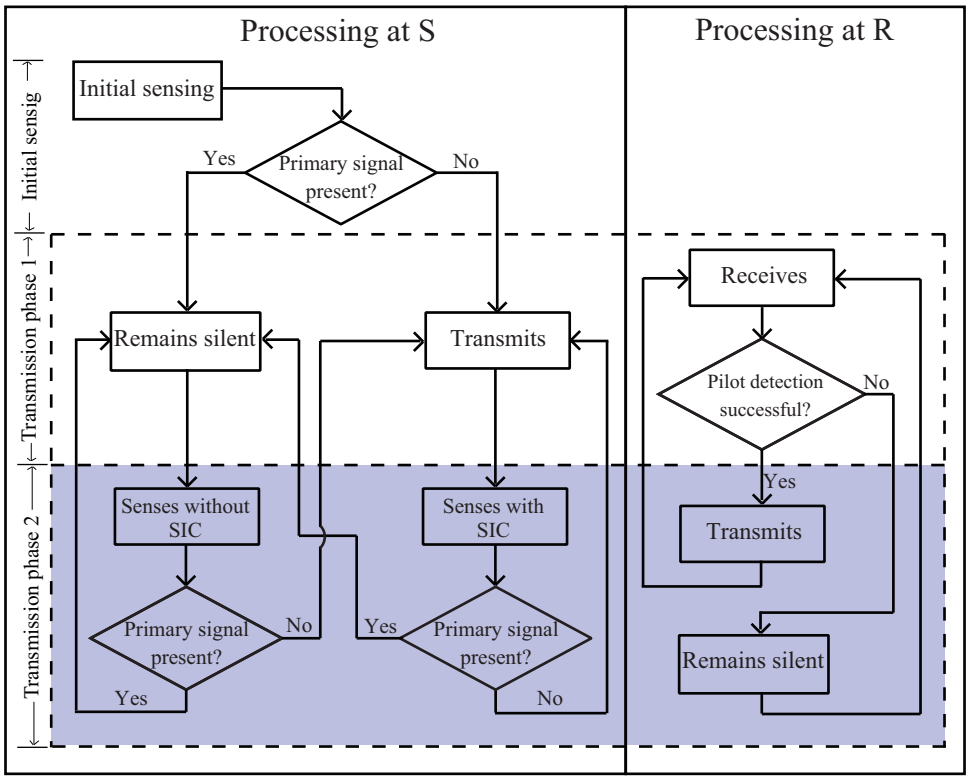

(b)

Figure 3.3. Diagram and flowchart for simultaneous sensing protocol.

In the simultaneous sensing protocol, an initial sensing is first performed at S during transmission setup. If no primary signal is detected, S transmits to R and D, otherwise S remains silent. In the meantime, R determines whether a secondary signal is received or not by detecting the pilot signal of the secondary

system. Similar to the dedicated sensing protocol, pilot detection is assumed to be successful if and only if S transmits in transmission phase 1. If the pilot is detected, R amplifies and forwards the signal it received to D in transmission phase 2, *without* any spectrum sensing. Otherwise R remains silent. The signal overheard by S in transmission phase 2 is then a combination of the primary signal transmitted by PT (if it exists), signal transmitted by R (if it exists) and AWGN. Note that the signal transmitted by R in transmission phase 2 will contain the primary signal component if both PT and S were active in transmission phase 1.

We first analyze the probability of detection for the simultaneous sensing protocol. There are two sensing scenarios to be considered. In Sensing Scenario 1, S remains silent in transmission phase 1 and hence knows that no secondary signal component will be present in transmission phase 2. Thus S directly performs sensing for the primary signal based on the signal it receives in transmission phase 2. On the other hand, in Sensing Scenario 2, S transmits in transmission phase 1 and performs sensing for the primary signal in transmission phase 2 after canceling out the secondary signal component (self-interference cancelation), which is known a priori by S. For both the sensing scenarios above, if no primary signal is determined to be present, S transmits in the next transmission phase. Otherwise, S remains silent.

It is clear that in the simultaneous sensing protocol, periodic sensing for the primary signal is performed at S during the time slots when R is supposed to transmit, thus removing the additional overhead incurred by dedicated sensing periods which are needed in the dedicated sensing protocol.

3.4.1 Detection Performance

We will first consider the detection performance of the simultaneous sensing protocol for the two sensing scenarios separately. Let N_s denote the number of samples collected for detection. We again assume that the sampling rate is equal to the symbol rate and note that S performs sensing over the entire transmission phase 2, thus $N_s = K$.

Sensing Scenario 1: S remains silent in transmission phase 1.

In this scenario, pilot detection at R fails due to the absence of secondary

signal in transmission phase 1 and accordingly, R remains silent in transmission phase 2. S knows a priori that no secondary signal component will be present in transmission phase 2, thus it directly performs sensing without self-interference cancelation (SIC). The detection probability for primary signal can be similarly obtained by following the derivations in Section 3.3. The only difference is that the number of samples collected for sensing is N_s, instead of N_d for the dedicated sensing protocol[5]. Thus the probability of detection under Sensing Scenario 1 is given by

$$P_d^{s,1} = J\left(N_s, \frac{P_p N_s \phi_{ps}}{\sigma^2}, 2\zeta_{s,1}\right) \tag{3.11}$$

where the detection threshold $\zeta_{s,1}$ can be computed from

$$P_{fa}^{s,1} = \frac{\Gamma(N_s,\ \zeta_{s,1})}{\Gamma(N_s)}, \tag{3.12}$$

given N_s and a target probability of false alarm $P_{fa}^{s,1}$.

Sensing Scenario 2: S transmits in transmission phase 1.

In this scenario, signal transmitted by S in transmission phase 1 is forwarded by R and received by S in transmission phase 2, presenting as self-interference to the secondary system. Thus, SIC is needed before spectrum sensing can be performed at S. Similar to Sensing Scenario 1, N_s samples are collected at S over transmission phase 2 for sensing.

Under $\mathcal{H}_0$, the lth sample of signal received at S in transmission phase 2, where $l \in \{1, 2, \cdots, K\}$, is given by

$$y_{s,0}(l) = \sqrt{P_s}\Delta x_s(l) + n'_s(l). \tag{3.13}$$

where $\Delta = g h_{sr} h_{rs}$, and $n'_s(l)$ denotes the lth sample of $n'_s \triangleq g h_{rs} n_r + n_s$.

Lemma 1. *Noise $n'_s(l)$ is Gaussian distributed with variance $2\sigma^2$, i.e., $n'_s(l) \sim \mathcal{CN}(0, 2\sigma^2)$.*

Proof: Note that

$$n'_s(l) = g h_{rs} n_r(l) + n_s(l),$$

[5]Note that $N_d = \lfloor \alpha K \rfloor$, where $0 < \alpha < 1$, and hence $N_d < N_s$.

where $n_r(l)$ and $n_s(l)$ denote the lth sample of n_r and n_s respectively. Since $h_{rs} \sim \mathcal{CN}(0, \phi_{rs})$, we have $h_{rs} = |h_{rs}|e^{j\theta_{rs}}$, where $\theta_{rs} \sim \mathcal{U}(0, 2\pi)$ denotes the argument of h_{rs} and the amplitude $|h_{rs}| = \sqrt{\gamma_{rs}} = \sqrt{\gamma_{sr}}$ follows a Rayleigh distribution. Since $g = \sqrt{\frac{1}{\gamma_{sr}}}$, we obtain

$$gh_{rs} = e^{j\theta_{rs}}.$$

The AWGN $n_r(l)$ can also be expressed as $n_r(l) = \sigma e^{j\theta_{n_r}}$, where $\theta_{n_r} \sim \mathcal{U}(0, 2\pi)$ denotes the argument of $n_r(l)$. Therefore, we have $gh_{rs}n_r(l) = \sigma e^{j\theta'}$, where $\theta' = \theta_{rs} + \theta_{n_r}$. It is clear that $\theta' \sim \mathcal{U}(0, 2\pi)$, thus $gh_{rs}n_r(l)$ is also AWGN with variance σ^2. Furthermore, since $n_s(l)$ is also AWGN with variance σ^2, we have $n'_s(l) \sim \mathcal{CN}(0, 2\sigma^2)$. This concludes the proof.

■

Note that the variance of n'_s is increased compared to that of n_s due to the AF relaying at R. Since P_s and $x_s(l)$ are known a priori, S is able to estimate the product channel Δ by making use of the self-interference component $\sqrt{P_s}\Delta x_s(l)$. Since $n'_s(l)$ is Gaussian distributed, the minimum variance unbiased estimation (MVUE) for Δ is given by [93]

$$\widehat{\Delta}_0 = \frac{\sum_{i=1}^{N_s} x_s(i)^* y_{s,0}(i)}{\sqrt{P_s}\sum_{i=1}^{N_s}|x_s(i)|^2} = \frac{1}{N_s\sqrt{P_s}}\sum_{i=1}^{N_s} x_s(i)^* y_{s,0}(i) \tag{3.14}$$

where we use the fact that $|x_s(i)|^2 = 1$. The estimation error under $\mathcal{H}_0$ is thus given by

$$\epsilon_0 = \Delta - \widehat{\Delta}_0 = -\frac{1}{N_s\sqrt{P_s}}\sum_{i=1}^{N_s} x_s(i)^* n'_s(i). \tag{3.15}$$

Thus S is able to use $\widehat{\Delta}_0$ to cancel out the self-interference component and obtain

$$\begin{aligned} y_{s,0}(l)' &= y_{s,0}(l) - \sqrt{P_s}\widehat{\Delta}_0 x_s(l) = \sqrt{P_s}\epsilon_0 x_s(l) + n'_s(l) \\ &= \left(1 - \frac{1}{N_s}\right) n'_s(l) - \frac{x_s(l)}{N_s}\sum_{i=1, i\neq l}^{N_s} x_s(i)^* n'_s(i). \end{aligned} \tag{3.16}$$

Noting the fact that $n'_s(l) \sim \mathcal{CN}(0, 2\sigma^2)$ from Lemma 1, it is straightforward that

$$y_{s,0}(l)' \sim \mathcal{CN}\left(0, \frac{2\sigma^2(N_s-1)}{N_s}\right).$$

The energy detection statistic is given by $D_s = \frac{1}{\sigma^2}\sum_{l=1}^{N_s} |y_{s,0}(l)'|^2$. Let $D'_s = \frac{N_s}{N_s-1}D_s$, and it is clear that $D'_s \sim \mathcal{X}^2_{2N_s}$. The probability of false alarm is thus given by

$$P_{fa}^{s,2} = \Pr\{D_s > \zeta_{s,2} |\ \mathcal{H}_0\} = \Pr\left\{D'_s > \frac{N_s\zeta_{s,2}}{N_s-1} |\ \mathcal{H}_0\right\} = \frac{\Gamma\left(N_s, \frac{N_s\zeta_{s,2}}{2(N_s-1)}\right)}{\Gamma(N_s)} \quad (3.17)$$

where $\zeta_{s,2}$ is the detection threshold.

Next, under $\mathcal{H}_1$, the lth sample of signal received at R in transmission phase 1, where $l \in \{1, 2, \cdots, N_s\}$, is given by

$$y_{r,1}(l) = \sqrt{P_s}h_{sr}x_s(l) + \sqrt{P_p}h_{pr}x_p^1(l) + n_r(l) \quad (3.18)$$

where $n_r(l)$ is the lth sample of n_r. The lth sample of signal received by S in transmission phase 2 is thus given by

$$y_{s,1}(l) = \sqrt{P_s}\Delta x_s(l) + \sqrt{P_p}gh_{pr}h_{rs}x_p^1(l) + \sqrt{P_p}h_{ps}x_p^2(l) + n'_s(l). \quad (3.19)$$

We denote $\widetilde{n}_s(l) = \sqrt{P_p}gh_{pr}h_{rs}x_p^1(l) + \sqrt{P_p}h_{ps}x_p^2(l) + n'_s(l)$, and following the same derivations in Lemma 1, it can be shown that $\widetilde{n}_s(l) \sim \mathcal{CN}(0, P_p(\phi_{ps}+\phi_{pr}) + 2\sigma^2)$. Similarly, S estimates Δ by using the MVUE

$$\widehat{\Delta}_1 = \frac{1}{N_s\sqrt{P_s}}\sum_{l=1}^{N_s} x_s(l)^* y_{s,1}(l). \quad (3.20)$$

Thus the signal at S after SIC is given by

$$y_{s,1}(l)' = \sqrt{P_s}\epsilon_1 x_s(l) + \widetilde{n}_s(l), \quad (3.21)$$

where $\epsilon_1 = \Delta - \widehat{\Delta}_1$ denotes the estimation error under $\mathcal{H}_1$.

The energy detection statistic is thus given by $D_s = \frac{1}{\sigma^2}\sum_{l=1}^{N_s} |y_{s,1}(l)'|^2$. It is

clear that $D'_s \sim \mathcal{X}^2_{2N_s}\left(\frac{P_p N_s \gamma}{\sigma^2}\right)$, where $\gamma \sim \mathcal{E}(\phi)$, and $\phi = \phi_{ps} + \phi_{pr}$. The probability of detection, conditioned on γ, is given by

$$P_d^{s,2}|_\gamma = \Pr\left\{ D'_s > \frac{N_s \zeta_{s,2}}{N_s - 1} \middle| \, \mathcal{H}_1, \, \gamma \right\} = Q_{N_s}\left(\sqrt{\frac{P_p N_s \gamma}{\sigma^2}}, \sqrt{\frac{N_s \zeta_{s,2}}{N_s - 1}} \right). \quad (3.22)$$

Averaging across γ, the probability of detection under Sensing Scenario 2 is given by

$$P_d^{s,2} = \int_0^\infty Q_{N_s}\left(\sqrt{\frac{P_p N_s \gamma}{\sigma^2}}, \sqrt{\frac{N_s \zeta_{s,2}}{N_s - 1}} \right) \frac{e^{-\frac{\gamma}{\phi}}}{\phi} d\gamma = J\left(N_s, \frac{P_p N_s \phi}{2\sigma^2}, \frac{N_s \zeta_{s,2}}{N_s - 1} \right) \quad (3.23)$$

It is worth mentioning that spectrum sensing with SIC in a two-user cognitive radio network was investigated in [88], where the SIC is assumed to be perfect, regardless of the presence of primary signal. In [63], we have also derived the probability of detection for the simultaneous sensing protocol when SIC at S is presumed to be perfect. However, as shown above, in this chapter we have considered a more realistic scenario where imperfect SIC caused by channel estimation error is considered.

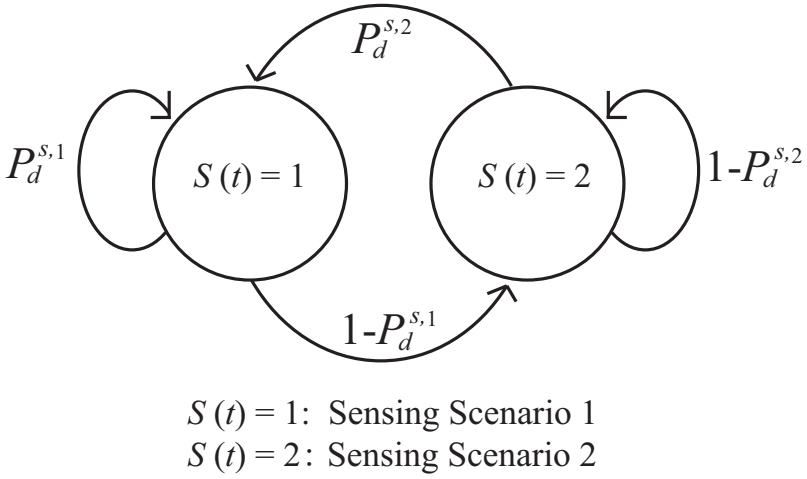

Figure 3.4. State transition graph of Markov chain $S(t)$.

We denote the sensing state at S in sensing slot t as $S(t)$, and $S(t) = 1$, $S(t) = 2$ denote Sensing Scenario 1 and 2, respectively. It is clear that $S(t)$, $t = 1, 2, 3, \cdots$ forms a Markov chain of order 1 [76], i.e., the sensing scenario in the current sensing

slot only depends on the previous sensing scenario. We show the state transition graph of this Markov chain in Figure 3.4. The transition matrix is given by

$$\boldsymbol{P} = \begin{bmatrix} P_d^{s,1} & 1 - P_d^{s,1} \\ P_d^{s,2} & 1 - P_d^{s,2} \end{bmatrix} \tag{3.24}$$

where the (i,j)th element of $\boldsymbol{P}$ is defined as $P_{i,j} = \Pr\{S(t+1) = j | S(t) = i\}$, and $i, j \in \{1, 2\}$. It is easy to derive the stationary distribution of $S(t),\ t = 1, 2, 3, \cdots$ as

$$\boldsymbol{\pi} = \begin{bmatrix} \pi_1, \pi_2 \end{bmatrix}, \tag{3.25}$$

where $\pi_1 = \frac{P_d^{s,2}}{1 - P_d^{s,1} + P_d^{s,2}}$ and $\pi_2 = \frac{1 - P_d^{s,1}}{1 - P_d^{s,1} + P_d^{s,2}}$.

The average probability of detection with the simultaneous sensing protocol is thus given by

$$P_d^s = \pi_1 P_d^{s,1} + \pi_2 P_d^{s,2} = \frac{P_d^{s,2}}{1 - P_d^{s,1} + P_d^{s,2}}. \tag{3.26}$$

Comparing (3.12) and (3.17), and letting $P_{fa}^{s,1} = P_{fa}^{s,2} (\triangleq P_{fa}^s)$, we have $\frac{2(N_s - 1)}{N_s} \zeta_{s,1} = \zeta_{s,2}$. Substituting (3.11), (3.23), and $\frac{2(N_s - 1)}{N_s} \zeta_{s,1} = \zeta_{s,2}$ into (3.26), we have

$$P_d^s = \frac{J\left(N_s, \frac{P_p N_s (\phi_{ps} + \phi_{pr})}{2\sigma^2}, 2\zeta_s\right)}{1 - J\left(N_s, \frac{P_p N_s \phi_{ps}}{\sigma^2}, 2\zeta_s\right) + J\left(N_s, \frac{P_p N_s (\phi_{ps} + \phi_{pr})}{\sigma^2}, 2\zeta_s\right)} \tag{3.27}$$

where the detection threshold ζ_s is calculated from $P_{fa}^s = \frac{\Gamma(N_s,\ \zeta_s)}{\Gamma(N_s)}$, given N_s and a target probability of false alarm P_{fa}^s.

3.4.2 Average Collision Time

In the first time slot, transmission is from S to R, and hence a collision, only occurs when spectrum sensing in the previous sensing slot fails to detect the primary signal, which has a probability of $(1 - P_d^s)$. Furthermore, we note that when the secondary system is active, S transmits in the entire first time slot. Thus the ACT of the first time slot is given by

$$C_1^s = (1 - P_d^s).$$

For the second time slot, a collision happens when S transmits in the first time slot, which has a probability of $(1 - P_d^s)$. Again, R transmits in the entire second time slot when it is active. Thus the ACT of the second time slot is also given by

$$C_2^s = (1 - P_d^s)\,.$$

The overall ACT of the simultaneous sensing protocol is therefore given by

$$C^s = \frac{C_1^s + C_2^s}{2} = 1 - P_d^s. \tag{3.28}$$

We can observe from (3.8) that C^d decreases with α and $C^d = 0$ with $\alpha = 1$. Thus with $\alpha > \alpha^*$ where α^* is a certain threshold, we have $C^d < C^s$. This indicates that the dedicated sensing protocol is capable of better protecting the primary system in terms of ACT with a large α. This will however lead to a lower AUT for the secondary system.

3.4.3 Average Utilization Time

Transmission from S to R occurs when spectrum sensing in the previous sensing slot correctly determines the channel vacancy, which has a probability of $\left(1 - P_{fa}^s\right)$. Since S uses the entire first time slot for data transmission, the AUT in the first time slot is given by

$$U_1^s = \left(1 - P_{fa}^s\right).$$

For the second time slot, R transmits as long as S transmits in the first time slot, which has a probability of $\left(1 - P_{fa}^s\right)$. Noting R also transmits for the entire second time slot when it is active, the AUT in the second time slot is also given by

$$U_2^s = \left(1 - P_{fa}^s\right).$$

The overall AUT of the simultaneous sensing protocol is therefore given by

$$U^s = \frac{U_1^s + U_2^s}{2} = 1 - P_{fa}^s. \tag{3.29}$$

It is obvious from (3.29) that U^s decreases with increasing P_{fa}^s. Comparing (3.9) and (3.29) and letting $P_{fa}^d = P_{fa}^s \neq 0$, it can be easily seen that $U^s > U^n$ for any $0 < \alpha < 1$. Thus the simultaneous sensing protocol strictly outperforms the dedicated sensing protocol in terms of AUT.

3.4.4 Overall System Utilization Time

Applying the same weighting factors w_p as in (3.10), the OSUT for the simultaneous sensing protocol is defined as

$$G^s \triangleq w_p\,(1 - C^s) + (1 - w_p)U^s. \tag{3.30}$$

In the following section, we will show that with pragmatic values for w_p, the simultaneous sensing protocol achieves a greater OSUT compared to the dedicated sensing protocol.

3.5 Simulation Results and Discussions

The average probability of detection for the dedicated and simultaneous sensing protocols is shown in Figure 3.5, where $\frac{P_p}{\sigma^2}$ varies from 0 dB to 20 dB. We assume $N_s = 50$, $P_{fa}^d = P_{fa}^s = 0.1$, and $\phi_{pr} = 0.1$. Three cases where the average channel gain for PT→S link is smaller than, equal to, and larger than that for PT→R link, i.e., $\phi_{ps} = 0.01$, $\phi_{ps} = 0.1$, and $\phi_{ps} = 1$ respectively, are considered. For the dedicated sensing protocol, $\alpha = 0.3$ is used. For comparison, we also show the theoretical results of P_d^d and P_d^s given in (3.7) and (3.27), respectively.

From Figure 3.5, it is clear that the theoretical results for P_d^d and P_d^s agree exactly with the simulation results, and both P_d^d and P_d^s increase with a larger ϕ_{ps}. It can be observed that $P_d^s > P_d^d$ for all three cases of ϕ_{ps} (except at the extreme case $\frac{P_p}{\sigma^2} = 0$ dB when $\phi_{ps} = 0.01$, where both P_d^d and P_d^s are small and thus is not of interest). This observation indicates that the simultaneous sensing protocol achieves a better detection performance even when 30% of each time slot is assigned for spectrum sensing in the dedicated sensing protocol. Furthermore, this performance improvement for the simultaneous sensing protocol is achieved regardless of the relative strengths of the average channel gains of PT→S and

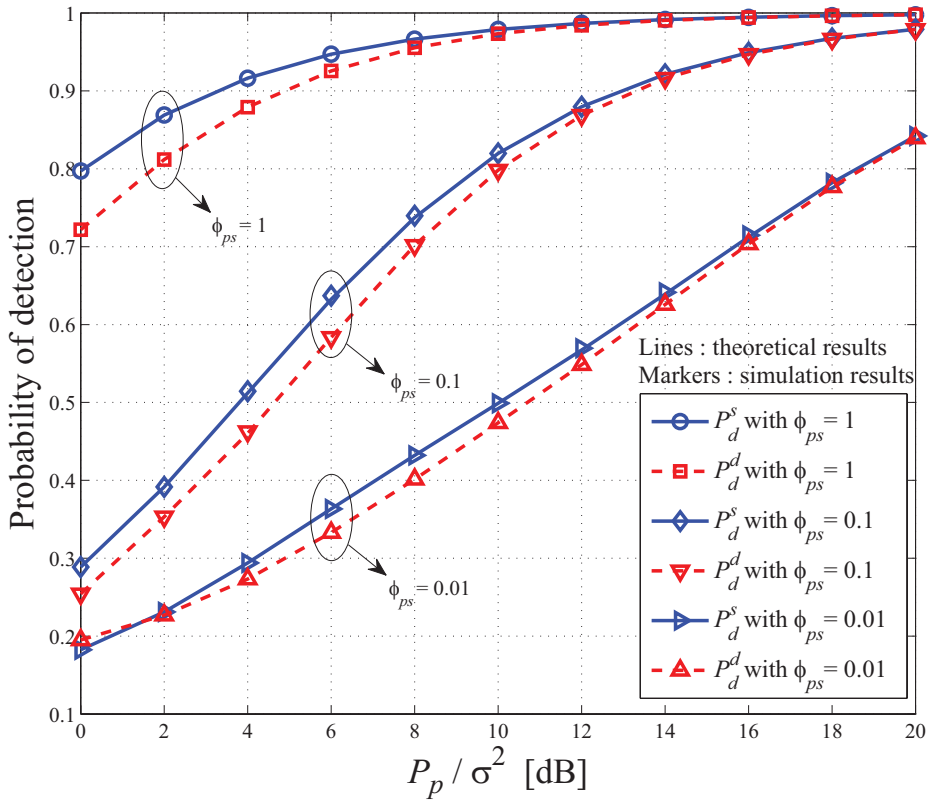

Figure 3.5. Probability of detection for the dedicated and simultaneous sensing protocols with $N_s = 50$, $P_{fa}^d = P_{fa}^s = 0.1$, $\phi_{pr} = 0.1$, and $\alpha = 0.3$.

PT→R links. Note that the simultaneous sensing protocol achieves this detection performance without requiring any dedicated sensing slots which are needed in the dedicated sensing protocol.

In Figure 3.6, we show the theoretical and simulation results of P_d^d with different values of α, where P_d^s is also shown for comparison purposes. We let $\frac{P_p}{\sigma^2} = 10$ dB, and α varies from 0.1 to 0.9. The rest of the parameters remains the same as in Figure 3.5. It is obvious from Figure 3.6 that while P_d^s is independent of α, P_d^d increases with α. This observation is intuitively satisfying since with a larger α, a larger percentage of time in each transmission phase is assigned for spectrum sensing in the dedicated sensing protocol. For all three cases of ϕ_{ps}, $P_d^d > P_d^s$ when $\alpha > \alpha' \approx 0.4$, indicating that the dedicated sensing protocol achieves a better detection performance. However, this improvement of the dedicated sensing protocol is obtained at the expense of losing up to 40% of the data transmission

time. Specifically, in the case with $\phi_{ps} = 1$, the gap between P_d^d and P_d^s is much smaller than that with $\phi_{ps} = 0.01$ and $\phi_{ps} = 0.1$, which indicates that the detection performance loss for the simultaneous sensing protocol becomes smaller when PT→S link is strong. Furthermore, although spectrum sensing is only performed at S for the simultaneous sensing protocol, the value of α' where the dedicated sensing protocol outperforms the simultaneous sensing protocol does not change significantly even when PT→S link is weaker than PT→R link.

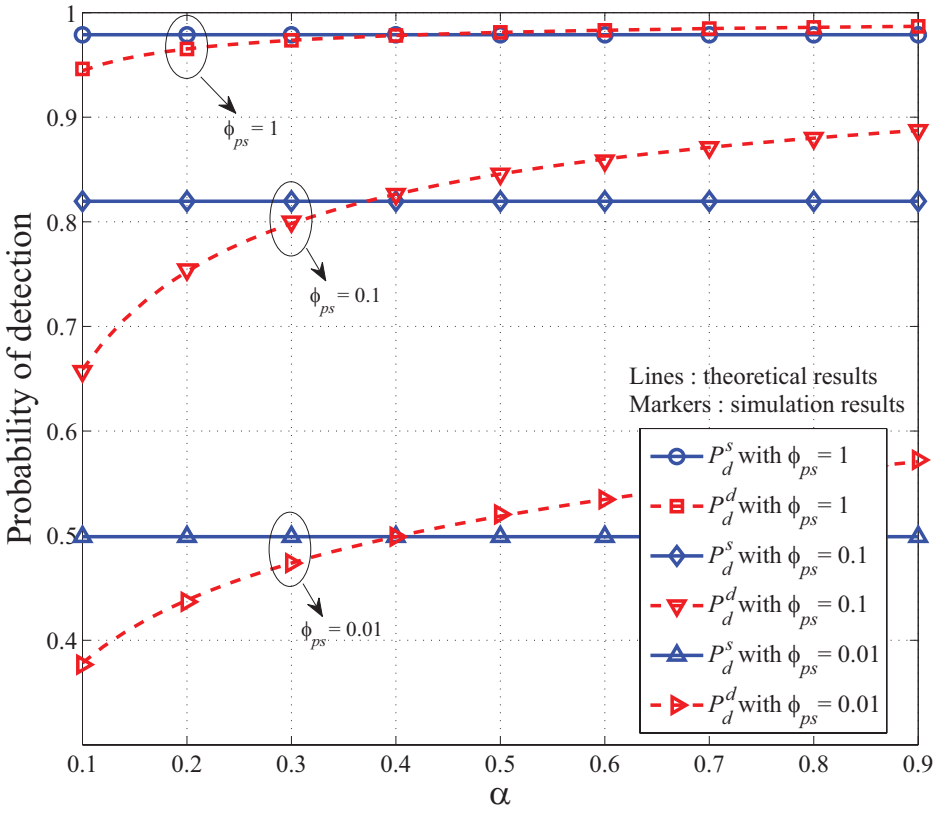

Figure 3.6. Probability of detection for the dedicated and simultaneous sensing protocols with different values of α and $\frac{P_p}{\sigma^2} = 10$ dB, $N_s = 50$, $P_{fa}^d = P_{fa}^s = 0.1$, and $\phi_{pr} = 0.1$.

In Figure 3.7, we show the theoretical results of ACT for both the dedicated and simultaneous sensing protocols, i.e., C^d and C^s, which are given in (3.8) and (3.28), respectively. We let $\frac{P_p}{\sigma^2} = 10$ dB, and α varies from 0 to 1. The rest of the parameters remains the same as in Figure 3.5. It is clear that C^d decreases with increasing α while C^s is independent of α. Furthermore, when PT→S link is strong, i.e., $\phi_{ps} = 1$, both the dedicated and simultaneous sensing protocols cause

less interference to the primary system as compared to the cases where PT→S link is weaker, i.e., $\phi_{ps} = 0.1$ and $\phi_{ps} = 0.01$.

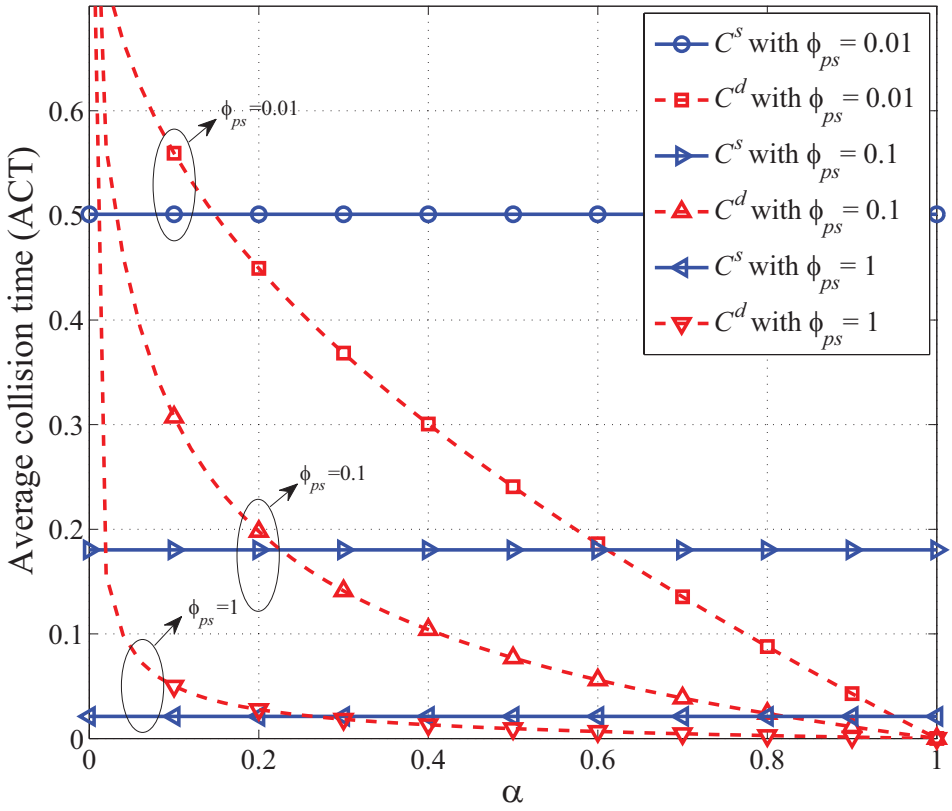

Figure 3.7. Theoretical results of average collision time (ACT) for the dedicated and simultaneous sensing protocols with different values of α and $\frac{P_p}{\sigma^2} = 10$ dB, $N_s = 50$, $P_{fa}^d = P_{fa}^s = 0.1$, and $\phi_{pr} = 0.1$.

Specifically, for the case of $\phi_{ps} = 0.1$, we can observe that $C^d < C^s$ for $\alpha > \alpha^* = 0.24$. With a larger α, more time is allocated for spectrum sensing in the dedicated sensing protocol, and this will not only increase P_d^d but also reduce the possible collision time $(1 - \alpha)$. Furthermore, since spectrum sensing is performed in every time slot with the dedicated sensing protocol, one miss-detection at S or R will only cause a collision that lasts for $(1-\alpha)$ of a time slot. On the other hand, for the simultaneous sensing protocol, one miss-detection will cause a collision that lasts for 2 time slots.

Although the dedicated sensing protocol achieves a smaller ACT when α is large, it will result in a significant spectrum efficiency loss for the secondary system.

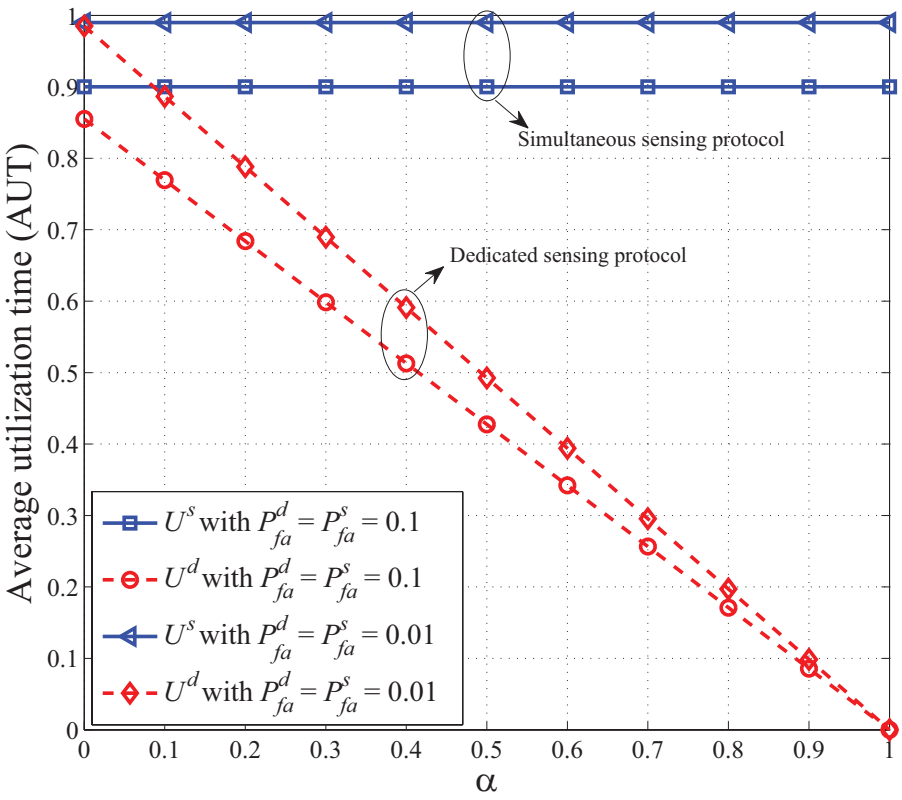

Figure 3.8. Theoretical results of average utilization time (AUT) for the dedicated and simultaneous sensing protocols with different values of α.

In Figure 3.8, we show the theoretical results of AUT for both the dedicated and simultaneous sensing protocols, i.e., U^d and U^s, which are given in (3.9) and (3.29), respectively. Here we consider two cases where $P^d_{fa} = P^s_{fa} = 0.1$ and $P^d_{fa} = P^s_{fa} = 0.01$, which correspond to scenarios where the secondary system is conservative and aggressive in accessing the spectrum band, respectively. The rest of the parameters remain the same as in Figure 3.7.

It can be observed from Figure 3.8 that both U^d and U^s increase when the secondary system is more aggressive in accessing the spectrum band, i.e., $P^d_{fa} = P^s_{fa} = 0.01$. Furthermore, with the dedicated sensing protocol, U^d decreases with increasing α, due to decreased data transmission time $(1-\alpha)$. On the other hand, with the simultaneous sensing protocol, U^s is independent of α. We note that both U^d and U^s remains unchanged with $\phi_{ps} = 0.01$, $\phi_{ps} = 0.1$, and $\phi_{ps} = 1$, since P^d_{fa}

and P_{fa}^{s} are fixed. For all values of α, we can observe that $U^{s} > U^{d}$, indicating that the simultaneous sensing protocol always achieves a higher spectrum efficiency compared to the dedicated sensing protocol. For example, when $P_{fa}^{d} = P_{fa}^{s} = 0.1$ and $\alpha = \alpha^{*} = 0.24$, we have $C^{d} = C^{s}$ according to Figure 3.7. At the same time, from Figure 3.8, we have $U^{s} = 0.9$, which is significantly better than $U^{d} = 0.65$. Thus the simultaneous sensing protocol is capable of significantly recovering the spectrum efficiency loss inherent in the dedicated sensing protocol.

Comparing Figure 3.7 and Figure 3.8, it is clear that we should not utilize the dedicated sensing protocol with $\alpha \leq \alpha^{*}$, since in this case the simultaneous sensing protocol outperforms the dedicated sensing protocol in terms of both ACT and AUT. On the other hand, with $\alpha > \alpha^{*}$, the dedicated sensing protocol is able to provide better protection to the primary system at the expense of a significant loss in secondary spectrum efficiency. Practically as long as C^{s}, or equivalently P_{d}^{s}, is lower than a predefined target, i.e., primary system is sufficiently protected, the simultaneous sensing protocol should be utilized in order to achieve a higher spectrum efficiency for the secondary system. For example, in IEEE 802.22 [37], the target probability of detection is set to be 0.9. However, if the simultaneous sensing protocol cannot meet the target for primary system, dedicated sensing protocol with a large α should be utilized.

We show in Figure 3.9 the theoretical results of OSUT for both the dedicated and simultaneous sensing protocols, i.e., G^{d} and G^{s}, which are given in (3.10) and (3.30) respectively. We let $\frac{P_p}{\sigma^2} = 20$ dB, $\phi_{ps} = \phi_{pr} = 0.1$, and α varies from 0 to 1. The rest of the parameters remain the same as Figure 3.5. Two pragmatic weighting factors $w_p = 0.95$ and $w_p = 0.8$ are considered.

It can be observed from Figure 3.9 that G^{s} is independent of α, since both C^{s} and U^{s} are independent of α. On the other hand, G^{d} varies with α and there exists an optimal value for α which maximizes G^{d}. For both cases of $w_p = 0.95$ and $w_p = 0.8$, we can observe that $G^{s} > G^{d}$ for all values of α, which indicates that the simultaneous sensing protocol always outperforms the dedicated sensing protocol in terms of OSUT. Furthermore, we can observe that the gap between G^{d} and G^{s} with $w_p = 0.8$ is larger than that with $w_p = 0.95$. This observation indicates that the simultaneous sensing protocol performs especially well when w_p is small.

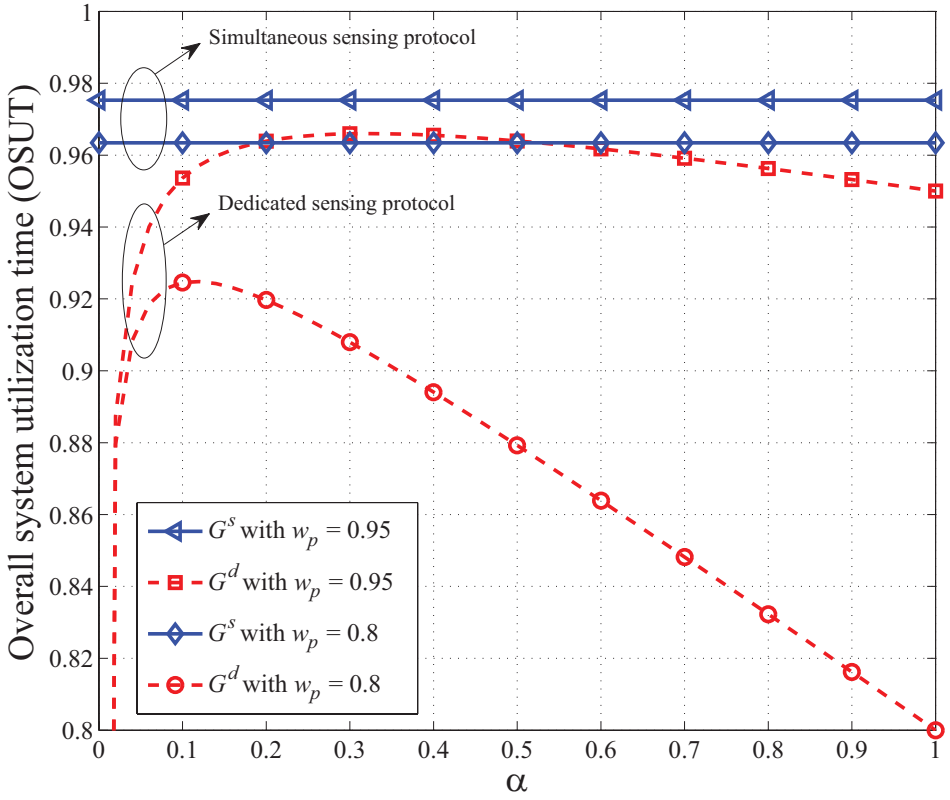

Figure 3.9. Theoretical results of overall system utilization time (OSUT) for the dedicated and simultaneous sensing protocols with different values of α and $\frac{P_p}{\sigma^2} = 20$ dB, $N_s = 50$, $P_{fa}^d = P_{fa}^s = 0.1$, $\phi_{ps} = \phi_{pr} = 0.1$, and $\sigma_e^2 = 0$.

3.6 Summary

We proposed a simultaneous spectrum sensing protocol for a cognitive dual-hop relay system and compared its performance with a straightforward dedicated sensing protocol. The simultaneous sensing protocol does not require dedicated sensing periods and performs spectrum sensing simultaneously during secondary relay transmission. We showed that the simultaneous sensing protocol outperforms the dedicated sensing protocol in terms of both average collision time and average utilization time, when short sensing periods are applied for the dedicated sensing protocol. On the other hand, when sensing periods become large, the dedicated sensing protocol is able to achieve a smaller average collision time, i.e., less interference to the primary system. However, this is at the expense of a significant loss in secondary spectrum efficiency. Furthermore, we showed that for practical priority

weighting factors, the simultaneous sensing protocol achieves a higher overall system utilization time, which takes the performance and different priorities of both the primary and secondary systems into consideration.

Chapter 4

Opportunistic Spectrum Access with Cooperative Amplify-and-Forward Relaying

4.1 Introduction

Apart from the interweave protocols based on "detect-and-avoid" principle as discussed in Chapter 3, cognitive radios were also considered in the framework of overlay spectrum sharing where two different wireless systems are allowed to operate over the same portion of spectrum albeit with different priorities in [39, 42, 94]. The higher priority for primary system is guaranteed by the constraint that secondary system accesses the spectrum with minimal interference to the primary system.

Recently, a number of spectrum sharing models for secondary spectrum access have emerged in literature [43, 44, 45, 95, 96, 97, 98] as spectrum regulatory policies evolve [99, 100]. In particular, theoretical throughput bounds and optimal power allocation for overlay spectrum sharing protocol have been considered in [95] and [96]. A spectrum leasing protocol has been proposed in [97], where the primary system *fully* controls the spectrum sharing mechanism based on cooperative transmission. Specifically, the primary system obtains instantaneous or statistical channel state information (CSI) of both primary and secondary systems,

and the primary transmitter decides whether to lease a certain portion of its own transmission time to the secondary system. In return, the secondary system has to spare a fraction of the leased time to help relay the primary transmission. In [43, 44, 45, 98], the role of cooperative transmission in spectrum sharing has been studied from an information theoretical perspective. In has been shown in [45] that when the cooperation takes place only through physical channels (no genie-aided information available), cognitive cooperation does not improve the network degrees of freedom.

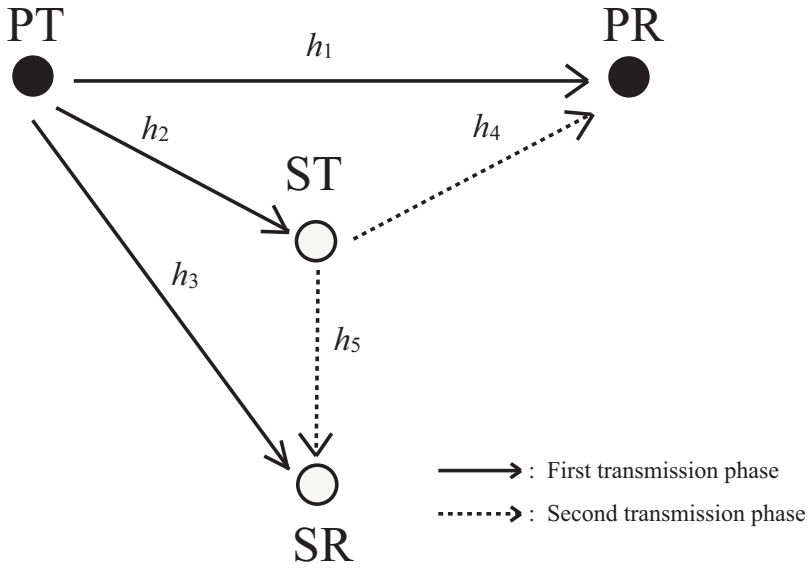

Figure 4.1. Cooperative spectrum sharing system.

Different from the information theoretical studies in [43, 44, 45, 98], in this chapter, we propose a practical spectrum sharing protocol based on cooperative amplify-and-forward relay transmission, which also falls into the category of overlay cognitive radio scheme [45]. The system configuration is shown in Figure 4.1. The primary system, comprising of a primary transmitter (PT) and primary receiver (PR), has the license to operate in a certain spectrum band and it supports the relaying functionality [3]. The secondary system, comprising of a secondary transmitter (ST) and secondary receiver (SR), can only opportunistically operate in this spectrum band by exploiting the situation when PT→PR link is weak. This situation provides a chance for ST to serve as an amplify-and-forward relay for the primary system. In this chapter, we assume that the secondary system is highly

advanced and intelligent, and it is able to emulate the same radio protocols (e.g., channel coding, synchronization, etc.) as the primary system [45].

Cooperative relaying transmission has been studied extensively in literature [3, 24] and also has been widely considered in standards, e.g. IEEE 802.16j, for the purposes of diversity gain, coverage extension, etc. In [24], opportunistic relaying is introduced, where the source terminal initializes a cooperative transmission by broadcasting a ready-to-send (RTS) signal and the destination terminal responds with a clear-to-send (CTS) signal. By overhearing these RTS and CTS signals, each potential relay terminal in the system is able to estimate the end-to-end channel gain from the source terminal, via itself, to the destination terminal. With this channel knowledge, each potential relay terminal is able to locally decide whether to participate in the cooperative transmission. Correspondingly, the cooperative relaying transmission ensues with the relay terminal which has the highest end-to-end channel gain.

In the proposed opportunistic spectrum sharing protocol, we apply a similar control signal handshake scheme. Specifically, when the PT→PR link becomes weak due to shadowing and/or fading, i.e. the channel gain drops below a certain threshold, PT will seek cooperation from neighboring terminals to enhance its transmission performance by sending out a cooperation request message (CRM). This CRM is then responded by PR with a cooperation acknowledge message (CAM). Unlike the RTS signal in [24], the CRM also indicates a request target rate for the primary system. Upon receiving both CRM and CAM, ST is able to estimate the channel gains of PT→ST and ST→PR links, and decide accordingly whether it is able to assist the primary system in achieving this request target rate by serving as an amplify-and-forward relay for the primary system. If positive, ST responds by sending a cooperation confirm message (CCM) to PT and PR[1], and the primary system correspondingly switches to a two-phase amplify-and-forward relaying transmission mode, with ST as the relay terminal. However, if ST is not able to assist the primary system in achieving the request target rate, it will simply remain silent and the primary system hence retains the direct transmission from PT to PR.

[1]Control signals CRM, CAM, CCM are all implemented in the MAC layer. We assume they are well protected by robust coding and modulation, and thus their receptions at the respective receivers are error free.

Once the two-phase cooperation is confirmed, secondary spectrum access is achieved by adopting the following transmission protocol. In the first transmission phase, the primary signal is transmitted by PT to PR, and is also overheard by ST and SR. At ST, the primary signal is amplified according to its power constraint, and a linearly weighted combination of the amplified primary signal and the secondary signal is generated. The weight denoted by α ($0 \leq \alpha \leq 1$), is the power allocation factor controlling the fraction of the total transmit power at ST that is allocated for relaying the primary signal. The weight α is chosen to ensure that the request target rate of primary system is achieved.

This composite signal is then broadcasted by ST in the second transmission phase (relaying phase). At PR, the primary signal is decoded based on the received signals in the two transmission phases which are combined through maximum ratio combining (MRC), while the secondary signal is treated as noise. At SR, interference cancelation is applied to first cancel out the primary signal component which is received in the first transmission phase, before retrieving the secondary signal transmitted in the second transmission phase. Note that the choice of $\alpha = 1$ in our proposed protocol reduces to the case of cooperative relaying with the amplify-and-forward protocol considered in [3].

In the proposed opportunistic spectrum sharing protocol, the primary system only has to be aware of an "amplify-and-forward relaying mode" operation. The primary system does not have to be cognizant of whether the relaying terminal belongs to the primary or secondary system, nor does it need to know the choice of α. From the perspective of the primary system, ST acts as an amplify-and-forward relay and appears to be part of a conventional cooperative communication system [3]. The onus is on the secondary system to "disguise" itself as a relay for the primary system in exchange for the chance to access the spectrum. It is also worth mentioning that the term "opportunistic" takes on different meanings in [94] and this chapter. Specifically, in [94], it indicates that secondary access can be achieved by exploiting the "spectrum hole" which is not occupied by the primary system. In this chapter, it indicates that secondary transmission opportunities can be obtained by exploiting the "vulnerable primary direct link" which can become weak due to shadowing and/or fading.

We analyze the proposed protocol by deriving the achievable rates of the pri-

mary and secondary systems. We show that when the channel gain of PT→PR link is smaller than a certain threshold, ST is able to assist the primary system in achieving the request target rate by selecting a proper value for α. Closed-form expression for α will be derived, and we will show that ST is able to decide whether to access the spectrum through a simple calculation of α. We also derive the probability that ST is able to gain opportunistic access to the licensed spectrum band. Simulation results confirm the efficiency of the proposed spectrum sharing protocol.

4.2 Protocol Description and Performance Analysis

The system configuration under consideration is shown in Figure 4.1. The channels over links PT→PR, PT→ST, PT→SR, ST→PR, and ST→SR are modeled to be Rayleigh flat fading with channel coefficients denoted by h_1, h_2, h_3, h_4, and h_5 respectively. Assuming channel reciprocity, the channel coefficient of link SR→ST is also given by h_5. We thus have $h_i \sim \mathcal{CN}(0, \beta_i)$, where β_i denotes the respective average channel gain and $i \in \{1, 2, 3, 4, 5\}$. We also denote the respective channel gains as $\gamma_i = |h_i|^2$. Let x_p and x_s denote the primary and secondary signals respectively, where $E\{x_p^* x_p\} = 1$ and $E\{x_s^* x_s\} = 1$. The transmit power at PT and ST is denoted by P_p and P_s respectively.

Since training symbols are incorporated in the CRM and CAM, ST is able to obtain γ_2 and γ_4 by overhearing the CRM and CAM and estimate the channel gains of the respective links through standard training-aided channel estimation methods. We assume that information regarding P_p is embedded in the CRM and thus can be acquired by ST. Furthermore, we also assume that the CAM contains information regarding γ_1, which can be estimated at PR by making use of the training symbols in CRM. Therefore, ST can also obtain γ_1 by overhearing the CAM from PR. The above assumptions for P_p and γ_1 are not unreasonable as these information would most likely be exchanged in practice, between the source and destination terminals, in a conventional system that supports the relay functionality.

4.2.1 Achievable Rate for Primary System

We first consider the situation where only the primary system is operating, i.e. there is no spectrum sharing. The primary signal is transmitted from PT to PR over channel h_1, with transmit power P_p. Thus, the achievable rate of the primary system is given by

$$R_n = \log_2\left(1 + \frac{P_p\gamma_1}{\sigma^2}\right) \tag{4.1}$$

where σ^2 is the variance of the AWGN at PR.

With the proposed spectrum sharing protocol, when the channel gain of PT→PR link γ_1 falls below a certain threshold due to shadowing and/or fading, a CRM which indicates a request target rate R_t where $R_t \geq R_n$, is sent out by PT. We define a ratio

$$\zeta = \frac{R_t}{R_n}. \tag{4.2}$$

We also denote the achievable rate of the primary system under the proposed scheme, with a power allocation factor of α, as $R_p(\alpha)$.

Upon receiving the CRM and the corresponding CAM from PT and PR, ST will first decide whether it is able to assist the primary system in achieving R_t by calculating $R_p(1)$, which is the achievable rate of the primary system where ST serves as an amplify-and-forward relay for the primary system and devotes all of its power for relaying the primary signal, i.e. $\alpha = 1$. If $R_p(1) \geq R_t$, ST[2] will broadcast a CCM to both PT and PR, and the primary system correspondingly switches to a two-phase amplify-and-forward relaying mode, with ST as the relay terminal. Otherwise, if $R_p(1) < R_t$, ST will simply remain silent. Without receiving any CCM, the primary system will retain its direction transmission from PT to PR, and secondary access is not possible.

Assuming that $R_p(1) \geq R_t$, the two-phase amplify-and-forward cooperation is established. In the first transmission phase, as shown by the solid lines in Figure 4.1, the primary signal x_p is broadcast by PT. Denoting the signal received by ST

[2]As shown later in this subsection, $R_p(1)$ is the highest achievable rate for the primary system through cooperation. Thus, the primary request target rate and hence secondary spectrum access are achievable if and only if $R_p(1) \geq R_t$.

in the first transmission phase as y_1^{st}, we have

$$y_1^{st} = \sqrt{P_p} h_2 x_p + n_1^{st}, \tag{4.3}$$

where $n_1^{st} \sim \mathcal{CN}(0, \sigma^2)$ is the AWGN at ST in the first transmission phase. Similarly, the signal received at PR in the first transmission phase is given by

$$y_1^{pr} = \sqrt{P_p} h_1 x_p + n_1^{pr}, \tag{4.4}$$

where $n_1^{pr} \sim \mathcal{CN}(0, \sigma^2)$ denotes the AWGN at PR in the first transmission phase.

After reception in the first transmission phase, ST normalizes the received signal based on its power constraint and further amplifies it with the power allocation factor α, followed by superpositioning its own secondary signal x_s to generate a composite signal

$$x_2^{st} = \sqrt{\alpha} g y_1^{st} + \sqrt{P_s(1-\alpha)} x_s \tag{4.5}$$

where $0 \leq \alpha \leq 1$, and the power normalization factor is given by $g = \sqrt{\frac{P_s}{P_p \gamma_2 + \sigma^2}}$.

In the second transmission phase, as shown by the dotted lines in Figure 4.1, the composite signal x_2^{st} is broadcast to both PR and SR. The signal received at PR is given by

$$\begin{aligned} y_2^{pr} &= h_4 x_2^{st} + n_2^{pr} \\ &= \left(\sqrt{P_p \alpha} g h_2 h_4\right) x_p + \left(\sqrt{P_s(1-\alpha)} h_4\right) x_s + \sqrt{\alpha} g h_4 n_1^{st} + n_2^{pr} \end{aligned} \tag{4.6}$$

where $n_2^{pr} \sim \mathcal{CN}(0, \sigma^2)$ is the AWGN at PR in the second transmission phase. Signals y_1^{pr} and y_2^{pr} are then combined at PR for the decoding of x_p. Note that the two-phase transmission of x_p can be written as an equivalent single-input-multiple-output (SIMO) channel,

$$\boldsymbol{y} = \boldsymbol{h} x_p + \boldsymbol{n} \tag{4.7}$$

where $\boldsymbol{h} = \sqrt{P_p}\,[h_1,\ \sqrt{\alpha} g h_2 h_4]^{\mathrm{T}}$, $\boldsymbol{n} = \left[n_1^{pr},\ \sqrt{P_s(1-\alpha)} h_4 x_s + \sqrt{\alpha} g h_4 n_1^{st} + n_2^{pr}\right]^{\mathrm{T}}$, and $\boldsymbol{y} = [y_1^{pr},\ y_2^{pr}]^{\mathrm{T}}$. The channel vector $\boldsymbol{h}$ can be estimated at PR by using standard training-aided channel estimation techniques[3], and MRC is then used to

[3]Note that PR does not need to have explicit knowledge of α as only the products $\sqrt{P_p} h_1$ and $\sqrt{\alpha} g h_2 h_4$ (the elements of $\boldsymbol{h}$) are required for MRC.

combine y_1^{pr} and y_2^{pr}. To obtain an expression for the achievable rate, we need to normalize the noise variances to obtain

$$\tilde{\boldsymbol{y}} = \begin{bmatrix} \frac{y_1^{pr}}{\sqrt{\sigma^2}} \\ \frac{y_2^{pr}}{\sqrt{\lambda}} \end{bmatrix} = \tilde{\boldsymbol{h}} x_p + \tilde{\boldsymbol{n}} \tag{4.8}$$

where $\tilde{\boldsymbol{h}} = \sqrt{P_p}\left[\frac{h_1}{\sqrt{\sigma^2}}, \frac{\sqrt{\alpha} g h_2 h_4}{\sqrt{\lambda}}\right]^{\mathrm{T}}$, $\lambda = P_s(1-\alpha)\gamma_4 + \alpha g^2 \gamma_4 \sigma^2 + \sigma^2$, and $E\{\tilde{\boldsymbol{n}}\tilde{\boldsymbol{n}}^{\mathrm{H}} | \boldsymbol{h}\} = \boldsymbol{I}_2$.

The achievable rate between PT and PR, with cooperation and power allocation factor α, is thus given by

$$\begin{aligned} R_p(\alpha) &= \frac{1}{2}\log_2\left(\det\left(\boldsymbol{I}_2 + \tilde{\boldsymbol{h}}\tilde{\boldsymbol{h}}^{\mathrm{H}}\right)\right) \\ &= \frac{1}{2}\log_2\left(1 + \frac{P_p\gamma_1}{\sigma^2} + \frac{P_p\gamma_2\gamma_4 g^2 \alpha}{P_s(1-\alpha)\gamma_4 + \alpha g^2 \gamma_4 \sigma^2 + \sigma^2}\right) \end{aligned} \tag{4.9}$$

where the factor of $\frac{1}{2}$ accounts for the fact that the transmission of x_p is carried out over two transmission phases.

It is clear from (4.9) that $R_p(\alpha)$ is increasing in α, thus the highest achievable rate for the primary system through cooperation is $R_p(1)$. If $R_p(1) < R_t$, the secondary system is not able to assist the primary system in achieving the request target rate, and hence no secondary spectrum access can take place. Thus, in order to achieve secondary spectrum access, we require

$$R_p(1) \geq R_t. \tag{4.10}$$

Substituting (4.1), (4.2), and (4.9) into (4.10), we obtain the inequality

$$\rho^{2\zeta} - \rho - Q \leq 0 \tag{4.11}$$

where $\rho = \frac{P_p\gamma_1}{\sigma^2} + 1$ and $Q = \frac{P_p\gamma_2\gamma_4 g^2}{g^2\gamma_4\sigma^2 + \sigma^2}$. To determine the threshold for γ_1 such that (4.10) holds true, we will take γ_1 as the variable and the rest of the terms as indeterminates. Thus, we can write $f(\gamma_1) = \rho^{2\zeta} - \rho - Q$.

Proposition 4.2.1. *The condition in (4.10) holds true if and only if* $0 < \gamma_1 \leq \gamma_1^*(\gamma_2, \gamma_4, \zeta)$, *where* $\gamma_1^*(\gamma_2, \gamma_4, \zeta)$ *is the one and only one real positive root for equa-*

tion $f(\gamma_1) = 0$.

Proof: It can be easily derived that

$$\frac{\partial f(\gamma_1)}{\partial \gamma_1} = \frac{P_p}{\sigma^2}\left(2\zeta\left(\frac{P_p\gamma_1}{\sigma^2}+1\right)^{2\zeta-1}-1\right), \tag{4.12}$$

and

$$\frac{\partial^2 f(\gamma_1)}{\partial \gamma_1^2} = 2\zeta(2\zeta-1)\left(\frac{P_p}{\sigma^2}\right)^2\left(\frac{P_p\gamma_1}{\sigma^2}+1\right)^{2\zeta-2}. \tag{4.13}$$

Since $\zeta \geq 1$, it is clear that $\frac{\partial f(\gamma_1)}{\partial \gamma_1} > 0$ and $\frac{\partial^2 f(\gamma_1)}{\partial \gamma_1^2} > 0$, with $\gamma_1 > 0$. Thus, $f(\gamma_1)$ is monotonously increasing with $\gamma_1 > 0$. Together with the fact that $f(0) = -Q < 0$, it is clear from the illustration in Figure 4.2 that the equation $f(\gamma_1) = 0$ has one and only one real positive root, which is denoted as $\gamma_1^*(\gamma_2, \gamma_4, \zeta)$. Thus (4.10) holds true if and only if $0 < \gamma_1 \leq \gamma_1^*(\gamma_2, \gamma_4, \zeta)$. This concludes the proof.

■

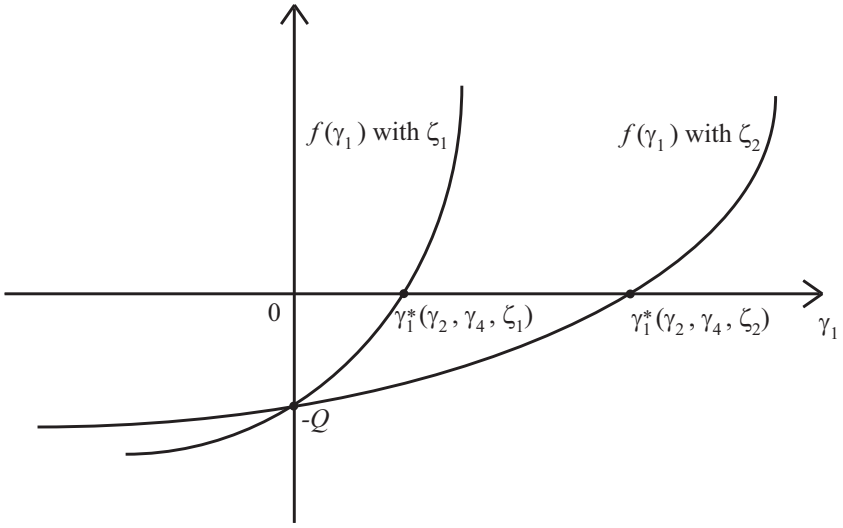

Figure 4.2. Illustrative diagram for $f(\gamma_1)$ where $\zeta_1 > \zeta_2$.

Proposition 1 indicates that when the primary direct link PT→PR becomes weak and the instantaneous channel gain γ_1 falls below the threshold $\gamma_1^*(\gamma_2, \gamma_4, \zeta)$, ST is able to assist the primary system in achieving the request target rate and at the same time gain opportunistic access to the licensed spectrum band.

In the following, we derive the value of α which achieves

$$R_p(\alpha) = R_t. \tag{4.14}$$

Substituting (4.1), (4.2), and (4.9) into (4.14), it can be easily derived that

$$\alpha = \frac{P_s\gamma_4 + \sigma^2}{\frac{P_p\gamma_2\gamma_4 g^2}{\rho^{2\zeta}-\rho} + P_s\gamma_4 - g^2\gamma_4\sigma^2}. \tag{4.15}$$

It is obvious from (4.15) that $\alpha \geq 0$ and α increases with ζ, which indicates that in order to satisfy a larger primary request target rate, ST has to devote more of its transmit power to relay the primary signal.

Proposition 4.2.2. *Secondary spectrum access is achievable if and only if* $0 \leq \alpha \leq 1$*, where* α *is given by (4.15).*

Proof: In order to achieve secondary spectrum access, we require that (4.10) holds true. Substituting (4.1), (4.2), and (4.9) into (4.10), and after some manipulations, (4.10) can be expressed as

$$\frac{P_p\gamma_2\gamma_4 g^2}{\rho^{2\zeta}-\rho} \geq g^2\gamma_4\sigma^2 + \sigma^2. \tag{4.16}$$

Substituting (4.16) into the denominator of (4.15), we obtain

$$0 \leq \alpha \leq \frac{P_s\gamma_4 + \sigma^2}{P_s\gamma_4 + \sigma^2} = 1. \tag{4.17}$$

This completes the forward proof. For the reverse proof, when $0 \leq \alpha \leq 1$, from (4.15) we have

$$1 + \frac{P_p\gamma_1}{\sigma^2} + \frac{P_p\gamma_2\gamma_4 g^2}{g^2\gamma_4\sigma^2 + \sigma^2} \geq \left(1 + \frac{P_p\gamma_1}{\sigma^2}\right)^{2\zeta}. \tag{4.18}$$

By taking the logarithm on both sides of (4.18), we obtain $R_p(1) \geq R_t$, i.e. (4.10) holds true and spectrum access is achievable. This concludes the proof.

■

From Proposition 2, ST only needs to calculate α through (4.15) to decide whether secondary spectrum access is possible. If $0 \leq \alpha \leq 1$, ST will send out the

CCM and apply the calculated α directly for transmission such that $R_p(\alpha) = R_t$ is achieved. Otherwise, if $\alpha > 1$, ST will remain silent and the primary system retains its direct transmission from PT to PR.

The average achievable rate for primary system with the proposed spectrum sharing protocol is thus given by

$$E\{R_p\} = \int_0^\infty \int_0^\infty \left(\underbrace{\int_0^{\gamma_1^*(\gamma_2,\gamma_4,\zeta)} \frac{R_t}{\beta_1} e^{-\frac{\gamma_1}{\beta_1}} d\gamma_1}_{\text{Cooperative relaying transmission}} + \underbrace{\int_{\gamma_1^*(\gamma_2,\gamma_4,\zeta)}^\infty \frac{R_n}{\beta_1} e^{-\frac{\gamma_1}{\beta_1}} d\gamma_1}_{\text{Direct transmission}} \right) \cdot \frac{e^{-\left(\frac{\gamma_2}{\beta_2}+\frac{\gamma_4}{\beta_4}\right)}}{\beta_2\beta_4} d\gamma_2 d\gamma_4. \tag{4.19}$$

Since $R_t \geq R_n$, we have $E\{R_p\} \geq E\{R_n\}$, and equality only holds with $\zeta = 1$. This indicates that with $\zeta > 1$, the primary system can always benefit from the proposed spectrum sharing protocol in terms of average achievable rate. Since the integral in (4.19) is intractable, we will analyze $E\{R_p\}$ by numerical methods in the next section.

4.2.2 Probability of Opportunistic Spectrum Access

The probability that ST is able to gain opportunistic access to the licensed spectrum band, conditioned on γ_2, γ_4, and ζ is given by

$$P_{\text{OA}} = \Pr\{\gamma_1 < \gamma_1^*(\gamma_2,\gamma_4,\zeta) | \gamma_2,\gamma_4,\zeta\} = 1 - e^{-\frac{\gamma_1^*(\gamma_2,\gamma_4,\zeta)}{\beta_1}}. \tag{4.20}$$

From (4.12), it is clear that $\frac{\partial f(\gamma_1)}{\partial \gamma_1}$ is increasing in ζ with $\gamma_1 > 0$, thus $\gamma_1^*(\gamma_2,\gamma_4,\zeta)$ decreases with ζ. For example, we show an illustrative diagram of $f(\gamma_1)$ with $\zeta = \zeta_1$ and $\zeta = \zeta_2$ in Figure 4.2, where $\zeta_1 > \zeta_2$. It is obvious that

$$\frac{\partial f(\gamma_1)}{\partial \gamma_1}\Big|_{\zeta=\zeta_1} > \frac{\partial f(\gamma_1)}{\partial \gamma_1}\Big|_{\zeta=\zeta_2}$$

with $\gamma_1 > 0$, and hence $\gamma_1^*(\gamma_2,\gamma_4,\zeta_1) < \gamma_1^*(\gamma_2,\gamma_4,\zeta_2)$. Therefore, P_{OA} decreases with increasing ζ. This observation is intuitive because the higher the primary request

target rate is, the smaller is the chance that ST is able to assist the primary system in achieving this request target rate. Averaging (4.20) across γ_2 and γ_4, the average probability that secondary spectrum access is possible can be expressed as

$$\overline{P_{\mathrm{OA}}} = 1 - \int_0^\infty \int_0^\infty \frac{1}{\beta_2\beta_4} e^{-\left(\frac{\gamma_1^*(\gamma_2,\gamma_4,\zeta)}{\beta_1}+\frac{\gamma_2}{\beta_2}+\frac{\gamma_4}{\beta_4}\right)} d\gamma_2 d\gamma_4. \tag{4.21}$$

Similarly, $\overline{P_{\mathrm{OA}}}$ also decreases with increasing ζ. The closed-form analysis of (4.21) is intractable, thus we will evaluate $\overline{P_{\mathrm{OA}}}$ by numerical simulation in the next section.

4.2.3 Achievable Rate for Secondary System

The signal received at SR in the first transmission phase is given by

$$y_1^{sr} = \sqrt{P_p} h_3 x_p + n_1^{sr}. \tag{4.22}$$

where $n_1^{sr} \sim \mathcal{CN}(0, \sigma^2)$ is the AWGN at SR in the first transmission phase. At SR, an estimate of x_p is obtained using (4.22) as

$$\widehat{x}_p = \frac{y_1^{sr}}{\sqrt{P_p} h_3} = x_p + \frac{n_1^{sr}}{\sqrt{P_p} h_3}. \tag{4.23}$$

The signal received at SR in the second transmission phase is given as

$$\begin{aligned} y_2^{sr} &= h_2 y_2^{st} + n_2^{sr} \\ &= (\sqrt{P_p \alpha} g h_2 h_5) x_p + (\sqrt{P_s(1-\alpha)} h_5) x_s + \sqrt{\alpha} g h_5 n_1^{st} + n_2^{sr}. \end{aligned} \tag{4.24}$$

where $n_2^{sr} \sim \mathcal{CN}(0, \sigma^2)$ is the AWGN at SR in the second transmission phase.

The secondary signal x_s is retrieved at SR as follows. The estimate $\widehat{x}_p$ in (4.23) is used to cancel out the interference component $(\sqrt{P_p \alpha} g h_2 h_5) x_p$ from y_2^{sr}, to obtain

$$\begin{aligned} \widehat{y_2^{sr}} &= y_2^{sr} - (\sqrt{P_p \alpha} g h_2 h_5) \widehat{x}_p \\ &= (\sqrt{P_s(1-\alpha)} h_5) x_s - \frac{\sqrt{\alpha} g h_2 h_5 n_1^{sr}}{h_3} + \sqrt{\alpha} g h_5 n_1^{st} + n_2^{sr}. \end{aligned} \tag{4.25}$$

Note that only the product $\sqrt{P_p\alpha}gh_2h_5$ is needed for the cancelation and it can be obtained in practice through the use of training symbols. Knowledge of the individual channel coefficients h_2 and h_5 is not required.

The achievable rate for ST→SR link is thus given by

$$R_s(\alpha) = \frac{1}{2}\log_2\left(1 + \frac{P_s(1-\alpha)\gamma_3\gamma_5}{\alpha g^2(\gamma_2+\gamma_3)\gamma_5\sigma^2 + \gamma_3\sigma^2}\right). \tag{4.26}$$

where the factor of $\frac{1}{2}$ accounts for the fact that the transmission of x_s is carried out over two transmission phases. The average achievable rate for the secondary system with the proposed spectrum sharing protocol is thus given by

$$E\{R_s\} = \int_0^{\infty}\int_0^{\gamma_1^*(\gamma_2,\gamma_4,\zeta)} \frac{R_s(\alpha)e^{-\left(\sum_{i=1}^{5}\frac{\gamma_i}{\beta_i}\right)}}{\prod_{i=1}^{5}\beta_i} d\gamma_1 d\boldsymbol{\gamma}, \tag{4.27}$$

where $\boldsymbol{\gamma} = [\gamma_2, \gamma_3, \gamma_4, \gamma_5]$. It is obvious that $R_s(\alpha)$ is monotonically decreasing with α. Thus, $E\{R_s\}$ decreases with increasing ζ. This observation indicates that when the primary system has a larger request target rate, the secondary system has a smaller chance to access the spectrum band, and for each access, ST has to devote a larger fraction of its transmit power to relay the primary signal which result in a lower average achievable rate for the secondary system. We will analyze $E\{R_s\}$ through numerical simulation in the next section.

4.2.4 Summary of The Proposed Protocol

1. PT sends out CRM when γ_1 falls below a certain threshold and hence the PT→PR link is not able to support a rate of R_t. PR responds by sending out CAM.

2. ST obtains P_p, ζ, γ_1, γ_2 and γ_4 from CRM and CAM.

3. ST calculates α and checks whether $0 \leq \alpha \leq 1$ is satisfied. If positive, go to step 4. Otherwise, go to step 5.

4. ST responds to CRM by sending out CCM, and two-phase amplify-and-forward cooperation ensues accordingly, with the power allocation factor α calculated in step 3.

5. ST remains silent and primary system retains its direct transmission over PT→PR link.

4.2.5 Remarks

Comparing (4.9) and (4.26), we can observe that with increasing α, more power is allocated by ST for relaying the primary signal and less power is used for secondary signal transmission which cause a respective increase and decrease in the achievable rates for the primary and secondary systems. From (4.15), it is obvious that when $\rho = \frac{P_p\gamma_1}{\sigma^2} + 1 \gg 1$, we have $\alpha \approx 1$ which indicates that in order to achieve the primary request target rate, ST has to allocate almost all of its power to relay the transmission of primary system which will cause $R_s(\alpha) \approx 0$. In this case, the proposed spectrum sharing scheme will reduce to a conventional relaying system where ST purely plays the role of a relay. This represents the case where ST behaves as an altruistic cognitive user.

In this chapter, we assume that ST will respond to the cooperation request as long as $0 \leq \alpha \leq 1$. However, in practice, ST can have additional secondary achievable rate requirements for participating in the cooperation, e.g., $R_s(\alpha) > R_r$, where R_r is the secondary target rate. Thus ST joins the cooperative transmission only when $\{0 \leq \alpha \leq 1\} \bigcap \{R_s(\alpha) > R_r\}$. By having this requirement, ST only explores the transmission opportunities which can provide an achievable rate gain larger than R_r, and ignores those which require it to devote most of its power to relaying the primary signal and bring little gain to the secondary system. This represents the case where ST behaves as a selfish cognitive user.

From (4.9) and (4.26), it can also be observed that both R_p and R_s increase with increasing P_s. However, when $P_s \to \infty$, we have

$$R_p(\alpha) \to \frac{1}{2}\log_2\left(1 + \frac{P_p\gamma_1}{\sigma^2} + \frac{P_p\gamma_2\alpha}{(P_p\gamma_2 + \sigma^2)(1-\alpha) + \alpha\sigma^2}\right) \tag{4.28}$$

and

$$R_s(\alpha) \to \frac{1}{2}\log_2\left(1 + \frac{(P_p\gamma_2 + \sigma^2)(1-\alpha)\gamma_3}{(\gamma_2 + \gamma_3)\alpha\sigma^2}\right), \tag{4.29}$$

which indicates that we cannot improve R_p and R_s indefinitely by increasing P_s. Furthermore, we can also observe that $R_p(\alpha)$ is independent of γ_3 and γ_5, while

$R_s(\alpha)$ increases with increasing γ_3 and γ_5. Thus for a given α, we can increase the achievable rate for the secondary system, without affecting the achievable rate for the primary system, by either increasing γ_3 or γ_5. This indicates that the proposed scheme will be especially attractive for short-range cognitive radios operating near PT.

4.3 Simulation Results and Discussions

We show the average achievable rates for primary and secondary systems with the proposed spectrum sharing protocol in Figure 4.3, where $P_p = P_s$ and $\frac{P_p}{\sigma^2}$ varies from 0 dB to 20 dB. We assume that the direct link from PT to PR experiences an extra attenuation of $L_s = 20$ dB (i.e., $\beta_1 = -20$ dB) due to shadowing, as compared to the other links. We assume $\beta_i = 0$ dB, $i = \{2, 3, 4, 5\}$. We consider three cases where $\zeta = 1$, $\zeta = 1.5$, and $\zeta = 2$ respectively. It can be observed from Figure 4.3 that $E\{R_p\}$ increases with ζ and coincides with $E\{R_n\}$ when $\zeta = 1$, whereas $E\{R_p\}$ is larger than $E\{R_n\}$ with $\zeta > 1$. On the other hand, $E\{R_s\}$ decreases with ζ but still achieves reasonable values, through opportunistic access, for all values of ζ. This observation confirms that both primary and secondary systems obtain benefits in terms of average achievable rate with the proposed opportunistic spectrum sharing protocol.

In Figure 4.4, we show $\overline{P_{\text{OA}}}$ given in (4.21). We let $\frac{P_p}{\sigma^2} = \frac{P_s}{\sigma^2} = 10$ dB and consider three cases where $\zeta = 1$, $\zeta = 1.5$, and $\zeta = 2$ respectively. From Figure 4.4, we can observe that $\overline{P_{\text{OA}}}$ increases with L_s, which agrees with the intuition that the weaker PT→PR link is, the higher is the chance that the secondary system can provide rate improvement to the primary system through cooperation, and at the same time gain secondary access to the spectrum. For example, with $L_s = 20$ dB, ST is able to gain transmission opportunities in more than 90% of the channel realizations, for all three values of ζ. Furthermore, we can observe that $\overline{P_{\text{OA}}}$ decreases with increasing ζ, which is due to the more stringent primary request target rate requirement.

In Figure 4.5, we show the average achievable rates for primary and secondary systems with different values of L_s. We let $\frac{P_p}{\sigma^2} = \frac{P_s}{\sigma^2} = 10$ dB, $\beta_i = 0$ dB, $i = \{2, 3, 4, 5\}$, and L_s vary from 0 dB to 30 dB. We consider two cases where $\zeta = 1$

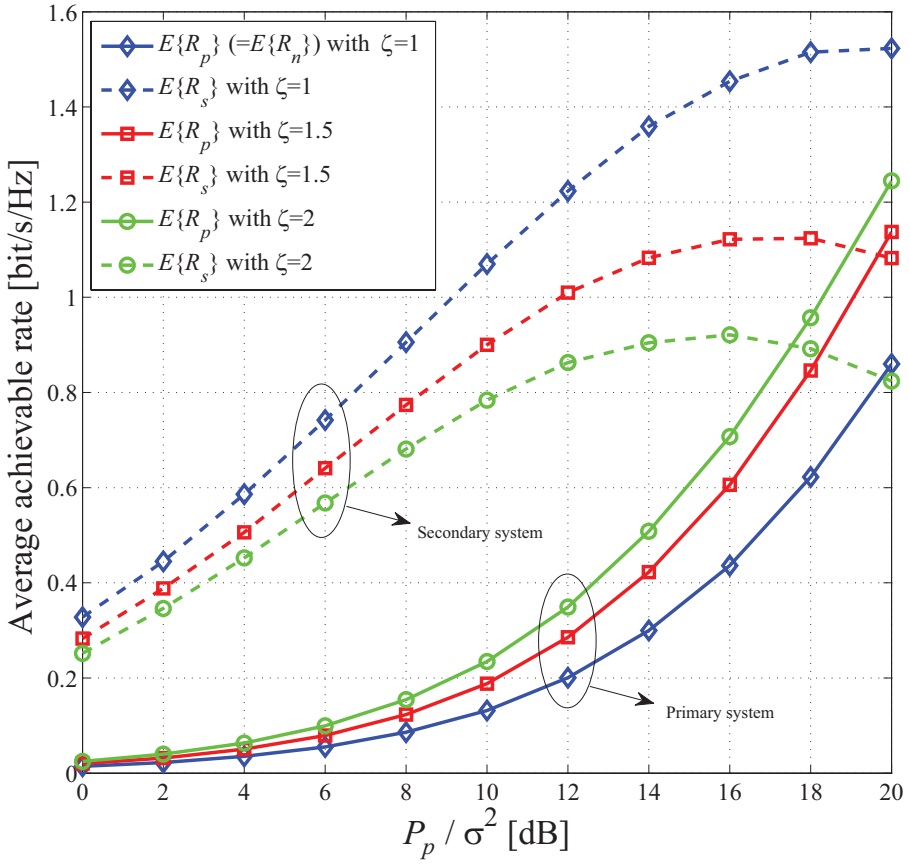

Figure 4.3. Average achievable rates for proposed opportunistic spectrum sharing protocol.

and $\zeta = 2$ respectively.

It can be observed from Figure 4.5 that $E\{R_p\}$ decreases with increasing L_s. This is because a weaker PT→PR link leads to a smaller R_n and hence a smaller primary request target rate $R_t = \zeta R_n$. Thus, $E\{R_p\}$ decreases with L_s, which can be easily observed from (4.19). When L_s is small, due to a small $\overline{P_{\text{OA}}}$, $E\{R_p\}$ with $\zeta = 2$ almost overlaps with $E\{R_n\}$. With increasing L_s, $E\{R_p\}$ is improved as compared to $E\{R_n\}$. On the other hand, $E\{R_s\}$ increases with increasing L_s. When the PT→PR link is weak, more transmission opportunities can be exploited by the secondary system and for each transmission opportunity, ST only needs to allocate a small fraction of its transmit power for relaying the primary signal, which all lead to an increase in $E\{R_s\}$. Furthermore, we can observe that while $E\{R_p\}$

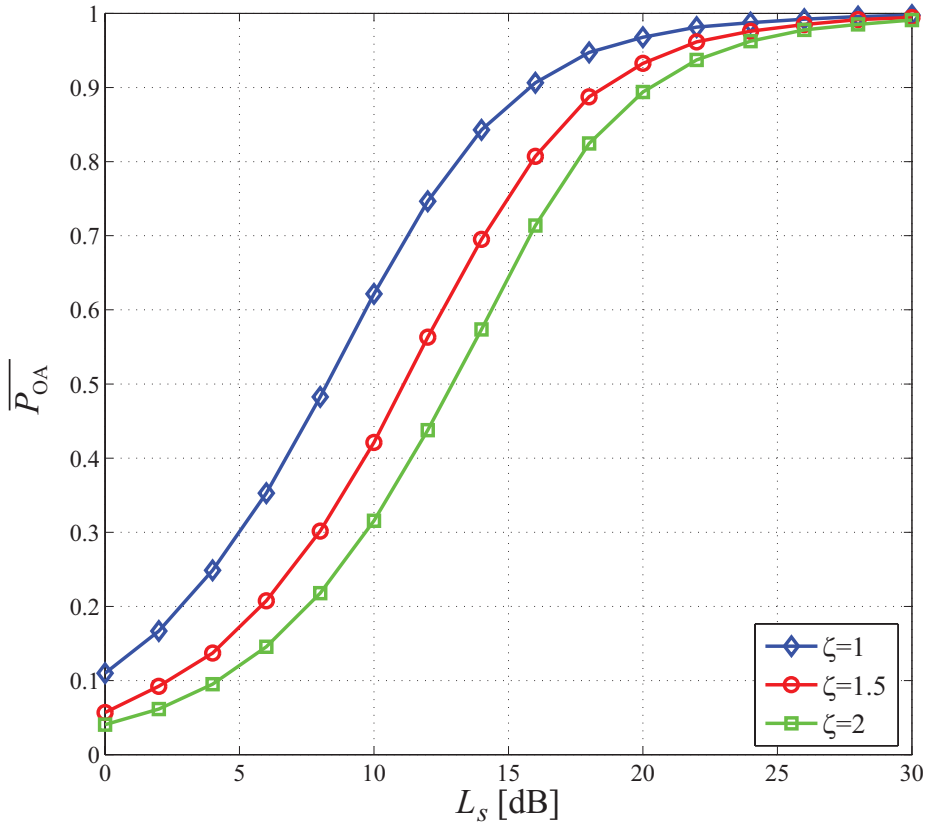

Figure 4.4. $\overline{P_{\mathrm{OA}}}$ with different values of ζ.

is improved with $\zeta = 2$ as compared to the case with $\zeta = 1$, $E\{R_s\}$ decreases with larger ζ due to the more stringent primary request target rate requirement.

In Figure 4.6, we show $E\{R_p\}$ and $E\{R_s\}$ with various values of P_s, β_3, and β_5. We let $\zeta = 2$, $\beta_1 = -20$ dB, $\beta_2 = \beta_4 = 0$ dB, $\frac{P_p}{\sigma^2} = 20$ dB, and $\frac{P_s}{\sigma^2}$ varies from 0 dB to 50 dB. We consider three cases where $\beta_3 = \beta_5 = -10$ dB, 0 dB, and 10 dB, respectively. It can be observed from Figure 4.6 that both $E\{R_p\}$ and $E\{R_s\}$ increase with P_s, when P_s is small. However, rate ceilings appear for both $E\{R_p\}$ and $E\{R_s\}$ when P_s becomes large. This coincides with our remark in Section 4.2.5 that we cannot improve the achievable rates for the primary and secondary systems indefinitely by increasing the transmit power at ST. Furthermore, we can observe that while $E\{R_p\}$ is independent of β_3 and β_5, $E\{R_s\}$ increases with increasing β_3 and β_5, which confirms our theoretical derivations in (4.9) and (4.26). This

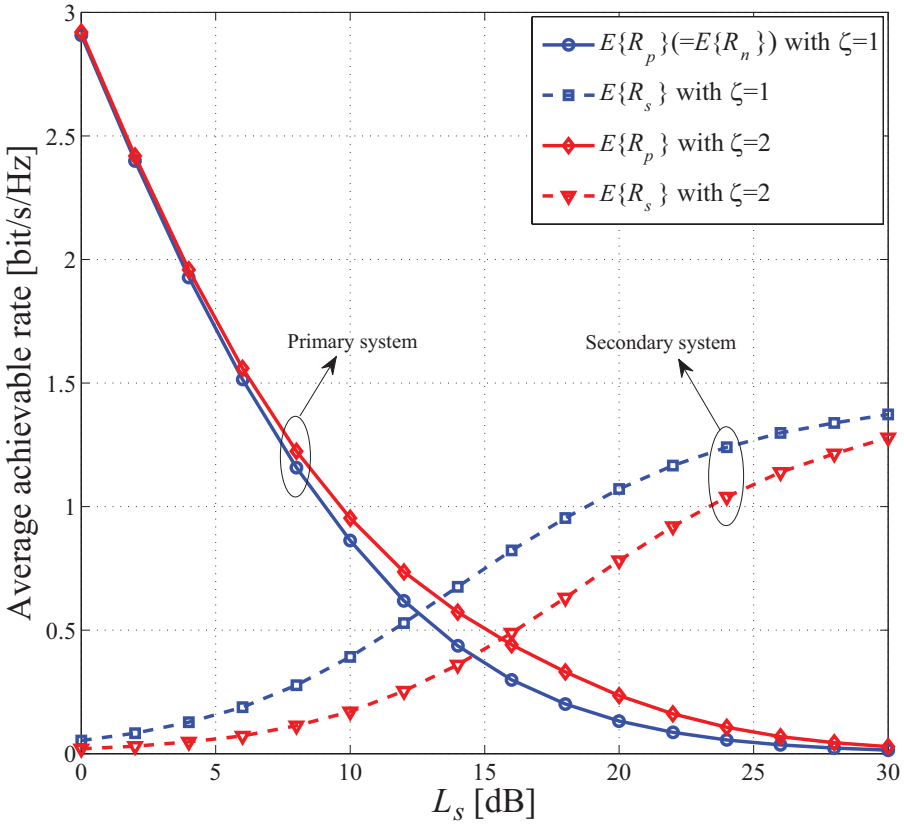

Figure 4.5. Average achievable rates for proposed opportunistic spectrum sharing protocol with different values of L_s.

indicates that when PT→SR and ST→SR links are strong, the achievable rate performance of secondary system can be significantly improved without affecting the primary system.

4.4 Summary

We proposed an opportunistic spectrum sharing protocol using cooperative transmission, which exploits the geographical location as well as the fading of wireless channels. Specifically, when the link between primary transmitter and receiver is weak due to shadowing and/or fading, the secondary transmitter is able to assist the primary system in improving its rate performance by serving as an amplify-

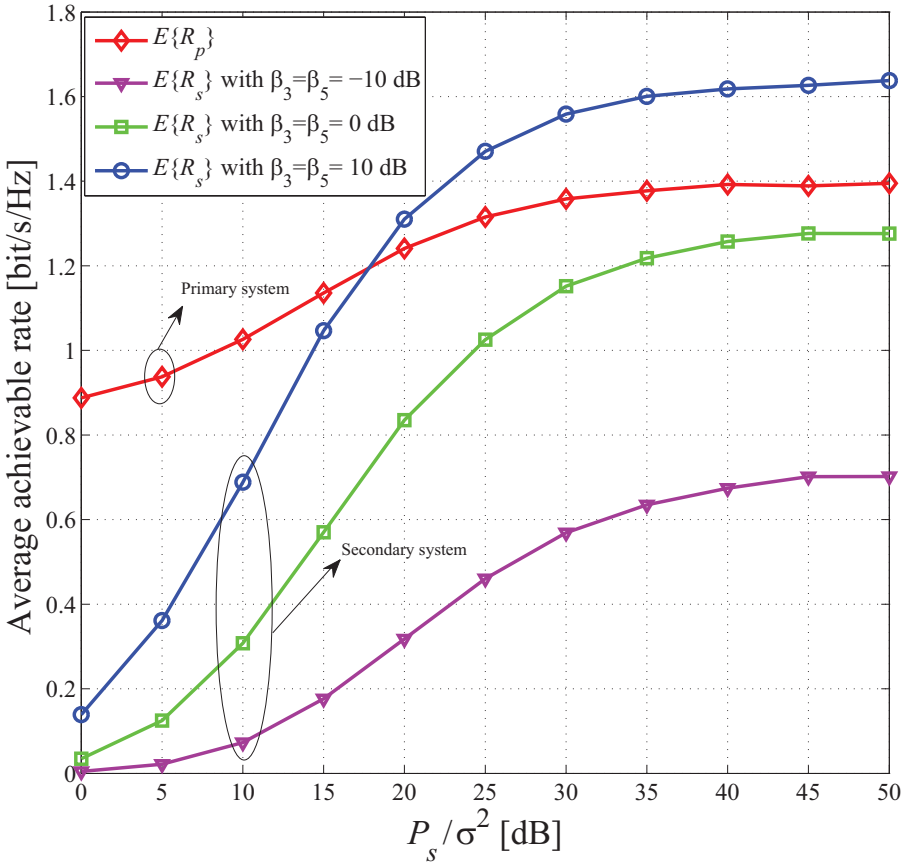

Figure 4.6. Average achievable rates for proposed opportunistic spectrum sharing protocol with $\frac{P_p}{\sigma^2} = 20$ dB and $\zeta = 2$.

and-forward relay for the primary system with a fraction of its own transmit power. At the same time, secondary transmission is accomplished by superimposing the secondary signal to the primary signal component in the relaying phase.

We derive the achievable rates for both primary and secondary systems and show that when the channel gain of the link from primary transmitter to receiver is lower than a certain threshold, primary request target rate can be achieved by the proposed cooperation scheme, and hence a transmission opportunity is obtained by the secondary system. We derive the probability for this opportunistic spectrum access and also the value for the power allocation factor at secondary transmitter which achieves the primary request target rate. Simulations results confirm that both primary and secondary systems benefit from the proposed opportunistic spectrum sharing protocol in terms of average achievable rate.

Chapter 5

Secondary Spectrum Access with Cooperative Decode-and-Forward Relaying

5.1 Introduction

In Chapter 4, the secondary system obtains the spectrum access opportunistically by exploiting the faded primary transmission link, thus explicit control message exchanges between the primary and secondary systems are required (although the primary system is oblivious to the secondary access). In this chapter, we propose a spectrum sharing protocol based on controlled cooperative DF relaying, where a fixed power allocation factor is used at the secondary transmitter and thus no explicit control message exchange is needed. Unlike in Chapter 4, we derive a critical region in terms of geographical location and power allocation factor. We show that within this critical region, the secondary transmitter is always able to access the spectrum band without degrading the outage performance of the primary system.

The primary system, comprising of a primary transmitter (PT) and primary receiver (PR), has licensed rights to operate in a certain portion of the spectrum and it supports the relaying functionality [3]. The secondary system, comprising of a secondary transmitter (ST) and secondary receiver (SR), can only operate

on a secondary basis in this spectrum, with the constraint that its operation does not affect the primary system performance. Furthermore, we assume that the secondary system is able to emulate the radio protocols (e.g., channel coding, synchronization, etc.) of the primary system. We quantify the primary system priority in terms of its outage probability. Note that in [101, 102], an alternate metric of priority namely average rate was used.

The secondary system insures the primary system performance by adopting the following transmission protocol. In the first transmission phase, the primary signal transmitted by PT to PR is also received and decoded by ST and SR[1]. The primary signal is then regenerated at ST and superimposed with the secondary signal. A fraction, α where $0 \leq \alpha \leq 1$, of the total power at ST is allocated to the primary signal, with the remaining power assigned to the secondary signal. This weighted linear composite signal is then broadcasted by ST in the second transmission phase. At PR, a maximum ratio combination (MRC) of the received signals in the two transmission phases is applied to retrieve the primary signal. At SR, interference cancelation is first applied to cancel the primary signal component and then the secondary signal is retrieved. Note that the choice of $\alpha = 1$ in our proposed protocol reduces to the case of cooperative relaying with the decode-and-forward protocol as considered in [3].

In the proposed spectrum sharing protocol, the primary system only has to be aware of a "decode-and-forward relaying mode" operation. This switch to a relaying mode can be easily conveyed to the primary system through the use of control messages. The primary system does not have to be cognizant of whether the relaying node is a node belonging to the primary system or the secondary system, nor does it need to know the choice of α. From the perspective of the primary system, ST acts as a decode-and-forward relay and appears to be part of a conventional cooperative communication system [3].

We analytically derive the outage probabilities of the primary and secondary systems under the proposed protocol. We show that as long as ST is located within a critical radius from PT, there exists a threshold value for α, above which

[1]If ST fails to decode, it will remain silent in the second transmission phase, and PR will try to decode by using only the signal it received in the first transmission phase. An outage will be declared for the secondary system if either ST or SR (or both) fails to decode the primary signal. The details of the proposed protocol will be explained in the next section.

the secondary system can operate without affecting the outage performance of the primary system. By controlling α, the outage probability of the primary system can either be maintained to be the same as the case without spectrum sharing, or it can be improved by a desired margin.

5.2 System Model and Performance Analysis

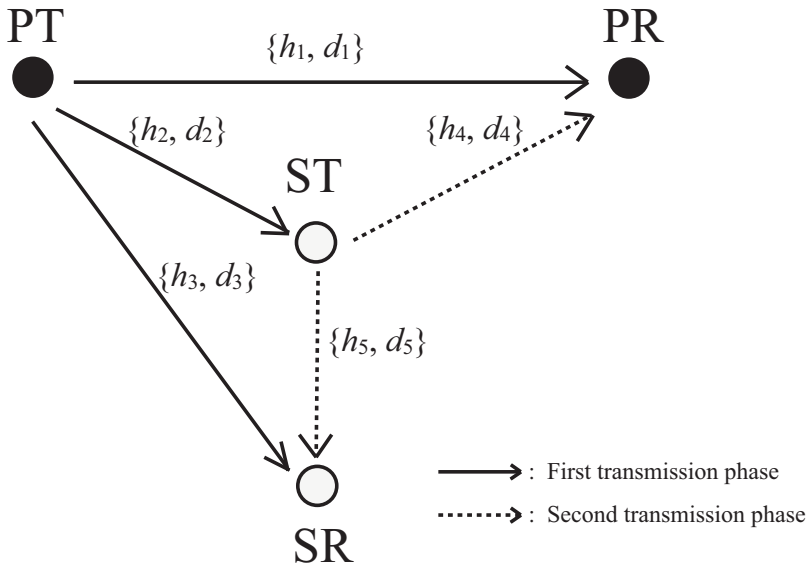

Figure 5.1. System configuration.

The system configuration of the proposed scheme is shown in Figure 5.1. The channels over links PT→PR, PT→ST, PT→SR, ST→PR, and ST→SR are modeled to be Rayleigh flat fading with channel coefficients denoted by h_1, h_2, h_3, h_4, and h_5 respectively. We have $h_i \sim \mathcal{CN}(0, d_i^{-\nu})$, $i = 1, 2, 3, 4, 5$, where ν is the path loss exponent and d_i is the normalized distance between the respective transmitters and receivers. This normalization is done with respect to the distance between PT and PR, i.e., $d_1 = 1$. Thus each of the links can be characterized by the set of parameters $\{h_i, d_i\}$ as shown in Figure 5.1, and we also denote $\gamma_i = |h_i|^2$. We assume that all the channel coefficients remain static in two transmission phases. Let x_p and x_s denote the primary and secondary signals respectively, with zero mean and $E\{x_p^* x_p\} = 1$, $E\{x_s^* x_s\} = 1$. The transmit power at PT and ST is denoted as P_p and P_s respectively.

5.2.1 Outage Performance of Primary System

We consider a two-phase transmission protocol. In the first transmission phase, as shown by the solid lines in Figure 5.1, the primary signal x_p is transmitted by PT. Denoting the signals received by PR, ST, and SR in the first transmission phase as y_{11}, y_{21}, and y_{31} respectively, we have

$$y_{j1} = \sqrt{P_p} h_j x_p + n_{j1} \tag{5.1}$$

where $j = 1, 2, 3$. Here, $n_{j1} \sim \mathcal{CN}(0, \sigma^2)$ is the additive white Gaussian noise (AWGN) in the respective receivers for the first transmission phase. The achievable rate between PT and ST is thus given by

$$R_2 = \frac{1}{2} \log_2 \left(1 + \frac{P_p \gamma_2}{\sigma^2} \right),$$

where the factor of $\frac{1}{2}$ accounts for the fact that the overall transmission is being split into two phases. After reception in the first transmission phase, ST attempts to decode x_p. If the decoding is successful, ST regenerates x_p. A composite signal z_s is generated by linearly combining the regenerated signal x_p with power αP_s and the secondary signal x_s with power $(1 - \alpha)P_s$, where α $(0 \leq \alpha \leq 1)$ is the power allocation factor. Thus

$$z_s = \sqrt{\alpha P_s} x_p + \sqrt{(1 - \alpha) P_s} x_s.$$

In the second transmission phase, as depicted by the dotted lines in Figure 5.1, z_s is broadcasted and received by PR and SR. The signal received at PR is given by

$$y_{12} = h_4 z_s + n_{12} = \left(\sqrt{\alpha P_s} h_4 \right) x_p + \left(\sqrt{(1 - \alpha) P_s} h_4 \right) x_s + n_{12},$$

where $n_{12} \sim \mathcal{CN}(0, \sigma^2)$ is the AWGN at PR in the second transmission phase. Signals y_{11} and y_{12} are then combined at PR using MRC for the decoding of x_p. Note that the two-phase transmission of x_p can be written as an equivalent single-input-multiple-output (SIMO) channel, i.e., $\boldsymbol{y} = \boldsymbol{h} x_p + \boldsymbol{n}$, where $\boldsymbol{y} = [y_{11},\ y_{12}]^{\mathrm{T}}$, $\boldsymbol{h} = \left[\sqrt{P_p} h_1,\ \sqrt{\alpha P_s} h_4 \right]^{\mathrm{T}}$ and $\boldsymbol{n} = \left[n_{11},\ \sqrt{(1 - \alpha) P_s} h_4 x_s + n_{12} \right]^{\mathrm{T}}$. After normal-

izing the noise variances, we obtain

$$\tilde{\boldsymbol{y}} = \left[\frac{y_{11}}{\sqrt{\sigma^2}}, \frac{y_{12}}{\sqrt{\lambda}}\right]^{\mathrm{T}} = \tilde{\boldsymbol{h}} x_p + \tilde{\boldsymbol{n}} \tag{5.2}$$

where $\tilde{\boldsymbol{h}} = \left[\frac{\sqrt{P_p}h_1}{\sqrt{\sigma^2}}, \frac{\sqrt{P_s\alpha}h_4}{\sqrt{\lambda}}\right]^{\mathrm{T}}$, $\lambda = P_s(1-\alpha)\gamma_4 + \sigma^2$, and $E\{\tilde{\boldsymbol{n}}\tilde{\boldsymbol{n}}^{\mathrm{H}}|\boldsymbol{h}\} = \boldsymbol{I}_2$. The channel vector $\boldsymbol{h}$ can be estimated at PR by using standard preamble-aided channel estimation techniques[2], thus y_{11} and y_{12} are combined by MRC, and the achievable rate between PT and PR, conditioned on the successful decoding at ST, is given by

$$\begin{aligned} R_1^{\mathrm{MRC}} &= \frac{1}{2}\log_2\left(\det\left(\boldsymbol{I}_2 + \tilde{\boldsymbol{h}}\tilde{\boldsymbol{h}}^{\mathrm{H}}\right)\right) \\ &= \frac{1}{2}\log_2\left(1 + \frac{P_p\gamma_1}{\sigma^2} + \frac{P_s\alpha\gamma_4}{P_s(1-\alpha)\gamma_4 + \sigma^2}\right). \end{aligned} \tag{5.3}$$

On the other hand, when ST fails to decode in the first transmission phase, it will remain silent in the second transmission phase. In this case, it is still possible for PR to decode for x_p through the direct link from PT to PR, and the achievable rate between PT and PR is given by $R_1 = \log_2\left(1 + \frac{P_p\gamma_1}{\sigma^2}\right)$. The outage probability of the primary signal transmission with target rate R_{pt} is thus given as

$$\begin{aligned} P_{\mathrm{out}}^{p} &= \Pr\{R_2 > R_{pt}\}\Pr\left\{R_1^{\mathrm{MRC}} < R_{pt}\right\} + \Pr\{R_2 < R_{pt}\}\Pr\left\{\frac{1}{2}R_1 < R_{pt}\right\} \\ &= 1 - \Pr\{R_2 > R_{pt}\}\Pr\{R_1^{\mathrm{MRC}} > R_{pt}\} - \Pr\{R_2 < R_{pt}\}\Pr\left\{\frac{1}{2}R_1 > R_{pt}\right\} \end{aligned} \tag{5.4}$$

where the factor of $\frac{1}{2}$ in the second term above accounts for the fact that the overall transmission is being split into two phases. Since $\gamma_1 \sim \mathcal{E}(1)$ and $\gamma_2 \sim \mathcal{E}(d_2^{-\nu})$, we have

$$\Pr\left\{\frac{1}{2}R_1 > R_{pt}\right\} = \Pr\left\{\gamma_1 > \frac{\sigma^2}{P_p}\rho_1\right\} = \exp\left(-\frac{\sigma^2}{P_p}\rho_1\right), \tag{5.5}$$

[2]Note that PR does not need to have explicit knowledge of α as only the products $\sqrt{P_p}h_1$ and $\sqrt{\alpha P_s}h_4$ (the elements of $\boldsymbol{h}$) are required for MRC.

$$\Pr\{R_2 > R_{pt}\} = \Pr\left\{\gamma_2 > \frac{\sigma^2}{P_p}\rho_1\right\} = \exp\left(-d_2^{\nu}\frac{\sigma^2}{P_p}\rho_1\right), \tag{5.6}$$

where $\rho_1 = 2^{2R_{pt}} - 1$. Assuming $P_s \gg \sigma^2$, we obtain

$$\begin{aligned}\Pr\{R_1^{\mathrm{MRC}} > R_{pt}\} &\approx \Pr\left\{\frac{1}{2}\log_2\left(1 + \frac{P_p\gamma_1}{\sigma^2} + \frac{\alpha}{1-\alpha}\right) > R_{pt}\right\} \\ &= \begin{cases} \exp\left(-\frac{\sigma^2}{P_p}\left(\rho_1 - \frac{\alpha}{1-\alpha}\right)\right) & 0 \le \alpha < \widehat{\alpha} \\ 1 & \widehat{\alpha} \le \alpha \le 1 \end{cases}\end{aligned} \tag{5.7}$$

where $\widehat{\alpha} = \frac{\rho_1}{\rho_1+1}$. Substituting (5.5), (5.6) and (5.7) into (5.4), we have

$$P_{\mathrm{out}}^{p} \approx \begin{cases} P_{\mathrm{out}}^{p,1} & 0 \le \alpha < \widehat{\alpha} \\ P_{\mathrm{out}}^{p,2} & \widehat{\alpha} \le \alpha \le 1 \end{cases} \tag{5.8}$$

where

$$P_{\mathrm{out}}^{p,1} = 1 - \exp\left(-\frac{\sigma^2}{P_p}\left((d_2^{\nu}+1)\rho_1 - \frac{\alpha}{1-\alpha}\right)\right) - \exp\left(-\frac{\sigma^2}{P_p}\rho_1\right) + \exp\left(-\frac{\sigma^2}{P_p}\rho_1(d_2^{\nu}+1)\right)$$

and

$$P_{\mathrm{out}}^{p,2} = 1 - \exp\left(-d_2^{\nu}\frac{\sigma^2}{P_p}\rho_1\right) - \exp\left(-\frac{\sigma^2}{P_p}\rho_1\right) + \exp\left(-\frac{\sigma^2}{P_p}\rho_1(d_2^{\nu}+1)\right).$$

5.2.2 Critical Radius from Primary Transmitter

Consider the scenario where the secondary system does not exist. In this case, x_p is transmitted through the direct link from PT to PR. The outage probability of the primary system with target rate R_{pt} in the absence of secondary access is thus given as

$$P_{\mathrm{out}}^{n} = \Pr\{R_1 < R_{pt}\} = 1 - \exp\left(-\frac{\sigma^2}{P_p}\rho_2\right) \tag{5.9}$$

where $\rho_2 = 2^{R_{pt}} - 1$.

We want to ensure that the outage probability of the primary system under the proposed scheme is equal to or smaller than the outage probability without

spectrum sharing, i.e.,

$$P_{\text{out}}^{p} \leq P_{\text{out}}^{n}. \tag{5.10}$$

From (5.8), we consider the spectrum sharing requirement in (5.10) for the following two cases.

Case 1: $\widehat{\alpha} \leq \alpha \leq 1$.

Substituting $P_{\text{out}}^{p,2}$ and (5.9) into (5.10), we obtain

$$d_2 \leq d_2^* = \left[\frac{P_p}{\rho_1 \sigma^2} \ln\left(\frac{\Phi_1 - 1}{\Phi_1 - \Phi_2}\right)\right]^{\frac{1}{\nu}} \tag{5.11}$$

where $\Phi_1 = \exp\left(-\frac{\sigma^2}{P_p}\rho_1\right)$ and $\Phi_2 = \exp\left(-\frac{\sigma^2}{P_p}\rho_2\right)$. Thus, as long as $d_2 \leq d_2^*$ and $\widehat{\alpha} \leq \alpha \leq 1$, we can achieve secondary access while satisfying (5.10). We draw the region that satisfies these two inequalities in a d_2-α plane and denote it as Region 1 in Figure 5.2.

Case 2: $0 \leq \alpha < \widehat{\alpha}$.

Substituting $P_{\text{out}}^{p,1}$ and (5.9) into (5.10), we obtain

$$\alpha \geq \alpha^* = \frac{P_p \ln\left(1 + \frac{\Phi_2 - \Phi_1}{\Phi_3}\right)}{P_p \ln\left(1 + \frac{\Phi_2 - \Phi_1}{\Phi_3}\right) + \sigma^2}. \tag{5.12}$$

where $\Phi_3 = \exp\left(-\frac{\sigma^2}{P_p}(d_2^{\nu} + 1)\rho_1\right)$. Note that α^* is monotonously increasing with respect to d_2 and it is easy to show that $\alpha^* \leq \widehat{\alpha}$ (equality holds when $d_2 = d_2^*$) when $d_2 \leq d_2^*$. Thus, as long as $d_2 < d_2^*$ and $\alpha^* \leq \alpha < \widehat{\alpha}$, (5.10) is satisfied. The region that satisfies these two inequalities is drawn in Figure 5.2 and is denoted as Region 2.

Combining Case 1 and Case 2, under the assumption of $P_s \gg \sigma^2$, we obtain the "critical region" of the proposed scheme, which is the union of Region 1 and Region 2 in Figure 5.2. The interpretation of this critical region is that there exists a critical radius d_2^* from PT such that as long as ST is located within this radius, i.e., $d_2 \leq d_2^*$, we can always find a suitable power allocation factor α between α^* and 1 to ensure that (5.10) is satisfied.

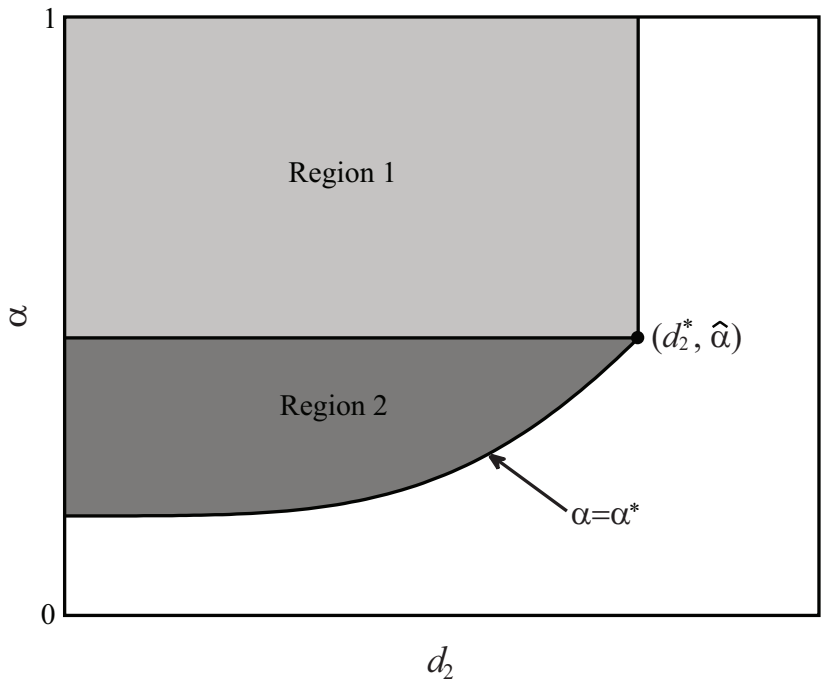

Figure 5.2. Diagram of critical region for proposed scheme.

5.2.3 Outage Performance of Secondary System

We now consider the processing at SR and obtain the outage probability of the secondary system. In the first transmission phase, the signal received at SR is given as

$$y_{31} = \sqrt{P_p} h_3 x_p + n_{31}.$$

The achievable rate between PT and SR is thus given as

$$R_3 = \frac{1}{2} \log_2 \left(1 + \frac{P_p \gamma_3}{\sigma^2} \right).$$

After the reception of y_{31}, SR attempts to decode x_p, and stores the decoding result if it succeeds.

In the second transmission phase, the signal received at SR is

$$\begin{aligned} y_{32} &= h_5 y_{22} + n_{32} \\ &= \left(\sqrt{\alpha P_s} h_5 \right) x_p + \left(\sqrt{(1-\alpha) P_s} h_5 \right) x_s + n_{32}. \end{aligned} \tag{5.13}$$

Here, $n_{32} \sim \mathcal{CN}(0, \sigma^2)$ is the AWGN at SR in the second transmission phase. Assuming the decoding of x_p at SR in the first transmission phase is successful, the interference component $\sqrt{\alpha P_s} h_5 x_p$ can be canceled out from (5.13) to obtain

$$y'_{32} = \left(\sqrt{(1-\alpha)P_s} h_5\right) x_s + n_{32}.$$

The achievable rate between ST and SR, conditioned on successful decoding of x_p at both ST and SR in the first transmission phase, is given as

$$R_5 = \frac{1}{2}\log_2\left(1 + \frac{P_s(1-\alpha)\gamma_5}{\sigma^2}\right).$$

Note that if ST or SR (or both) is not able to decode x_p, an outage is declared for the secondary system. Thus the outage probability of the secondary system transmission with target rates R_{pt} and R_{st} for primary and secondary systems respectively, is given by

$$\begin{aligned} P^s_{\text{out}} &= 1 - \Pr\{R_2 > R_{pt}\}\Pr\{R_3 > R_{pt}\}\Pr\{R_5 > R_{st}\} \\ &= 1 - \exp\left(-\left(\frac{\sigma^2(d_2^{\nu} + d_3^{\nu})\rho_1}{P_p} + \frac{\sigma^2 d_5^{\nu}\rho_3}{P_s(1-\alpha)}\right)\right) \end{aligned} \tag{5.14}$$

where $\rho_3 = 2^{2R_{st}} - 1$.

5.2.4 Observations and Remarks

We can observe from $P^{p,1}_{\text{out}}$ in (5.8) that with increasing α for $\alpha < \widehat{\alpha}$, more power at ST is allocated for relaying the primary signal and thus P^p_{out} decreases. However when $\alpha \geq \widehat{\alpha}$, P^p_{out} becomes independent of α and attains a constant minimum value. On the other hand, as can be observed from (5.14), with increasing α, less power at ST is used for x_s which causes an increase in P^s_{out}. This means that increasing α beyond $\widehat{\alpha}$ is counterproductive as it will only serve to increase P^s_{out} without any corresponding improvement in P^p_{out}. Thus, we should choose a power allocation factor in the range $\alpha^* \leq \alpha < \widehat{\alpha}$ to achieve an efficient outage performance tradeoff between primary and secondary systems while ensuring that (5.10) is satisfied. Supposing our goal is to minimize the outage probability of the primary system, it is obvious that the optimal power allocation factor is $\alpha = \widehat{\alpha}$.

Furthermore, it is worth noting that d_2^*, α^*, and $\widehat{\alpha}$ are independent of instantaneous channel realizations and can be easily obtained by ST. For instance, R_{pt} can be known by overhearing the communications between PT and PR during link setup and d_2 by channel estimation[3]. This simplicity is especially attractive for practical implementation.

Comparing (5.8) and (5.14), we can also observe that P_{out}^p is independent of P_s and d_5 for $P_s \gg \sigma^2$, while P_{out}^s decreases with increasing P_s and decreasing d_5. Thus for a given α, we can lower the outage probability of the secondary system, without affecting the outage probability of the primary system, by either increasing P_s or decreasing d_5.

5.3 Simulation Results and Discussions

We show the critical regions of the proposed scheme defined by (5.11) and (5.12) in a d_2-α plane for different R_{pt} in Figure 5.3 with a path loss exponent $\nu = 4$. It can be observed from Figure 5.3 that with decreased R_{pt}, the critical region becomes larger, which indicates that when the primary system has a lower performance requirement, secondary systems which are farther away from the primary transmitter are able to benefit from the proposed spectrum sharing scheme and the cooperating secondary system can allocate more power for its own transmission without deteriorating the primary system performance.

We consider the outage probabilities of the primary and secondary systems under different settings. We choose target rates $R_{pt} = R_{st} = 1$. The path loss exponent remains at $\nu = 4$, and $\frac{P_p}{\sigma^2} = \frac{P_s}{\sigma^2} = 20$ dB. For ease of presentation, we considered a system topology where PT, PR, ST, and SR are collinear. As shown in Figure 5.4, in a two-dimensional X-Y plane, PT and PR are located at points $(0, 0)$ and $(1, 0)$ respectively, thus $d_1 = 1$. ST moves on the positive X axis, whereas SR is located in the middle of PT and ST. Therefore, $d_4 = |1 - d_2|$ and $d_3 = d_5 = \frac{1}{2}d_2$. In Figure 5.5, we show both the theoretical and simulation results

[3]By measuring the average channel gain $\bar{\gamma}_2$ of PT-ST link, and overhearing the primary control signal regarding the average channel gain $\bar{\gamma}_1$ of PT-PR link, d_2 can be simply obtained by $d_2 = \left(\frac{\bar{\gamma}_1}{\bar{\gamma}_2}\right)^{\frac{1}{\nu}}$. We presume that, like most modern wireless systems, the primary system utilizes a feedback link for channel state information.

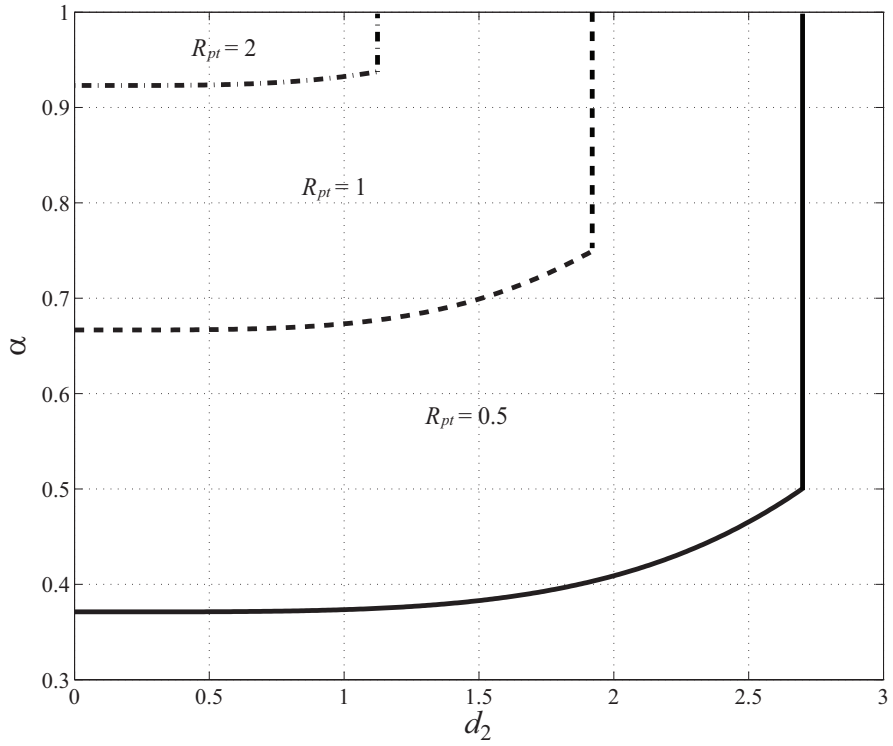

Figure 5.3. Critical regions for the proposed scheme for various values of R_{pt}.

of the outage probabilities for $d_2 = 0.5$, $d_2 = 1.2$, and $d_2 = d_2^* = 1.92$, as the power allocation factor α is varied.

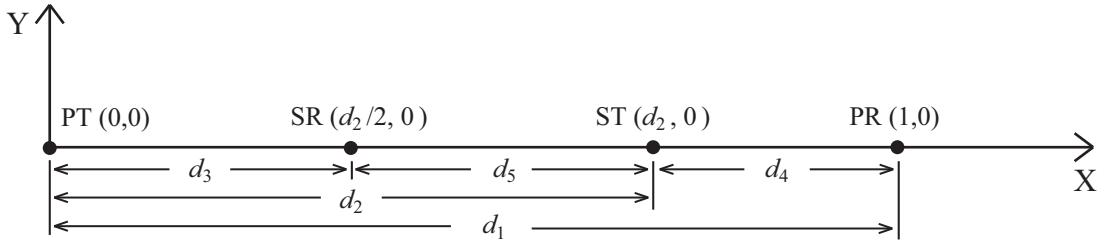

Figure 5.4. Locations of primary and secondary terminals.

From Figure 5.5 we can observe that the theoretical results agree excellently with the simulation results. When $\alpha < \widehat{\alpha} = 0.75$, the outage probability P_{out}^{p} decreases with increasing α, which is intuitively satisfying because more power is allocated at ST for the relaying of primary signal and less power is used for the transmission of secondary signal (which constitutes interference to the primary

system). However, an outage probability floor for P_{out}^{p} appears when $\alpha > \widehat{\alpha}$. This is because when α approaches unity, $\Pr\{R_1^{\text{MRC}} < R_{pt}\}$ becomes small, and the successful decoding at ST and PR in the first transmission phase becomes the limiting factor for primary system, i.e., $P_{\text{out}}^{p} \to \Pr\{R_2 < R_{pt}\}\Pr\{\frac{1}{2}R_1 < R_{pt}\}$. Thus increasing α further cannot reduce the outage probability of the primary system. This fact can also be analytically deduced from (5.8) as discussed in Section 5.2.4. Furthermore, since $\Pr\{R_2 < R_{pt}\}$ becomes larger with increasing d_2, the outage probability floor for P_{out}^{p} becomes higher with increasing d_2. Finally, when $d_2 = d_2^*$, the outage probability floor coincides with P_{out}^{n} which indicates that with $d_2 > d_2^*$, the proposed scheme is not able to satisfy the spectrum sharing requirement in (5.10).

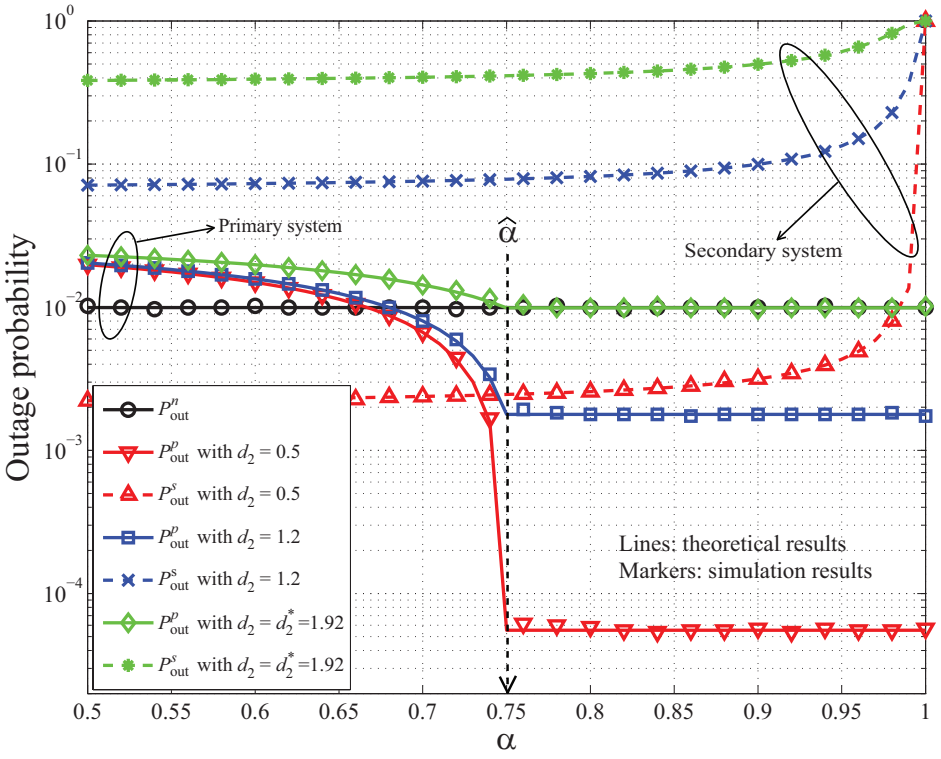

Figure 5.5. Outage probability comparison for $d_2 = 0.5$, $d_2 = 1.2$, and $d_2 = d_2^* = 1.92$.

For $d_2 = 0.5$, it is obvious that with $\alpha > \alpha^* = 0.67$, we have $P_{\text{out}}^{p} < P_{\text{out}}^{n}$ and the outage probability floor of P_{out}^{p} is lower than P_{out}^{n}. Thus, we are able to satisfy the spectrum sharing requirement in (5.10). Furthermore, P_{out}^{s} achieves reasonable values (except when α is close to 1) which indicates that with our

proposed spectrum sharing scheme, the secondary system is able to gain secondary spectrum access while providing the primary system a significant performance gain in terms of outage probability. Although not shown in Figure 5.5, with $d_2 < 0.5$, both primary and secondary systems achieve even better outage performance.

In Figure 5.6, we show the effect of P_s and d_5 on the outage performance of the primary and secondary systems. Again, we assume $R_{pt} = R_{st} = 1$ and $\nu = 4$. Here we choose $\alpha = \widehat{\alpha} = 0.75$, and fix $d_2 = d_3 = d_4 = 0.5$. We consider two different values for d_5. For each case, we fix $\frac{P_p}{\sigma^2} = 20$ dB and vary $\frac{P_s}{\sigma^2}$ from 10 dB to 30 dB.

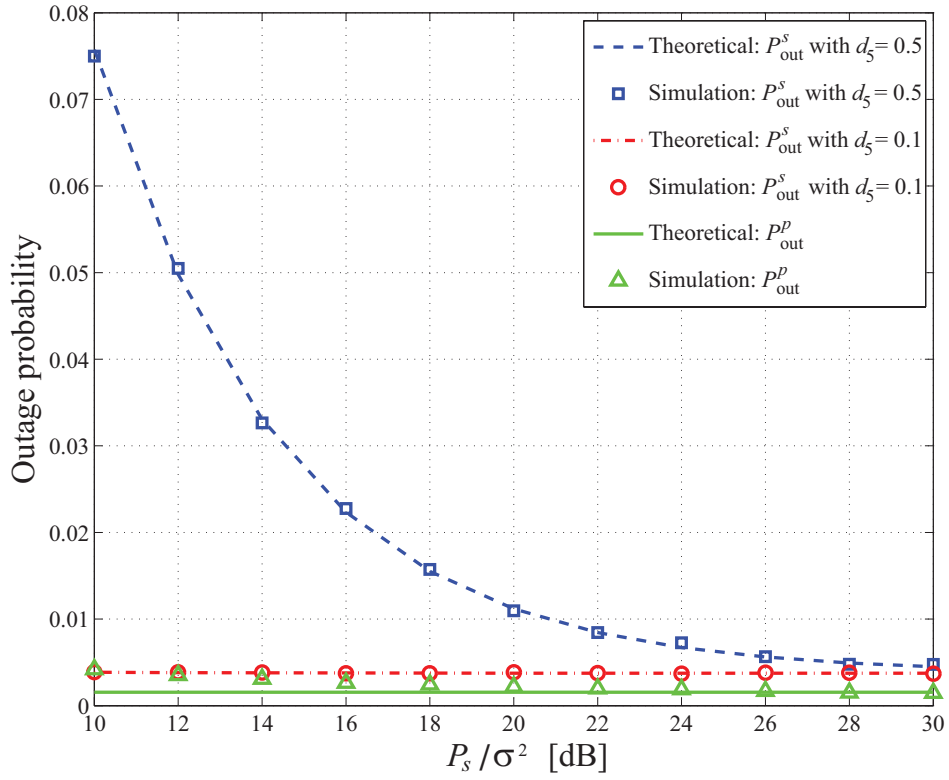

Figure 5.6. Outage probability for various values of P_s/σ^2.

From Figure 5.6, we can again observe that the theoretical results for P^s_{out} agree well with the simulation results, and the small gap between the theoretical and simulation results for P^p_{out} when P_s is small comes from the approximation we made in (5.7), which holds better for large P_s. It can be observed that while P^p_{out} is independent of d_5 and P_s (for $P_s \gg \sigma^2$), P^s_{out} is significantly affected by both

P_s and d_5. Specifically, when $d_5 = 0.1$ which corresponds to the scenario where ST and SR are located close to each other, the ST→SR channel gain is high and $\Pr\{R_5 < R_{st}\} \to 0$. Thus $P^s_{\text{out}} \approx 1 - \exp\left(-\frac{\sigma^2(d_2^\nu + d_3^\nu)\rho_1}{P_p}\right)$ which is independent of P_s. On the other hand, when $d_5 = 0.5$, the outage probability $\Pr\{R_5 < R_{st}\}$ is not negligible and by increasing P_s, $\Pr\{R_5 < R_{st}\}$ decreases significantly, causing a decrease in P^s_{out} which finally converges to $1 - \exp\left(-\frac{\sigma^2(d_2^\nu + d_3^\nu)\rho_1}{P_p}\right)$. We note that in the case where d_5 is small, very low outage probability P^s_{out} can be achieved, even with a small value of P_s, without affecting the outage performance of the primary system.

5.4 Secondary User Selection Based on Statistical Channel Information

5.4.1 Introduction

In this section, we study the proposed spectrum sharing protocol in a more general multi-user scenario and present a distributed secondary user selection scheme with statistical channel information which optimizes the performance for primary system. In our system model, the primary system comprises of a primary transmitter (PT) and primary receiver (PR). The secondary system comprises of M secondary transmitter-receiver pairs $\text{ST}_i - \text{SR}_i$, $i \in \{1, 2, \cdots, M\}$.

The best secondary user pair $\text{ST}_b - \text{SR}_b$, $b \in \{1, 2, \cdots, M\}$ which is able to provide the minimum outage probability for the primary system, is selected from the overall M pairs to access the spectrum band with ST_b serving as a cooperative decode-and-forward relay for the primary system. We will show later in this chapter that unlike [97], the secondary user selection in our proposed protocol is performed in a distributed fashion, thus the selection is totally oblivious to the primary system and no explicit communication between different secondary user pairs is required. Furthermore, the selection is done based on the knowledge or estimation of distance between PT to ST_i [103], which can be obtained locally by ST_i through 1) infrastructure for distance measurement (e.g., GPS receiver at ST_i) or 2) distance estimation with received average SNR. Thus no instantaneous channel state information (CSI) is required at ST_i.

The transmission from PT to PR with the cooperation of the secondary system is accomplished in two transmission phases. In the first phase, the primary signal transmitted by PT to PR is also received by ST_i and SR_i $\forall i$. As soon as PT finishes its transmission, each ST_i evaluates its achievable performance for the primary system by relaying the primary signal and starts a timer. The initial value of the timer is related to its geographical distance to PT [24]. Let ST_b be the node whose timer expires first among all ST_i. Then ST_b transmits a short *flag* signal, identifying its presence to both the primary and secondary systems. This *flag* informs PT−PR that a relay exists and is ready to cooperate in primary transmission. Upon receiving the *flag* signal from ST_b, all the unselected secondary user pairs ST_i−SR_i, $i = \{1, 2, \cdots, M\}\backslash\{b\}$ back off and remain silent. On the other hand, both PR and SR_b are aware that ST_b is selected and they will continue to receive in the second transmission phase. ST_b accesses the spectrum band with the proposed spectrum sharing protocol (Section 5.2) in the following two transmission phases. For simplicity of derivation, we assume the *flag* signal is short and well protected by coding/modulation, thus its transmission is instantaneous and error free.

In the proposed protocol, the primary system only has to be aware of a "decode-and-forward relaying with relay selection" operation. The switch to a relaying mode can be easily conveyed to the primary system through the use of control messages. Furthermore, the primary system is also totally oblivious to the distributed secondary user (relay) selection. From the perspective of the primary system, ST_b acts as a decode-and-forward relay and appears to be part of a conventional cooperative communication system.

5.4.2 Protocol Description and Performance Analysis

The system configuration of the proposed scheme is shown in Figure 5.7. The channels over links PT→PR, PT→ST_i, PT→SR_i, ST_i→PR, and ST_i→SR_i are modeled to be Rayleigh flat fading with channel coefficients denoted by h_1, $h_{2,i}$, $h_{3,i}$, $h_{4,i}$, and $h_{5,i}$ respectively, where $i \in \{1, 2, \cdots, M\}$. We assume $h_1 \sim \mathcal{CN}(0, d_1^{-\nu})$, where ν is the path loss exponent and d_1 is the normalized distance between PT and PR. Similarly, we have $h_{j,i} \sim \mathcal{CN}(0, d_{j,i}^{-\nu})$, $j \in \{2, 3, 4, 5\}$, where $d_{j,i}$ is the

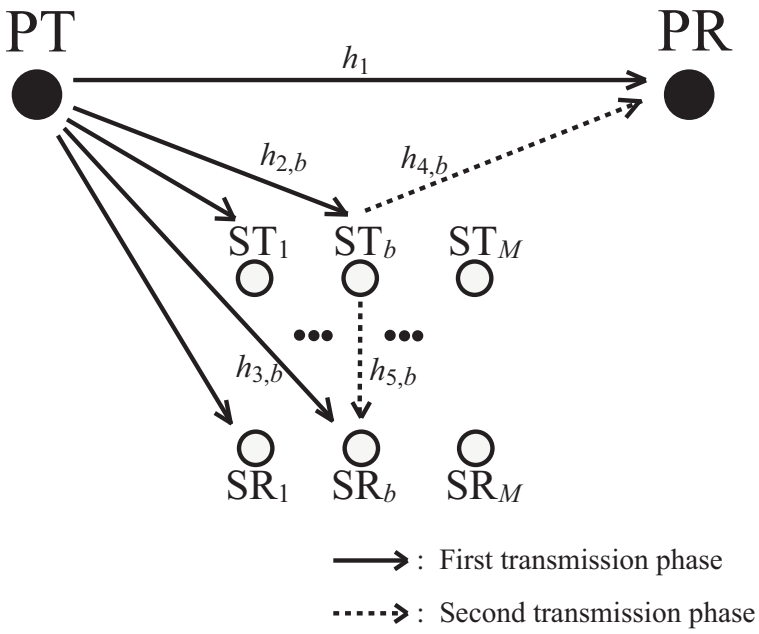

Figure 5.7. System configuration.

normalized distance between the respective transmitters and receivers. Without loss of generality, we assume this normalization is done with respect to the distance between PT and PR, thus $d_1 = 1$. We also denote $\gamma_1 = |h_1|^2$ and $\gamma_{j,i} = |h_{j,i}|^2$.

Let x_p and $x_{s,i}$ denote the primary signal and the secondary signal of ST_i respectively, with zero mean and $E\{x_p^* x_p\} = 1$, $E\{x_{s,i}^* x_{s,i}\} = 1$. The transmit power at PT and ST_i is denoted as P_p and P_s respectively. The variances of the additive white Gaussian noise (AWGN) at all receivers are assumed to be identical and denoted as σ^2.

In the following, we first derive the outage probability of the primary system with ST_i serving as a cooperative decode-and forward relay. Then we show that by applying the proposed secondary user selection scheme, i.e., when $i = b$, the outage probability for the primary system is minimized.

Following the derivations in Section 5.2.1, the outage probability of the primary signal transmission with ST_i serving as a relay and a target rate R_{pt}, is given by

$$P_{\mathrm{out}}^{p,i} \approx \begin{cases} P_{\mathrm{out},1}^{p,i} & 0 \le \alpha < \widehat{\alpha} \\ P_{\mathrm{out},2}^{p,i} & \widehat{\alpha} \le \alpha \le 1 \end{cases} \tag{5.15}$$

where

$$\begin{aligned} P_{\text{out},1}^{p,i} &= 1-\exp\left(-\frac{\sigma^2}{P_p}\left((d_{2,i}^{\nu}+1)\rho_1-\frac{\alpha}{1-\alpha}\right)\right) \\ &\quad -\exp\left(-\frac{\sigma^2}{P_p}\rho_1\right)+\exp\left(-\frac{\sigma^2}{P_p}\rho_1(d_{2,i}^{\nu}+1)\right) \end{aligned}$$

and

$$P_{\text{out},2}^{p,i}=1-\exp\left(-d_{2,i}^{\nu}\frac{\sigma^2}{P_p}\rho_1\right)-\exp\left(-\frac{\sigma^2}{P_p}\rho_1\right)+\exp\left(-\frac{\sigma^2}{P_p}\rho_1(d_{2,i}^{\nu}+1)\right).$$

It is clear from (5.15) that given a fixed α at all ST_i, $P_{\text{out}}^{p,i}$ is only dependent on $d_{2,i}$ and

$$\arg\min_i P_{\text{out}}^{p,i}=\arg\min_i d_{2,i}. \tag{5.16}$$

Thus selecting the best secondary user pair which provides the minimum outage probability for the primary system is equivalent to selecting the pair whose transmitter has the smallest geographical distance to PT or equivalently the largest average channel gain.

At each ST_i, information regarding $d_{2,i}$ can be obtained through 1) infrastructure for distance measurement (e.g., GPS receiver at ST_i) or 2) distance estimation with received average SNR. As soon as PT finishes its transmission in the first transmission phase, ST_i starts a count-down timer with initial value

$$T_i=\frac{d_{2,i}}{C} \tag{5.17}$$

where C is a normalization constant. It is obvious from (5.16) and (5.17) that ST_b, where $b=\arg\min_i T_i$, minimizes the outage probability for the primary system.

Therefore the best secondary transmitter ST_b has its timer reduced to zero first, and it broadcasts a *flag* signal accordingly to identify its presence. The rest of ST_i, $i=\{1,2,\cdots,M\}\setminus\{b\}$ will overhear the *flag* signal from ST_b and remain silent in the second transmission phase. Note that the proposed secondary user selection scheme is performed in a distributed fashion and thus it is totally oblivious to the primary system. In contrast, secondary users are selected by the primary system for spectrum leasing in [97].

It is clear that as long as ST_b is located within the critical radius from PT, distance, i.e., $d_{2,b} \leq d_2^*$, we can always apply a suitable power allocation factor α between α^* and 1 at ST_b to ensure that the outage performance of the primary system is not adversely affected.

Similarly, the outage probability of the secondary system transmission with target rate R_{st}, is given by

$$\begin{aligned} P_{\text{out}}^{s,i} &= 1 - \Pr\{R_{2,i} > R_{pt}\}\Pr\{R_{3,i} > R_{pt}\}\Pr\{R_{5,i} > R_{st}\} \\ &= 1 - \exp\left(-\left(\frac{\sigma^2(d_{2,i}^{\nu} + d_{3,i}^{\nu})\rho_1}{P_p} + \frac{\sigma^2 d_{5,i}^{\nu}\rho_3}{P_s(1-\alpha)}\right)\right) \end{aligned} \tag{5.18}$$

where $\rho_3 = 2^{2R_{st}} - 1$. From (5.18), it is clear that although $P_{\text{out}}^{s,i}$ decreases with a decreasing $d_{2,i}$, it may not be minimized by $i = b$, since $d_{3,i}$ and $d_{5,i}$ may not achieve their minimum with $i = b$. This observation indicates that while the proposed secondary user selection scheme minimizes the outage probability for the primary system, the outage performance for the secondary system is not optimized.

5.4.3 Simulation Results and Discussions

We first show the outage probabilities of the primary and secondary systems when there is only one secondary user pair $\mathrm{ST}_1 - \mathrm{SR}_1$, i.e., $M = 1$. In this case, no secondary user selection is needed. We choose target rates $R_{pt} = R_{st} = 1$. The path loss exponent $\nu = 4$, and $\frac{P_p}{\sigma^2} = \frac{P_s}{\sigma^2} = 20$ dB. For ease of presentation, we considered a system topology where PT, PR, ST_1, and SR_1 are collinear. As shown in Figure 5.4, in a two-dimensional X-Y plane, PT and PR are located at points $(0, 0)$ and $(1, 0)$ respectively, thus $d_1 = 1$. ST_1 moves on the positive X axis, whereas SR_1 is located in the middle of PT and ST_1. Therefore, $d_{4,1} = |1 - d_{2,1}|$ and $d_{3,1} = d_{5,1} = \frac{1}{2}d_{2,1}$. In Figure 5.8, we show both the theoretical and simulation results of the outage probabilities for $\alpha = 0.5$, $\alpha = \widehat{\alpha} = 0.75$, and $\alpha = 0.9$, as the distance $d_{2,1}$ is varied.

From Figure 5.8, similar observations as in Figure 5.5 can be made. Specifically, it is obvious that $P_{\text{out}}^{p,1}$ with $\alpha = \widehat{\alpha} = 0.75$ is lower than that with $\alpha = 0.5$. An outage probability floor for $P_{\text{out}}^{p,1}$ appears when $\alpha > \widehat{\alpha}$, and we can observe that the curve for $P_{\text{out}}^{p,1}$ with $\alpha = 0.9$ overlaps with that with $\alpha = \widehat{\alpha} = 0.75$. This observation

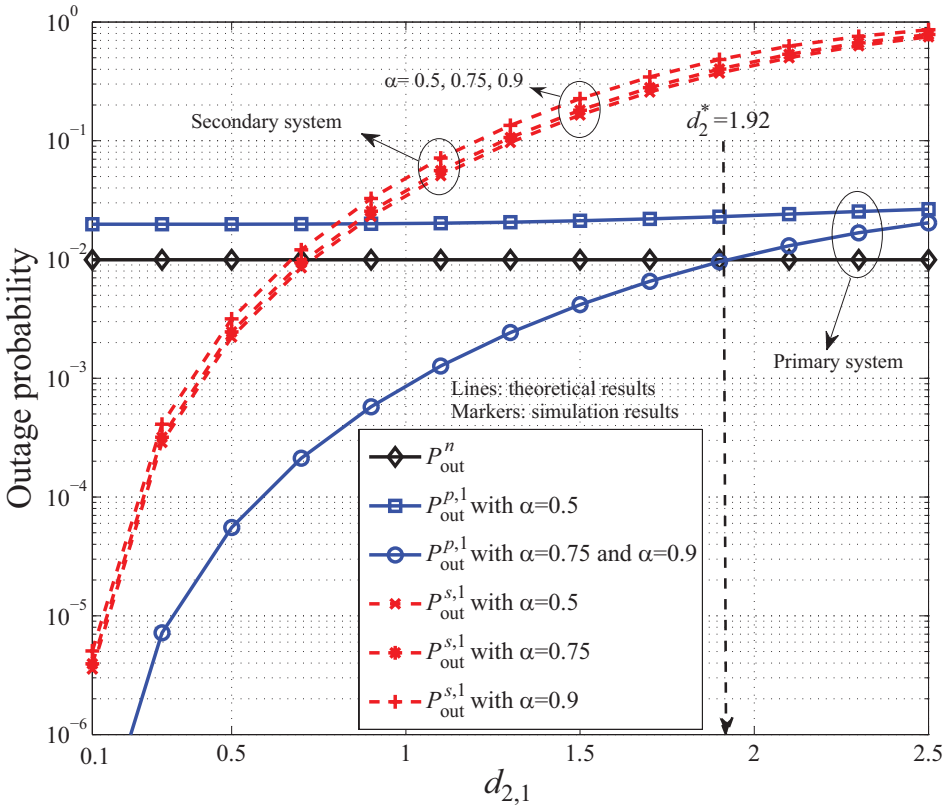

Figure 5.8. Outage probability comparison with $M = 1$. Three cases where $\alpha = 0.5$, $\alpha = \hat{\alpha} = 0.75$, and $\alpha = 0.9$ are considered.

indicates that increasing α further cannot reduce the outage probability of the primary system. This fact can also be analytically deduced from (5.15) as discussed in Section 5.4.2.

Furthermore, we can observe that both $P_{\text{out}}^{p,1}$ and $P_{\text{out}}^{s,1}$ increase with increasing $d_{2,1}$. Since $\Pr\{R_{2,1} < R_{pt}\}$ becomes larger with increasing $d_{2,1}$, the outage probability for $P_{\text{out}}^{p,1}$ becomes higher with increasing $d_{2,1}$. Finally, when $d_{2,1} = d_2^*$, it can be observed from Figure 5.8 that $P_{\text{out}}^{p,1}$ coincides with P_{out}^{n} which indicates that with $d_{2,1} > d_2^*$, the proposed protocol is not able to satisfy the spectrum sharing requirement in (5.10). On the other hand, $P_{\text{out}}^{s,1}$ achieves reasonable values (except when $d_{2,1}$ becomes large) which indicates that with our proposed spectrum sharing scheme, the secondary system is able to gain spectrum access while providing the primary system a significant performance gain in terms of outage probability.

In Figure 5.9, we show $P_{\text{out}}^{p,b}$ and $P_{\text{out}}^{s,b}$ with our proposed secondary user selection scheme given different values of M. We assume that PT and PR are located

at points $(0,0)$ and $(1,0)$ respectively, and $M \geq 1$ secondary user transmitters ST_i, $i \in \{1,2,\cdots,M\}$, are uniformly distributed within a circular area of radius $d_2^* = 1.92$ from PT. Furthermore, we assume SR_i is uniformly distributed on the circumference of a circle with center ST_i and radius 0.3, thus we have $d_{5,i} = 0.3\ \forall i$. We let $\frac{P_p}{\sigma^2} = \frac{P_s}{\sigma^2} = 20$ dB, $R_{pt} = R_{st} = 1$, $\nu = 4$, and $\alpha = \widehat{\alpha} = 0.75$. For comparison purposes, we also show $P_{\text{out}}^{p,r}$ and $P_{\text{out}}^{s,r}$, which denote the outage probabilities for the primary and secondary systems with a random secondary user selection scheme, as well as P_{out}^{n}. All the outage probabilities in Figure 5.9 are averaged through 10^5 secondary user distributions.

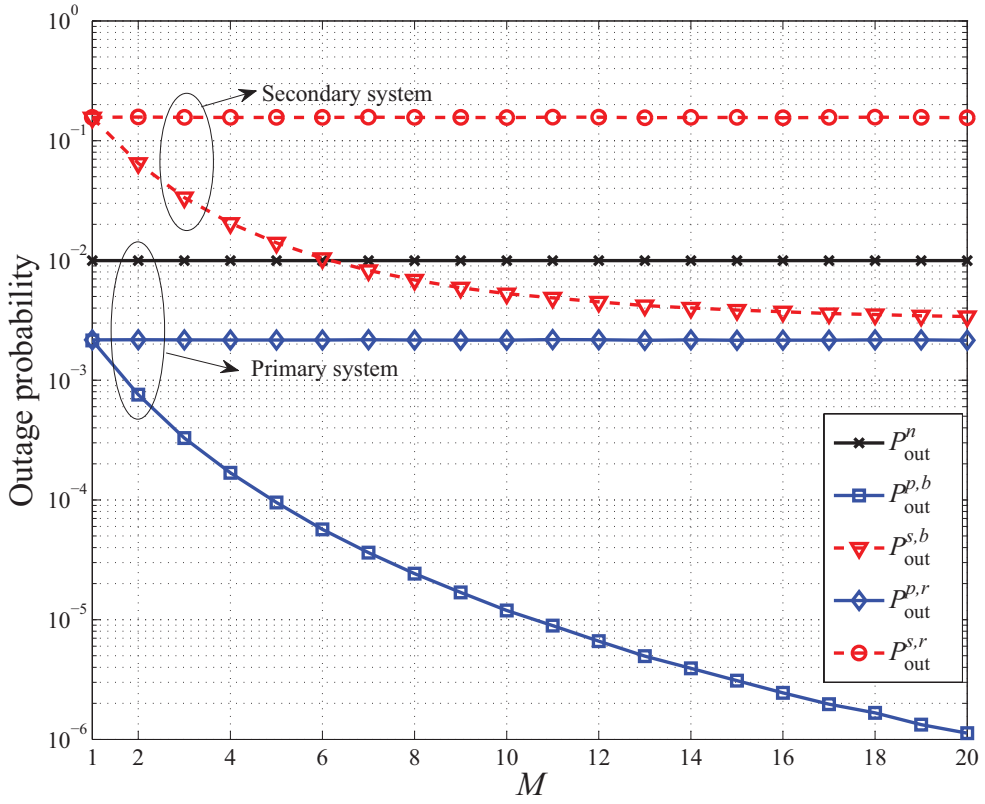

Figure 5.9. Outage probability for various values of M.

From Figure 5.9, it is clear that both $P_{\text{out}}^{p,b}$ and $P_{\text{out}}^{p,r}$ achieve smaller values than P_{out}^{n}, indicating the efficiency of the proposed spectrum sharing protocol in improving the outage performance for the primary system when the secondary transmitter is located within the critical distance d_2^* from PT. Furthermore, while $P_{\text{out}}^{p,r}$ and $P_{\text{out}}^{s,r}$ are independent of M, $P_{\text{out}}^{p,b}$ and $P_{\text{out}}^{s,b}$ decrease with M and are much smaller than

$P_{\text{out}}^{p,r}$ and $P_{\text{out}}^{s,r}$ with $M > 1$, respectively. This observation indicates that the proposed secondary user selection scheme benefits both the primary and secondary systems, which can also be easily observed from (5.15) and (5.18). However, the improvement of $P_{\text{out}}^{s,b}$ diminishes when M is large, because in this case the distance $d_{5,b} = 0.3$ becomes the limiting factor of the outage performance for the secondary system.

5.5 Summary

We presented a protocol where a secondary transmitter applies decode-and-forward relaying to transmit the primary signal along with its own secondary signal, such that the outage performance of the primary system is not affected. We derived a critical distance from the primary transmitter to the secondary transmitter. A secondary transmitter within this critical distance can properly choose the fraction of the transmit power to be allocated for relaying the primary signal so as to meet the outage probability requirement of the primary system, and at the same time achieves secondary spectrum access.

Furthermore, under a multi-user scenario, we proposed a distributed secondary user selection scheme to select the secondary user pair whose transmitter has the smallest geographical distance (average channel gain) to the primary transmitter for spectrum access. We show that the proposed secondary user selection scheme not only minimizes the outage probability for the primary system but also reduces the outage probability for the secondary system. Outage performance for both primary and secondary systems improves with increasing number of secondary transmitter-receiver pairs.

Chapter 6

Cooperative Spectrum Sharing Protocol with Two-step Distributed Secondary User Selection

6.1 Introduction

Unlike the protocols proposed in Chapter 4 and Chapter 5 where a single secondary user achieves the spectrum access by partially performing as a cooperative relay for the primary system, in this chapter we consider a more general multi-user scenario and propose a cooperative spectrum sharing protocol with two-step distributed secondary user selection. In this protocol, one secondary transmitter is first selected to serve as a cooperative relay for the primary system, and another secondary transmitter which maximizes the achievable rate of the secondary system is then selected to access the spectrum band along with the primary system.

The system configuration is shown in Figure 6.1. The primary system, comprising of a primary transmitter (PT) and primary receiver (PR), supports the relaying functionality [3]. In the secondary system, M secondary transmitters ST_i where $i \in \mathcal{M} = \{1, 2, \cdots, M\}$ communicate with a common secondary receiver SR, with the constraint that its operation does not adversely affect the primary system performance. We quantify the primary system priority in terms of its outage probability. Again, in this chapter, we assume that the secondary system has the

intelligence to emulate the radio protocols (e.g., channel coding, synchronization, etc.) of the primary system [45].

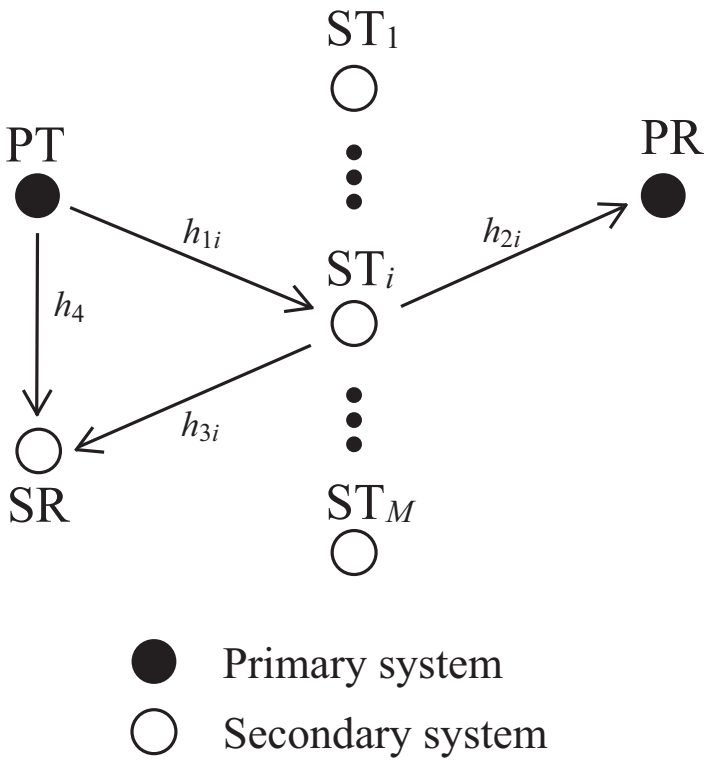

Figure 6.1. System model for proposed spectrum sharing protocol.

In the proposed spectrum sharing protocol, the secondary user selection stage consists of two steps. In the first step, one secondary transmitter ST_p is selected to assist (relay) the primary transmission in achieving a request target rate (if possible). With the cooperation of ST_p, the primary system is then able to tolerate some interference lower than a certain threshold in the relaying phase, without compromising its outage performance. In the second step, another secondary transmitter ST_s is then selected to access the spectrum simultaneously with ST_p in the relaying phase (if possible). Note that the second step is performed conditioned on the successful completion of the first step. Furthermore, ST_s has to comply with an interference constraint to ensure that the outage performance of the primary system is not degraded as compared to the case where there is no secondary spectrum access. Under this interference constraint, ST_s is selected such that the outage performance for the secondary system is optimized.

In the above two-step secondary user selection, we apply a control signal handshake scheme similar to the selective relaying protocol in [24, 104]. Specifically, with the assistance of control message exchange, a count-down timer mechanism is applied to select ST_p and ST_s in a distributed manner, and the whole selection process is accomplished in a secondary user selection window (SUSW) before data transmission begins. If the selections for both ST_p and ST_s succeed, cooperative DF relaying transmission for primary system with ST_p serving as a relay and second spectrum access by ST_s ensue simultaneously. Otherwise, if the selection for ST_p succeeds and the selection for ST_s fails, cooperative DF transmission for primary system ensues without secondary spectrum access. In this case, the proposed spectrum sharing protocol reduces to the conventional selective relaying scheme [24, 104]. Lastly, if the selection for neither ST_p nor ST_s succeeds, no data transmission ensues.

Under the case where the selections for both ST_p and ST_s are successful, two-phase cooperative DF transmission for the primary system and secondary spectrum access proceed after the SUSW. Specifically, in the first transmission phase, both ST_p and SR decode and regenerate the primary signal transmitted by PT. Note that while ST_p always successfully decodes[1], decoding at SR may or may not succeed. In the second transmission phase, ST_p forwards the regenerated primary signal to PR, which is also received at SR as interference to the secondary system. Simultaneously in the second transmission phase, ST_s transmits secondary signal to SR, which is also received at PR as interference to the primary system. Since ST_s is guaranteed to satisfy the interference constraint, its transmission does not affect the successful decoding at PR. At SR, if the decoding in the first transmission phase is successful, interference cancelation is first applied to cancel off the primary signal component and then the secondary signal is retrieved. Otherwise, SR decodes the secondary signal directly by considering the interference as noise.

It is worth mentioning that in the proposed spectrum sharing protocol, the primary system only has to be aware of a "DF relaying with relay selection" operation mode. The primary system does not have to be cognizant of whether the relaying nodes belong to the primary or secondary system, nor does it need to know whether secondary spectrum access is going on or not. The primary system is also

[1]Due to the selection process.

ignorant of the secondary control signals, and cooperative DF relaying transmission for the primary system ensues as long as selection for ST_p is successful. In other words, from the perspective of the primary system, the processing at PT and PR in the proposed spectrum sharing protocol is the same as a selective relaying scheme [24, 104]. Furthermore, we will show later that unlike [97], secondary user selection in our proposed protocol is performed in a distributed fashion [24], thus no central control terminal is required.

We analyze the outage performance of the primary and secondary systems under the proposed spectrum sharing protocol, and derive closed-form expressions for the outage probabilities. We show that the secondary system is able to access the spectrum band without degrading the outage performance of the primary system. The primary system is able to achieve the same outage performance as a conventional selective relaying scheme, given the same number of secondary users (relays) for selection. Furthermore, we show that the outage performance for both primary and secondary systems improves as the number of secondary users M increases.

6.2 System Model and Protocol Description

6.2.1 System Model

The system configuration of the proposed spectrum sharing protocol is shown in Figure 6.1. The primary direct link PT→PR is assumed to be weak due to shadowing and/or fading and is thus neglected for data transmission[2]. The channels over links PT→ ST_i, ST_i →PR, and ST_i →SR are modeled to be Rayleigh flat fading with channel coefficients denoted by h_{1i}, h_{2i}, and h_{3i} respectively, where $i \in \mathcal{M} = \{1, 2, \cdots, M\}$. We have $h_{\kappa i} \sim \mathcal{CN}(0, \Omega_{\kappa i})$, $\kappa = 1, 2, 3$, where $\Omega_{\kappa i}$ is the average channel gain between the respective transmitters and receivers. In this chapter, we assume that[3] $\Omega_{1i} = \Omega_1$, $\Omega_{2i} = \Omega_2$, and $\Omega_{3i} = \Omega_3$, $\forall i \in \mathcal{M}$. We also denote the instantaneous channel gain as $\gamma_{\kappa i} = |h_{\kappa i}|^2$. Similarly, the channel over link PT→SR is modeled as $h_4 \sim \mathcal{CN}(0, \Omega_4)$, where Ω_4 is the average channel gain of PT→SR link, and $\gamma_4 = |h_4|^2$. We assume all channel coefficients remain static

[2]This assumption is made purely for simplicity of derivation and it does not restrict the application of the proposed spectrum sharing protocol to the case where direct link exists.

[3]This assumption is made purely for mathematical tractability.

within a duration of two transmission phases.

Let x_p and $x_{s,i}$ denote the primary signal and the secondary signal of ST_i, $i \in \mathcal{M}$ respectively, with zero mean and $E\{x_p^* x_p\} = 1$, $E\{x_{s,i}^* x_{s,i}\} = 1$. The transmit power at PT and ST_i is denoted as P_p and P_s respectively. The variances of the additive white Gaussian noise (AWGN) at all receivers are assumed to be identical and denoted as σ^2.

6.2.2 Distributed Secondary User Selection

An illustration of the secondary user selection process is shown in Figure 6.2. The SUSW has a duration of t_w, and the distributed selection for ST_p and ST_s has to be accomplished within this duration. Note that t_w is a primary system parameter for relay selection and is known by the secondary system. For simplicity of analysis, we assume that the transmissions and processing of all control messages are instantaneous[4].

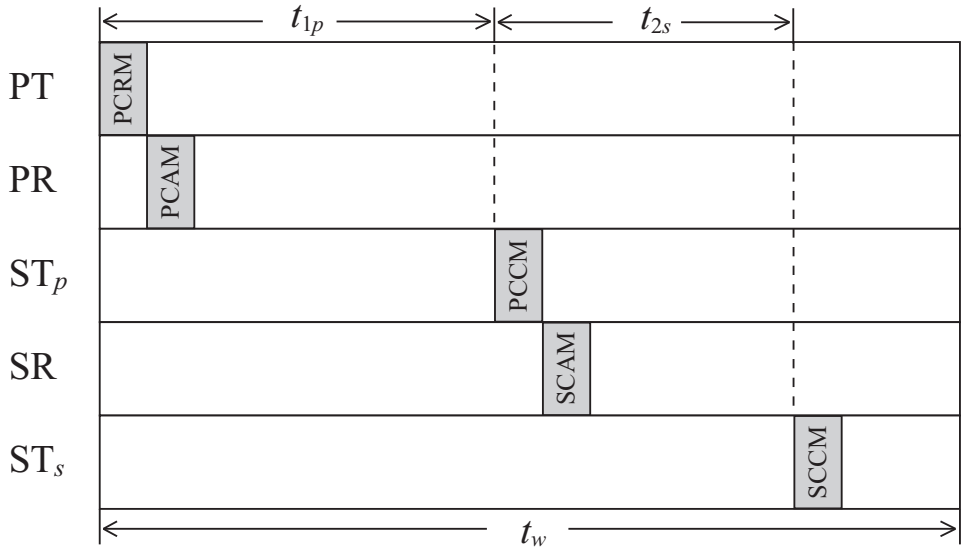

Figure 6.2. Illustration of the secondary user selection window.

[4]This assumption is reasonable since the control messages are generally short and are only used for the purposes of channel estimation and terminal identification [104].

6.2.2.1 Selection for ST_p

When PT→PR link becomes weak due to shadowing and/or fading, i.e. the channel gain drops below a certain threshold, PT will seek cooperation from neighboring terminals to enhance its transmission performance by transmitting a primary cooperation request message (PCRM) which also indicates a request target rate R_{pt} for the primary system. This PCRM is then responded by PR with a primary cooperation acknowledged message (PCAM).

By overhearing PCRM and PCAM, ST_i, $\forall i \in \mathcal{M}$, is able to estimate channel gains γ_{1i} and γ_{2i}. Accordingly, ST_i computes the achievable rate of PT→ ST_i and ST_i →PR links, which are respectively given by

$$R_{1i} = \frac{1}{2}\log_2\left(1 + \frac{P_p\gamma_{1i}}{\sigma^2}\right) \tag{6.1}$$

and

$$R_{2i} = \frac{1}{2}\log_2\left(1 + \frac{P_s\gamma_{2i}}{\sigma^2}\right), \tag{6.2}$$

where the factor of $\frac{1}{2}$ accounts for the fact that the overall transmission is being split into two phases. We denote

$$\mathcal{D} = \{i | i \in \mathcal{M}, R_{1i} > R_{pt}\},$$

and

$$\mathcal{F} = \{i | i \in \mathcal{D}, R_{2i} > R_{pt}\}.$$

It is clear that ST_i, $\forall i \in \mathcal{F}$ is able to assist the primary system in achieving R_{pt}.

Each secondary transmitter ST_i, $\forall i \in \mathcal{F}$ now starts a count-down timer with initial value

$$t_{1i} = \frac{\Gamma_1}{\gamma_{2i}} \tag{6.3}$$

where the normalization factor Γ_1 is given by $\Gamma_1 = \frac{\sigma^2}{P_s}\rho_p t_w$, and $\rho_p = 2^{2R_{pt}} - 1$. Secondary transmitter ST_p, $p \in \mathcal{F}$, where $p = \arg\max_{i\in\mathcal{F}} [\gamma_{2i}] = \arg\max_{i\in\mathcal{F}} [R_{2i}]$ has its timer reduced to zero first and hence broadcasts a primary cooperation confirmation message (PCCM) to identify its presence. All other ST_i, $i \in \mathcal{F} \setminus \{p\}$

upon hearing the PCCM will back off. It is clear from (6.3) that $t_{1i} < t_w$, $\forall i \in \mathcal{F}$, and thus PCCM is broadcasted as long as $|\mathcal{F}| \neq 0$. Upon receiving PCCM, the primary system is aware that R_{pt} can be achieved through cooperation, and the two-phase cooperative transmission from PT to PR with ST_p serving as a DF relay will ensue after the SUSW. On the other hand, in the event that $|\mathcal{F}| = 0$, no PCCM is broadcasted within the SUSW and hence the selection for ST_p fails. Accordingly, no primary and secondary data transmission ensues after the SUSW.

When the selection for ST_p succeeds, the relaying link of the primary system $\mathrm{ST}_p \rightarrow \mathrm{PR}$ will have a certain margin to tolerate interference from the secondary system while ensuring that R_{pt} is achieved. We denote the maximum tolerable interference threshold by I_p, and ST_p calculates I_p by letting

$$R_{pt} = R_{2p} = \frac{1}{2}\log_2\left(1 + \frac{P_s\gamma_{2p}}{I_p + \sigma^2}\right), \tag{6.4}$$

which leads to $I_p = \frac{P_s\gamma_{2p}}{\rho_p} - \sigma^2$. Since $|\mathcal{F}| \neq 0$, we have $\gamma_{2p} > \frac{\sigma^2}{P_s}\rho_p$, and therefore $I_p > 0$. Note that the information regarding I_p is also included in PCCM and broadcasted by ST_p. However, it is only understood by the secondary system and will be neglected by the primary system.

6.2.2.2 Selection for ST_s

Retrieving I_p from PCCM, each $\mathrm{ST}_i, \forall i \in \mathcal{M}\backslash\{p\}$ compares I_p with the interference it would cause to PR if it transmits its own secondary signal[5]. It is clear from (6.4) that any interference in the second transmission phase lower than I_p will result in $R_{2p} > R_{pt}$. Thus, secondary transmitter ST_i, $\forall i \in \mathcal{M} \setminus \{p\}$ is able to access the spectrum band in the second transmission phase without affecting the outage probability of the primary system as long as it causes less interference than I_p at

[5]Under conditions $R_{pt} < 0.5$, $\gamma_{2p} > \frac{\sigma^2}{P_s}\frac{\rho_p}{1-\rho_p}$, where $p = \arg\max_{i\in\mathcal{F}}[\gamma_{2i}] = \arg\max_{i\in\mathcal{M}}[\gamma_{3i}]$, ST_p could also be selected for secondary access by transmitting a superimposed signal of the primary and secondary systems. However, we ignore this extremely low probability case for simplicity and consistency. For more details regarding superimposed transmission in cooperative spectrum sharing, we would like to refer the reader to Chapter 5.

PR, i.e., $P_s\gamma_{2i} < I_p$. We denote

$$\mathcal{S} = \left\{ i | i \in \mathcal{M} \setminus \{p\}, \gamma_{2i} < \frac{I_p}{P_s} \right\},$$

and thus only ST_i, $\forall i \in \mathcal{S}$ will participate in the selection of ST_s.

Upon receiving PCCM, SR responds by broadcasting a secondary cooperation acknowledged message (SCAM), from which ST_i, $\forall i \in \mathcal{S}$ is able to estimate channel gain γ_{3i}. Given a secondary target rate R_{st}, each secondary transmitter ST_i, $\forall i \in \mathcal{S}$ now starts a count-down timer with initial value

$$t_{2i} = \frac{\Gamma_2}{\gamma_{3i}} \tag{6.5}$$

where the normalization factor $\Gamma_2 = \frac{\sigma^2}{P_s}\rho_s(t_w - t_{1p})$, and $\rho_s = 2^{2R_{st}} - 1$. Secondary transmitter ST_s, $s \in \mathcal{S}$, where $s = \arg\max_{i \in \mathcal{S}} [\gamma_{3i}]$ has its timer reduced to zero first and hence broadcasts a secondary cooperation confirmation message (SCCM) to identify its presence. All other ST_i, $i \in \mathcal{S} \setminus \{s\}$ upon hearing the SCCM will back off.

It is clear from (6.5) that $t_{2i} \leq (t_w - t_{1p})$ when $\gamma_{3i} \geq \frac{\sigma^2}{P_s}\rho_s$. Thus SCCM is broadcasted by ST_s within the SUSW as long as $\gamma_{3s} \geq \frac{\sigma^2}{P_s}\rho_s$, which is the minimum channel gain of $\mathrm{ST}_i \rightarrow$SR link required to achieve R_{st}. On the other hand, in the event that $|\mathcal{S}| = 0$ or $\gamma_{3s} < \frac{\sigma^2}{P_s}\rho_s$, no SCCM is broadcasted within the SUSW and hence the selection for ST_s fails. Accordingly, secondary spectrum access is not possible. Note that the primary system is ignorant of secondary control signals SCAM and SCCM, and thus the selection for ST_s is totally oblivious to the primary system. It is the onus of the secondary system to ensure that all secondary control messaging is completed within the SUSW.

Upon receiving SCCM, SR is aware that ST_s is selected for secondary spectrum access, and it will receive a combination of signals transmitted by ST_p and ST_s in the second transmission phase. All possible scenarios of the proposed secondary user selection and their corresponding consequences are summarized in Table 6.1. It is worth mentioning that all control messages PCRM, PCAM, PCCM, SCAM, and SCCM are implemented in the MAC layer. We assume that they are well protected by robust coding/modulation, and thus their receptions at the respective

receivers are error free.

Table 6.1. Secondary User Selection Scenarios and Corresponding Consequences

Scenario	Consequence
Selection for neither ST_p nor ST_s succeeds	No primary & secondary transmission
Only selection for ST_p succeeds	DF relaying with ST_p & no secondary transmission
Selections for both ST_p and ST_s succeed	DF relaying with ST_p & secondary spectrum access with ST_s

6.2.3 Cooperative Transmission for Primary System and Secondary Spectrum Access

In the event that both ST_p and ST_s are successfully selected within the SUSW, spectrum sharing is possible. In the first transmission phase, both ST_p and SR decode and regenerate the primary signal transmitted by PT. Note that ST_p always successfully decodes, but the decoding at SR may or may not succeed, depending on the channel gain of PT→SR link γ_4 and the primary target rate R_{pt}.

In the second transmission phase, ST_p forwards the regenerated primary signal to PR, which is also received at SR as interference to the secondary system. Simultaneously in the second transmission phase, ST_s transmits secondary signal to SR, which is also received at PR as interference to the primary system. Since ST_s satisfies interference constraint I_p, its transmission does not affect the successful decoding at PR.

At SR, if the decoding in the first transmission phase is successful, interference cancelation is first applied to cancel the primary signal component and then the secondary signal is retrieved. Otherwise, SR decodes the secondary signal directly by considering the interference as noise. If the achievable rate at SR is lower than R_{st}, an outage is declared for the secondary system.

6.3 Outage Performance Analysis

6.3.1 Outage Probability of Primary System

We will first derive the outage probability for the primary system with request target rate R_{pt}. From the protocol described in the previous section, it is clear that an outage for the primary system occurs if and only if $|\mathcal{F}| = 0$. The outage probability for the primary system is therefore given by

$$P_{\text{out}}^{p} = \Pr\{|\mathcal{F}| = 0\} = \sum_{k=0}^{M} \Pr\left\{\max_{i\in\mathcal{D}} [R_{2i}] < R_{pt} \big| |\mathcal{D}| = k\right\} \Pr\{|\mathcal{D}| = k\}. \quad (6.6)$$

We can easily obtain

$$\begin{aligned} \Pr\left\{\max_{i\in\mathcal{D}}[R_{2i}] < R_{pt}\big||\mathcal{D}| = k\right\} &= (\Pr\{R_{2i} < R_{pt}\})^{k} \\ &= \left[1 - \exp\left(-\Omega_2^{-1}\frac{\sigma^2}{P_s}\rho_p\right)\right]^{k} \end{aligned} \quad (6.7)$$

and

$$\begin{aligned} \Pr\{|\mathcal{D}| = k\} &= \binom{M}{k} (\Pr\{R_{1i} > R_{pt}\})^{k} (1 - \Pr\{R_{1i} > R_{pt}\})^{M-k} \\ &= \binom{M}{k} \left[\exp\left(-\Omega_1^{-1}\frac{\sigma^2}{P_p}\rho_p\right)\right]^{k} \left[1 - \exp\left(-\Omega_1^{-1}\frac{\sigma^2}{P_p}\rho_p\right)\right]^{M-k} \end{aligned} \quad (6.8)$$

Substituting (6.7) and (6.8) into (6.6), we have

$$\begin{aligned} P_{\text{out}}^{p} &= \sum_{k=0}^{M} \binom{M}{k} \left[1 - \exp\left(-\Omega_2^{-1}\frac{\sigma^2}{P_s}\rho_p\right)\right]^{k} \left[\exp\left(-\Omega_1^{-1}\frac{\sigma^2}{P_p}\rho_p\right)\right]^{k} \\ &\quad \cdot \left[1 - \exp\left(-\Omega_1^{-1}\frac{\sigma^2}{P_p}\rho_p\right)\right]^{M-k} \\ &= (1 - p_1 p_2)^{M} \end{aligned} \quad (6.9)$$

where $p_1 = \exp\left(-\Omega_1^{-1}\frac{\sigma^2}{P_p}\rho_p\right)$ and $p_2 = \exp\left(-\Omega_2^{-1}\frac{\sigma^2}{P_s}\rho_p\right)$.

It can be observed from (6.9) that P_{out}^{p} coincides with the outage probability

expression for *fixed selective decode-and-forward (FSDF) without direct link combining* [104], where the source and destination terminal communicate via one DF relay terminal which is selected from M potential relays. Thus, with the proposed spectrum sharing protocol, the primary system is able to achieve the same outage performance as the selective relaying scheme in [104] and at the same time, the secondary system is able to access the spectrum.

6.3.2 Outage Probability of Secondary System

In the following, we derive a closed-form upper bound for the outage probability of the secondary system with target rate R_{st}. When $|\mathcal{F}| = 0$, i.e. an outage occurs for the primary system, secondary spectrum sharing is not possible due to the absence of PCCM, thus an outage is declared for the secondary system immediately. On the other hand, when $|\mathcal{F}| \neq 0$, we assume ST_s, $s \in \mathcal{S}$ is selected to access the spectrum in the second transmission phase[6].

In the first transmission phase, PT transmits x_p and the signal received at SR is given by

$$y_{\mathrm{SR},1} = \sqrt{P_p} h_4 x_p + n_{\mathrm{SR},1} \tag{6.10}$$

where $n_{\mathrm{SR},1} \sim \mathcal{CN}(0, \sigma^2)$ denotes AWGN at SR in the first transmission phase. The achievable rate between PT and SR is thus given by

$$R_4^1 = \frac{1}{2} \log_2 \left(1 + \frac{P_p \gamma_4}{\sigma^2} \right) \tag{6.11}$$

where the factor of $\frac{1}{2}$ accounts for the fact that the overall transmission is being split into two phases. After the reception of $y_{\mathrm{SR},1}$, SR attempts to decode x_p and stores the decoding results if it succeeds. This decoding is successful if $R_4^1 \geq R_{pt}$ and

$$\Pr\{R_4^1 \geq R_{pt}\} = \exp\left(-\Omega_4^{-1} \frac{\sigma^2}{P_p} \rho_p \right). \tag{6.12}$$

In the second transmission phase, ST_s transmits secondary signal $x_{s,s}$ to SR while ST_p is relaying primary signal x_p to PR. The signal received at SR in the

[6]Note that SCCM might be absent due to $|\mathcal{S}| = 0$ or $\gamma_{3s} < \frac{\sigma^2}{P_s} \rho_s$. Both cases are taken into consideration in the following derivations.

second transmission phase is given by

$$y_{\mathrm{SR},2} = \sqrt{P_s} h_{3s} x_{s,s} + \sqrt{P_s} h_{3p} x_p + n_{\mathrm{SR},2}, \tag{6.13}$$

where $n_{\mathrm{SR},2} \sim \mathcal{CN}(0, \sigma^2)$ denotes AWGN at SR in the second transmission phase. If the decoding at SR in the first transmission phase is successful, interference component $\sqrt{P_s} h_{3p} x_p$ can be canceled out from (6.13) to obtain $\tilde{y}_{\mathrm{SR},2} = \sqrt{P_s} h_{3s} x_{s,s} + n_{\mathrm{SR},2}$, where channel coefficient h_{3p} can be estimated at SR through SCAM. SR can then use $\tilde{y}_{\mathrm{SR},2}$ for decoding of $x_{s,s}$. Otherwise, if the decoding at SR in the first transmission phase fails, SR will directly use $y_{\mathrm{SR},2}$ to decode for $x_{s,s}$ by treating the interference from x_p as noise.

The achievable rate between ST_s and SR conditioned on successful and unsuccessful decoding at SR in the first transmission phase is given by

$$R_{3s} = \begin{cases} \frac{1}{2}\log_2\left(1 + \frac{P_s \gamma_{3s}}{\sigma^2}\right) & R_4^1 \geq R_{pt} \\ \frac{1}{2}\log_2\left(1 + \frac{P_s \gamma_{3s}}{P_s \gamma_{3p} + \sigma^2}\right) & R_4^1 < R_{pt} \end{cases}. \tag{6.14}$$

The outage probability for the secondary system is thus given by

$$P_{\mathrm{out}}^s = P_{\mathrm{out}}^p + \sum_{k=1}^{M} \sum_{f=1}^{k} \Pr\left\{R_{3s} < R_{st} \;\middle|\; |\mathcal{F}| = f, |\mathcal{D}| = k\right\} \Pr\{|\mathcal{F}| = f, |\mathcal{D}| = k\}. \tag{6.15}$$

In (6.15), the first term denotes the case where an outage occurs for the primary system and thus leading to an outage for the secondary system. The second term denotes the case where no outage occurs for the primary system but an outage occurs for the secondary system. Note that the case where SCCM is absent within the SUSW is also taken into consideration in the second term of (6.15), since both scenarios of $|\mathcal{S}| = 0$ and $\gamma_{3s} < \frac{\sigma^2}{P_s}\rho_s$ will lead to $R_{3s} < R_{st}$.

It is easy to see that

$$\Pr\{|\mathcal{F}| = f, |\mathcal{D}| = k\} = \Pr\left\{|\mathcal{F}| = f \;\middle|\; |\mathcal{D}| = k\right\} \Pr\{|\mathcal{D}| = k\} \tag{6.16}$$

where

$$\begin{aligned}\Pr\left\{|\mathcal{F}| = f \;\middle|\; |\mathcal{D}| = k\right\} &= \binom{k}{f} \left(\Pr\{R_{2i} > R_{pt}\}\right)^f \left(1 - \Pr\{R_{2i} > R_{pt}\}\right)^{k-f} \\ &= \binom{k}{f} p_2^f (1-p_2)^{k-f}. \end{aligned} \tag{6.17}$$

Substituting (6.8) and (6.17) into (6.16), we have

$$\Pr\{|\mathcal{F}| = f, |\mathcal{D}| = k\} = P(f,k) = \binom{M}{k}\binom{k}{f} p_1^k (1-p_1)^{M-k} p_2^f (1-p_2)^{k-f}. \tag{6.18}$$

Proposition 6.3.1. *A closed-form upper bound for* $\Pr\left\{R_{3s} < R_{st} \;\middle|\; |\mathcal{F}| = f, |\mathcal{D}| = k\right\}$ *is given by*

$$\Pr\left\{R_{3s} < R_{st} \;\middle|\; |\mathcal{F}| = f, |\mathcal{D}| = k\right\} \leq P_{\text{out}}^{s,ub}(f,k) \tag{6.19}$$

where the detailed expression and derivations for $P_{\text{out}}^{s,ub}(f,k)$ *are given in Appendix B.*

A closed-form upper bound for the outage probability of the secondary system is thus given by

$$P_{\text{out}}^{s} \leq P_{\text{out}}^{s,ub} = P_{\text{out}}^{p} + \sum_{k=1}^{M}\sum_{f=1}^{k} P(f,k) P_{\text{out}}^{s,ub}(f,k) \tag{6.20}$$

where P_{out}^{p}, $P(f,k)$, and $P_{\text{out}}^{s,ub}(f,k)$ are given in (6.9), (6.18), and (B.32) respectively.

6.4 Simulation Results and Discussions

We show the simulation and theoretical results for the outage probability of the primary system under the proposed spectrum sharing protocol in Figure 6.3. For comparison purposes, we also show the simulation results for the outage probability of FSDF without direct link $P_{\text{out}}^{\text{FSDF}}$ [104]. We let $M = 10$, $\Omega_1 = \Omega_2 = 1$, and $\frac{P_p}{\sigma^2}$

varies from 10 dB to 30 dB. Two cases of P_s where $\frac{P_s}{\sigma^2} = 15$ dB and $\frac{P_s}{\sigma^2} = 20$ dB and two cases of R_{pt} where $R_{pt} = 1.5$ and $R_{pt} = 2$ are considered.

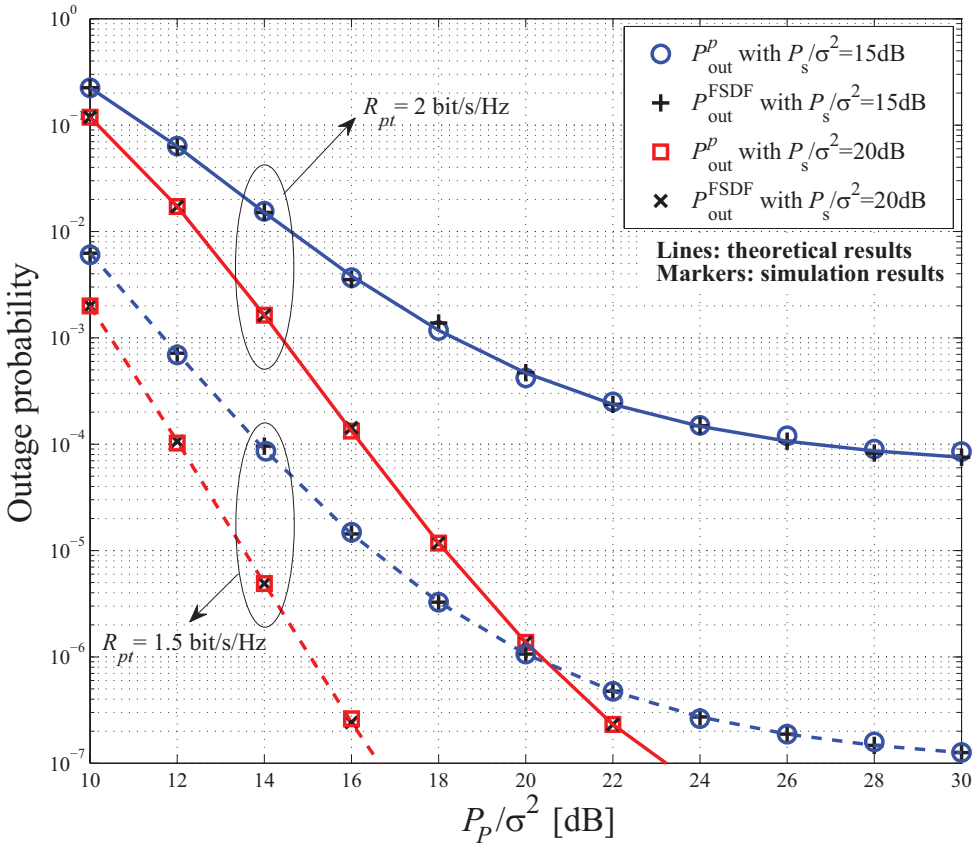

Figure 6.3. Outage probability of primary system with $M = 10$ and $\Omega_1 = \Omega_2 = 1$.

It can be observed from Figure 6.3 that the derived theoretical results of P^p_{out} agree exactly with the simulation results of P^p_{out} and $P^{\text{FSDF}}_{\text{out}}$, indicating that the primary system is able to achieve the same outage performance as a conventional selective relaying scheme [104]. We can also observe that P^p_{out} decreases with increasing P_p and P_s, and decreasing R_{pt}. Furthermore, with $\frac{P_s}{\sigma^2} = 15$ dB, a floor for P^p_{out} appears when P_p becomes large. This is because with a small P_s, successful decoding in the second transmission phase becomes the limiting factor

at PR, and thus further increasing the transmit power at PT will not reduce the overall primary outage probability.

In Figure 6.4, we show the simulation results for the outage probability of the secondary system and the theoretical upper bound derived in (6.20) is also plotted. We let $M = 10$, $\Omega_1 = \Omega_2 = \Omega_3 = 1$, $R_{pt} = 1.5$ bit/s/Hz, $R_{st} = 1$ bit/s/Hz, and $\frac{P_p}{\sigma^2}$ varies from 10 dB to 30 dB. Three cases of P_s where $\frac{P_s}{\sigma^2} = 10$ dB, 15 dB, and 20 dB and two cases of Ω_4 where $\Omega_4 = 1$ and $\Omega_4 = 10$ are considered.

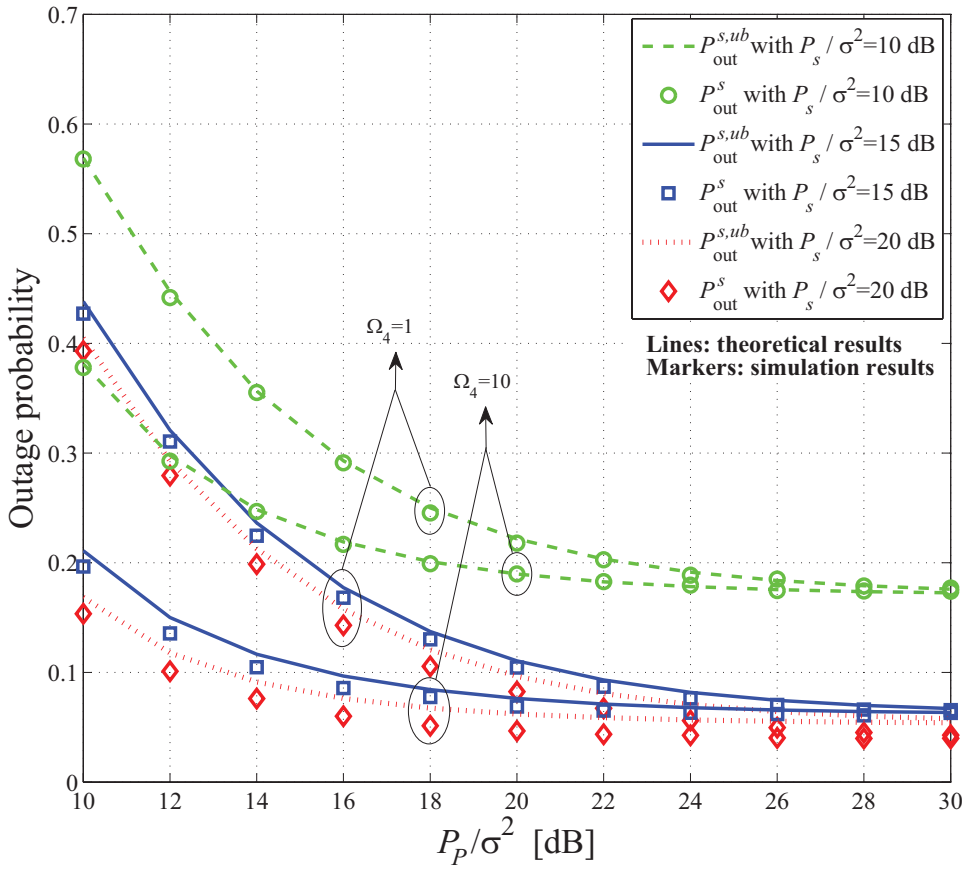

Figure 6.4. Outage probability of secondary system with $M = 10$, $\Omega_1 = \Omega_2 = \Omega_3 = 1$, $R_{pt} = 1.5$ bit/s/Hz, and $R_{st} = 1$ bit/s/Hz.

It can be observed from Figure 6.4 that $P_{\text{out}}^{s,ub}$ provides a good upper bound which is especially tight when P_s is small, i.e. $\frac{P_s}{\sigma^2} = 10$ dB. This observation coincides with the derivation in (B.27), where by using a smaller P_s we obtain a tighter lower bound for p_6 which leads to a tighter upper bound for P_{out}^{s}. We can

also observe that P_{out}^{s} decreases with increasing P_s. However, the performance gap between $\frac{P_s}{\sigma^2} = 20$ dB and $\frac{P_s}{\sigma^2} = 15$ dB is much smaller than that between $\frac{P_s}{\sigma^2} = 15$ dB and $\frac{P_s}{\sigma^2} = 10$ dB, i.e. the improvement by increasing P_s becomes saturated. This is because when P_s is large, the first transmission phase becomes the limiting factor at SR, and therefore P_{out}^{s} becomes independent of P_s. This observation indicates that the secondary system cannot reduce its outage probability unboundedly by increasing its transmit power P_s.

We can also observe from Figure 6.4 that P_{out}^{s} decreases with increasing P_p. However an outage probability floor appears for P_{out}^{s} when P_p becomes large. This can be attributed to the fact that with a large P_p, we have $|\mathcal{D}| \to M$, $p_1 \to 0$, and $p_4 \to 0$ [7]. In this case, the second transmission phase becomes the limiting factor at SR, and thus P_{out}^{s} becomes independent of P_p. Specifically, when both P_p and P_s are large, the limiting factor at SR is also the second transmission phase, thus P_{out}^{s} does not decreases unboundedly with increasing P_p and P_s.

Furthermore, it is noted that P_{out}^{s} with $\Omega_4 = 10$ is smaller than that with $\Omega_4 = 1$ due to a higher probability of interference cancelation at SR. This observation indicates that the proposed spectrum protocol performs especially well when the channel between PT and SR is strong. Comparing Figure 6.3 and Figure 6.4, we confirm that with the proposed spectrum sharing protocol, the secondary system is able to access the spectrum band without degrading the outage performance of the primary system. It is also worth mentioning that the secondary system achieves the above performance without causing any additional overhead to the primary system.

The outage probability for the primary system with different values of M is shown in Figure 6.5, where we also show $P_{\text{out}}^{\text{FSDF}}$ for comparison purposes. We let $\frac{P_p}{\sigma^2} = 20$ dB, $\Omega_1 = \Omega_2 = 1$, and M varies from 1 to 100. Two cases of R_{pt} where $R_{pt} = 2$ bit/s/Hz and $R_{pt} = 3$ bit/s/Hz, and three cases of P_s where $\frac{P_s}{\sigma^2} = 15$ dB, 20 dB, and 25 dB, are considered.

Again, we can observe from Figure 6.5 that the derived theoretical results agree exactly with the simulation results of P_{out}^{p} and $P_{\text{out}}^{\text{FSDF}}$. This observation indicates that with the proposed spectrum sharing protocol, the primary system is able to achieve exactly the same multi-user (multi-relay) diversity gain as the selective

[7] Refer to Appendix B.

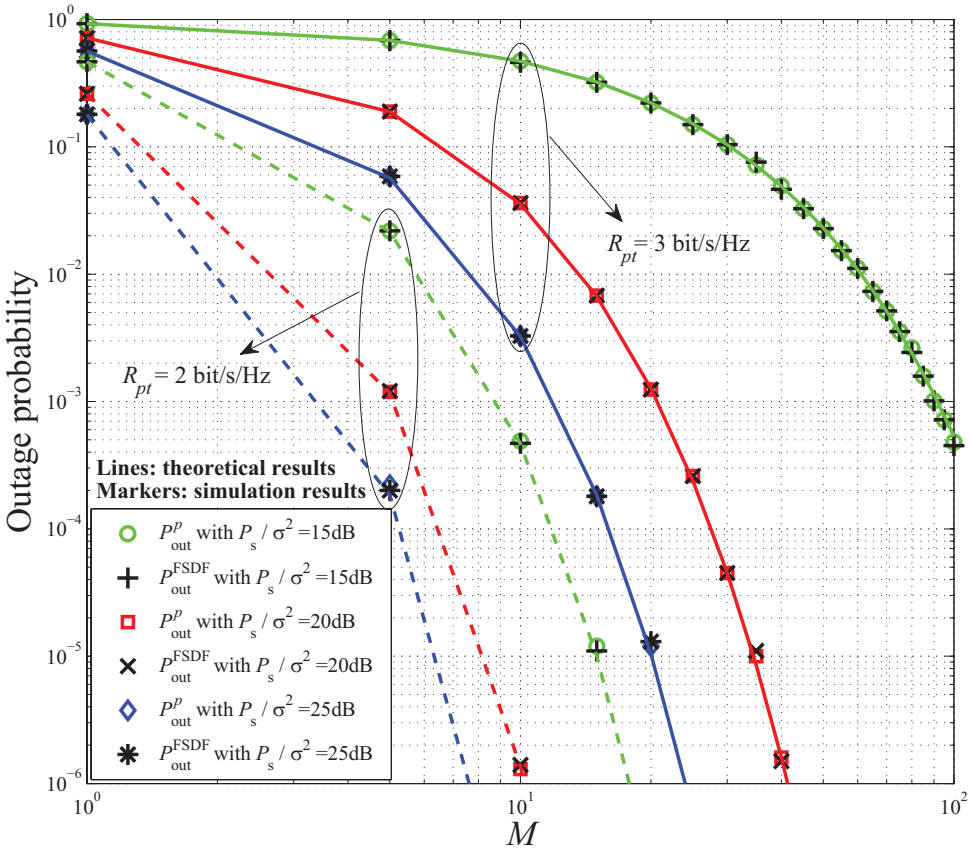

Figure 6.5. Outage probability of primary system with different values of M, where $\Omega_1 = \Omega_2 = 1$ and $\frac{P_p}{\sigma^2} = 20$ dB.

relaying scheme where the M secondary transmitters are purely designated as DF relays for the primary system. It can be observed that P^{p}_{out} decreases with increasing M, and the gaps between curves with $\frac{P_s}{\sigma^2} = 15$ dB, 20 dB and 25 dB increase with M, indicating an increased multi-user (multi-relay) diversity gain brought about by the cooperative transmission. We can also observe that P^{p}_{out} increases with R_{pt}, and it decreases with increasing P_p and P_s. The performance gap between $\frac{P_s}{\sigma^2} = 20$ dB and $\frac{P_s}{\sigma^2} = 25$ dB is smaller than that between $\frac{P_s}{\sigma^2} = 15$ dB and $\frac{P_s}{\sigma^2} = 20$ dB. This is because with a large P_s, outage in the first transmission phase dominates the overall primary outage performance, and thus the improvement by increasing P_s becomes saturated.

In Figure 6.6, we show the outage probability for the secondary system with

different values of M, where the theoretical upper bound $P_{\text{out}}^{s,ub}$ derived in (6.20) is also plotted. We let $\frac{P_p}{\sigma^2} = \frac{P_s}{\sigma^2} = 20$ dB, $\Omega_1 = \Omega_2 = \Omega_3 = \Omega_4 = 1$, and M varies from 1 to 100. Two cases of R_{pt} where $R_{pt} = 2$ bit/s/Hz and $R_{pt} = 1$ bit/s/Hz and two cases of R_{st} where $R_{st} = 1$ bit/s/Hz and $R_{st} = 0.5$ bit/s/Hz are considered.

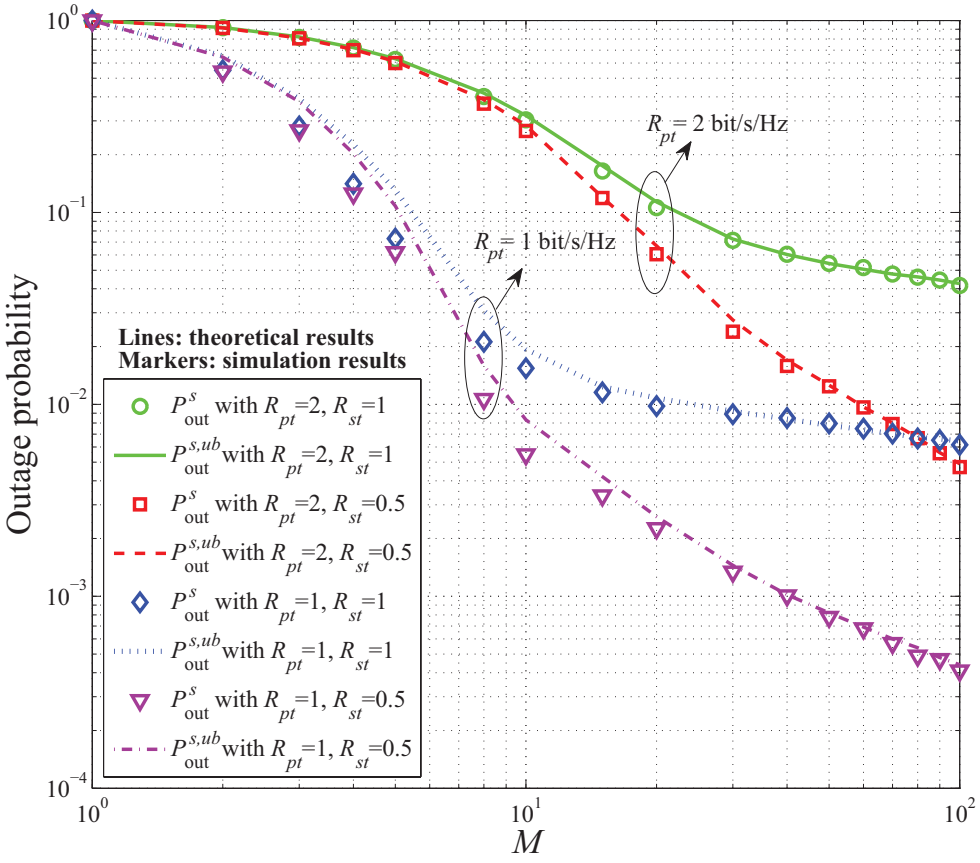

Figure 6.6. Outage probability of secondary system with different values of M, where $\Omega_1 = \Omega_2 = \Omega_3 = \Omega_4 = 1$ and $\frac{P_p}{\sigma^2} = \frac{P_s}{\sigma^2} = 20$ dB.

We can observe from Figure 6.6 that the derived $P_{\text{out}}^{s,ub}$ forms a tight upper bound for the simulation result of P_{out}^{s}, and P_{out}^{s} decreases with increasing M. We note that the upper bound $P_{\text{out}}^{s,ub}$ with $R_{pt} = 2$ is tighter compared to that with $R_{pt} = 1$. This coincides with the derivation in (B.27), where by using a larger R_{pt}

we obtain a tighter lower bound[8] for p_6 which leads to a tighter upper bound for P_{out}^{s}. Similarly, we can also observe that for both cases of $R_{pt} = 2$ bit/s/Hz and $R_{pt} = 1$ bit/s/Hz, $P_{\text{out}}^{s,ub}$ becomes tighter with increasing M. This is due to fact that with a larger M, we will have a larger probability to obtain a large γ_{2p}, which makes the lower bound in (B.27) tighter. Comparing Figure 6.5 and Figure 6.6, we note that both the primary and secondary systems are able to benefit from the increasing number of secondary transmitters. Furthermore, it can be concluded from Figure 6.3 and Figure 6.5 that the secondary system is able to improve the outage performance for the primary system by increasing P_s and M.

6.5 Summary

In this chapter, we proposed a cooperative spectrum sharing protocol with two-step distributed secondary user selection. In the proposed protocol, secondary transmitter ST_p is first selected from M secondary transmitters to assist the primary system in achieving a primary request target rate, by serving as a DF relay. Conditioned on the successful selection of ST_p, another secondary transmitter ST_s which is able to provide the optimal outage performance for the secondary system, is then selected to access the spectrum band simultaneously when ST_p is relaying the primary signal. Theoretical and simulation results confirm the efficiency of the proposed spectrum sharing protocol, and we show that the secondary system is able to access the licensed spectrum band without degrading the outage performance for the primary system nor causing additional overheads to the primary system, as compared to a conventional selective relaying scheme. Furthermore, we show that the outage performance for both the primary and secondary systems improves as the number of secondary transmitters M increases.

[8]Refer to Appendix B.

Chapter 7

Conclusion

As two of the most successful research areas in communications in the past decade, cooperation and cognition in wireless networks have drawn great research attention, and promising advancements have been achieved in both theory and practice. This dissertation is devoted to the joint investigation of these two fast-evolving paradigms for the purpose of spectrum efficiency enhancement.

We started off by considering a pure cooperative system where rate performance of two-way AF relaying was analyzed. Then we extended our scope and took more flexible spectrum utilization models based on CR into consideration. Various practical schemes and protocols which take advantage of both cooperation and cognition in the wireless systems were presented with theoretical analysis.

In Chapter 2, the moments of the harmonic mean of two independent gamma distributed random variables which have the same shape parameter but different scale parameters, were first derived. These novel results enable us to analyze two-way AF relaying under a practical scenario where the channel coefficients of the two hops have different average channel gains. We then extend the conventional two-way AF relaying to the scenario where source and destination terminals utilize two antennas to transmit Alamouti's OSTBC and the relay has only one antenna.

By deriving both upper and lower bounds of the average sum rates for the two-way relaying schemes with and without OSTBC in the high SNR regime, we proved that two-way relaying is capable of significantly recovering the spectrum efficiency loss of one-way relaying. These bounds also showed that the proposed two-way relaying scheme with OSTBC achieves a higher average sum rate than the single

antenna scheme without OSTBC. We also used these bounds to analytically derive the optimal power allocations for both two-way relaying schemes. Furthermore, an upper-bound for the PEP of two-way relaying with OSTBC was also derived, which verified that a diversity order of two is also achieved by the proposed scheme.

To address the inefficiency of current spectrum regulations, we shifted our focus to cooperative systems in a CR context from Chapter 3 onwards. In Chapter 3, we combine cooperative relaying transmission with interweave CR and consider the scenario where the secondary system is a dual-hop relay system. We presented a simultaneous spectrum sensing protocol for such a system and compared its performance with a straightforward dedicated sensing protocol. It was shown that by removing the dedicated sensing periods, the simultaneous sensing protocol significantly outperforms the dedicated sensing protocol in terms of spectrum efficiency for the secondary system. At the same time, the interference constraint of the primary system is also satisfied. Furthermore, we showed that for practical priority weighting factors, the simultaneous sensing protocol achieves a higher overall system utilization, which takes the performance and different priorities of both the primary and secondary systems into consideration.

Besides the interweave CR discussed in Chapter 3, we also combine cooperative relaying transmission with overlay CR. In Chapter 4, we proposed an opportunistic spectrum sharing protocol with AF relaying, which exploits the geographical location as well as the fading of wireless channels. A corresponding handshake mechanism was also presented. The achievable rate analysis revealed that when the channel gain of the link from primary transmitter to receiver is lower than a particular threshold, the primary request target rate can be achieved by the proposed cooperation scheme, and hence a transmission opportunity is obtained by the secondary system. Simulations results confirmed that both primary and secondary systems benefit from the proposed opportunistic spectrum sharing protocol in terms of average achievable rate.

Spectrum sharing protocol based on DF cooperative relaying was presented in Chapter 5, where the secondary transmitter decodes and retransmits primary signal along with its own secondary signal. A critical radius from the primary transmitter was derived, within which the secondary transmitter is able to achieve spectrum access without degrading the outage performance of the primary system

by properly choosing the transmission power for relaying the primary signal. Furthermore, we showed that by selecting the secondary transmitter which is located closest to the primary transmitter for spectrum access, not only is the outage probability for the primary system minimized, the outage probability for the secondary system is also reduced. Outage performance for both primary and secondary systems improves with increasing number of secondary transmitter-receiver pairs.

Last but not least, in Chapter 6 we extended our work on cooperative spectrum sharing protocol to a more general multi-user scenario for the secondary system, and presented a two-step distributed secondary user selection scheme. In this protocol, one secondary transmitter is first selected to assist the primary system in achieving a primary request target rate by serving as a DF relay. Conditioned on the successful selection in the first step, another secondary transmitter is then selected to access the spectrum band. Theoretical and simulation results confirmed the efficiency of the proposed spectrum sharing protocol. We showed that the secondary system is able to access the licensed spectrum band without degrading the outage performance of the primary system nor causing additional overheads to the primary system, when compared to a conventional selective relaying scheme. Furthermore, we show that the outage performance for both the primary and secondary systems improves as the number of secondary transmitters increases.

7.1 Future Research Topics

We introduced various protocols and schemes in this dissertation as a preliminary effort towards practical wireless systems which are able to utilize spectrum resources more efficiently. Following the routes that we have sketched, there are still many research issues that need to be addressed in order to implement the proposed schemes in practice. In this last section of the dissertation, we will pick up a few of the most pertinent topics and discuss them briefly.

7.1.1 Sensing-Transmission Tradeoff in Cognitive Relay System

In interweave CR, the secondary system is able to access the licensed spectrum band only if the primary transmission is determined to be absent. As evident in Chapter 3, there exists a tradeoff between the sensing capability and spectrum efficiency of the secondary system, which can be equivalently interpreted as a tradeoff between the primary and secondary systems. Specifically, longer sensing slots at the secondary system will lead to a better detection performance and hence a lower collision probability. However, this is achieved at the expense of shorter effective data transmission time for the secondary system.

This sensing-transmission tradeoff in a point-to-point secondary system has been studied in [83], where an optimal sensing duration which maximizes the sum throughput was derived. However, extending these results to a cognitive relay system is not a trivial task. First of all, in a cognitive relay system, the detection performed at a relay is dependent on the detection at the source. Thus, the overall optimization problem cannot be simply decomposed into two independent subproblems. Secondly, the geographical separation between the source and relay means that identical sensing duration at both terminals is not necessarily an optimal choice. Therefore, this optimization also needs to take into account the network topology and channel model.

7.1.2 Multi-hop and Multi-user Cognitive Relay System

In Chapter 3, our discussions were limited to a dual-hop single-relay scenario. Apparently, an extension of the proposed protocol to a more general multi-hop multi-user scenario would be desirable. The following key questions need to be answered in order to accomplish this extension.

- In a multi-hop relay system, how should the sensing and transmission be scheduled at each terminal, such that our "sensing with cancelation" idea can still be applied and therefore the overall spectrum efficiency is improved?
- In a multi-user relay system, should all the available relays participate in the sensing-transmission protocol? If we select only a subset of the relays for cooper-

ation, then what is the proper criterion for deciding the size and members of this subset? If more than one relay is selected, should they operate autonomously or cooperatively?

In Chapter 6, we considered a multi-user scenario for the proposed cooperative spectrum sharing protocol, but multi-hop scenario has not been taken into consideration. Furthermore, in the proposed secondary user selection scheme, only one secondary transmitter is selected for primary relaying and secondary transmission respectively. However, no optimality is guaranteed by this option. Intuitively, the performance for both primary and secondary system would be improved when more secondary transmitters (relays) cooperatively participate in the transmission. The performance analysis and the corresponding changes needed for such protocols are interesting problems.

It is worth mentioning that in this thesis our focus is on the physical layer and all the results are derived under the assumption that all the transmitters always have data packets to transmit. However, this may not be true in practice. To apply the proposed protocols in more practical scenarios, transmission scheduling based on data traffic of the transmitters needs to be taken into consideration. This is especially necessary for the protocols in Section 5.4 and Chapter 6 where multiple secondary transmitters compete for transmission opportunities. Extensions of combining higher-layer scheduling with the proposed spectrum sharing protocol are also interesting directions.

7.1.3 Implementation Issues

For simplicity of derivation and mathematical tractability, we made several assumptions in our proposed protocols. These assumptions are reasonable and have been widely used in the literature. However, complete or partial failure in achieving these assumptions in practical implementations may have serious impacts on the performance of the overall system. Thus these issues need to be studied in detail.

- In Chapter 4, 5 and 6 , we assumed that the secondary system is highly advanced and intelligent, and it is able to emulate the same radio protocols (e.g.,

channel coding, synchronization, etc.) as the primary system. This assumption can be realized by adopting sophisticated signal detection techniques and adaptive transmission strategies. However, the errors incurred in the related signal processing should be evaluated and taken into consideration when designing a practical system.

- In Chapter 4, 5, and 6, we assumed that the transmission of control signals are instantaneous and error-free. However, these assumptions are definitely not true in practice. Although the error probability for control signals can be driven down to close zero through robust coding and modulation, propagation delays are inevitable and cannot be reduced. This will lead to possible collisions between control signals from different terminals as discussed in [24], and the impact of these collisions needs to be analyzed.

- In order to implement the proposed spectrum sharing protocol, some policy issues also need to be taken into consideration. Specifically, we assumed that the primary system is aware of a "DF relaying mode" operation in Chapter 5, and we assumed that the primary system is aware of a "DF relaying with relay selection" operation mode in Chapter 6. Thus, there is a need to develop primary systems that have awareness – at least to some extent, of the ongoing spectrum sharing.

Appendix A

Proof for Theorem 2.2.1

Let $Z = \frac{1}{2}H(X,Y) = \frac{XY}{X+Y}$, we have

$$\begin{aligned} \underset{X}{\mathcal{E}}[Z^n|Y] &= \int_0^\infty \left(\frac{xy}{x+y}\right)^n x^{\alpha-1}\frac{e^{-\frac{x}{\beta_1}}}{\beta_1^\alpha\Gamma(\alpha)}dx \\ &= \frac{1}{\beta_1^\alpha\Gamma(\alpha)}\int_0^\infty (1+\frac{1}{y}x)^{-n}x^{\alpha+n-1}e^{-\frac{x}{\beta_1}}dx \end{aligned} \tag{A.1}$$

We calculate (A.1) with the help of [75, Eq.(3.383.5)] to obtain,

$$\underset{X}{\mathcal{E}}[Z^n|Y] = \frac{\Gamma(\alpha+n)}{\beta_1^\alpha\Gamma(\alpha)}\left(\frac{1}{y}\right)^{-\alpha-n}\Psi(\alpha+n,\alpha+1,\frac{y}{\beta_1}) \tag{A.2}$$

where $\Psi(\cdot,\cdot,\cdot)$ is the confluent hypergeometric function [75, Eq. (9.210.2)]. Since X and Y are independent, by using the relation

$$\mathcal{E}(Z^n) = \underset{Y}{\mathcal{E}}\left[\underset{X}{\mathcal{E}}[Z^n|Y]\right] \tag{A.3}$$

we have

$$\mathcal{E}(Z^n)=\frac{\Gamma(\alpha+n)}{(\beta_1\beta_2)^\alpha\Gamma(\alpha)^2}\int_0^\infty y^{2\alpha+n-1}\Psi(\alpha+n,\alpha+1,\frac{y}{\beta_1})e^{-\frac{y}{\beta_2}}dy. \tag{A.4}$$

Changing the variable as $y = \beta_1 t$ and applying [75, Eq. (7.621.6)], we obtain

$$\mathcal{E}\{Z^n\} = \frac{\beta_{\min}^{\alpha+n}}{\beta_{\max}^\alpha}\frac{\Gamma(2\alpha+n)B(\alpha+n,\alpha+n)}{\Gamma(\alpha)^2}$$

$$\times \quad {}_2F_1\left(2\alpha+n, \alpha+n; 2\alpha+2n; 1-\frac{\beta_{\min}}{\beta_{\max}}\right) \tag{A.5}$$

Since $\mathcal{E}(H(X,Y)) = 2^n\mathcal{E}(Z^n)$, (2.2) is evident. This concludes the proof.

Appendix B

Proof for Proposition 6.3.1

First of all, we express

$$\begin{aligned}
&\Pr\left\{R_{3s} < R_{st} \;\middle|\; |\mathcal{F}| = f, |\mathcal{D}| = k\right\} \\
&= \Pr\left\{R_{3s} < R_{st} \;\middle|\; \mathbb{C}_1\right\} \Pr\{\gamma_{2p} < \gamma_{t2} \;\middle|\; |\mathcal{F}| = f, |\mathcal{D}| = k\} \\
&+\Pr\left\{R_{3s} < R_{st} \;\middle|\; \mathbb{C}_2\right\} \Pr\left\{\gamma_{2p} \geq \gamma_{t2} \;\middle|\; |\mathcal{F}| = f, |\mathcal{D}| = k\right\}. \qquad \text{(B.1)}
\end{aligned}$$

where $\mathbb{C}_1 = \{\gamma_{2p} < \gamma_{t2}, |\mathcal{F}| = f, |\mathcal{D}| = k\}$, $\mathbb{C}_2 = \{\gamma_{2p} \geq \gamma_{t2}, |\mathcal{F}| = f, |\mathcal{D}| = k\}$ and $\gamma_{t2} = \frac{\sigma^2}{P_s}\rho_p(\rho_p + 1)$.

We first consider $\mathbb{C}_1$. Under the condition $\mathbb{C}_1$, since $\gamma_{2p} < \gamma_{t2}$, we have $\gamma_{t1} = \frac{\sigma^2}{P_s}\rho_p > \frac{\gamma_{2p}}{\rho_p} - \frac{\sigma^2}{P_s} = \frac{I_p}{P_s}$, where γ_{t1} denotes the minimal channel gain required to achieve R_{pt} for the primary system. Furthermore, $\gamma_{2i} \geq \gamma_{t1}$, $\forall i \in \mathcal{F}$. Thus, it is clear that $\gamma_{2i} > \frac{I_p}{P_s}$, $\forall i \in \mathcal{F}$, i.e. $P_s\gamma_{2i} > I_p$, $\forall i \in \mathcal{F}$ and therefore $\mathcal{S} \cap \mathcal{F} = \emptyset$. In other words, all ST_i in $\mathcal{F}$ are not able to satisfy the interference constraint and thus are not eligible for secondary spectrum access. Thus, we have $0 \leq |\mathcal{S}| \leq (M - f)$ under $\mathbb{C}_1$, and

$$\Pr\left\{R_{3s} < R_{st} \;\middle|\; \mathbb{C}_1\right\} = \sum_{j=0}^{M-f} \Pr\left\{R_{3s} < R_{st} \;\middle|\; |\mathcal{S}| = j, \mathbb{C}_1\right\} \Pr\left\{|\mathcal{S}| = j \;\middle|\; \mathbb{C}_1\right\} \qquad \text{(B.2)}$$

where

$$\begin{aligned}&\Pr\left\{R_{3s} < R_{st} \;\middle|\; |\mathcal{S}| = j, \mathbb{C}_1\right\}\\&= \Pr\left\{R_{3s} < R_{st} \;\middle|\; R_4^1 \geq R_{pt}, |\mathcal{S}| = j, \mathbb{C}_1\right\} \Pr\left\{R_4^1 \geq R_{pt}\right\}\\&+\Pr\left\{R_{3s} < R_{st} \;\middle|\; R_4^1 < R_{pt}, |\mathcal{S}| = j, \mathbb{C}_1\right\} \Pr\left\{R_4^1 < R_{pt}\right\}. \qquad \text{(B.3)}\end{aligned}$$

Noting that $s = \underset{i\in\mathcal{S}}{\arg\max}\ [\gamma_{3i}] = \underset{i\in\mathcal{S}}{\arg\max}\ [R_{3i}]$, and substituting (6.14) into (B.3), we have

$$\Pr\left\{R_{3s} < R_{st} \;\middle|\; R_4^1 \geq R_{pt}, |\mathcal{S}| = j, \mathbb{C}_1\right\} \;=\; \left[1 - \exp\left(-\Omega_3^{-1}\frac{\sigma^2}{P_s}\rho_s\right)\right]^j \qquad \text{(B.4)}$$

On the other hand, when $R_4^1 < R_{pt}$, R_{3s} is dependent on γ_{3p}. Thus, averaging across γ_{3p}, we can obtain

$$\begin{aligned}&\Pr\left\{R_{3s} < R_{st} \;\middle|\; R_4^1 < R_{pt}, |\mathcal{S}| = j, \mathbb{C}_1\right\}\\&= \int_0^\infty \left[1 - p_3 \exp\left(-\Omega_3^{-1}\rho_s\gamma_{3p}\right)\right]^j p_{\gamma_{3p}}(\gamma_{3p})d\gamma_{3p} = \sum_{l=0}^{j}\binom{j}{l}\frac{(-p_3)^{j-l}}{\rho_s(j-l)+1}\end{aligned} \qquad \text{(B.5)}$$

where $p_3 = \exp\left(-\Omega_3^{-1}\frac{\sigma^2}{P_s}\rho_s\right)$ and $p_{\gamma_{3p}}(\gamma_{3p}) = \Omega_3^{-1}\exp(-\Omega_3^{-1}\gamma_{3p})$ denotes the probability density function (p.d.f.) of γ_{3p}. Substituting (6.12), (B.4), and (B.5) into (B.3), we have

$$\begin{aligned}&\Pr\left\{R_{3s} < R_{st} \;\middle|\; |\mathcal{S}| = j, \mathbb{C}_1\right\}\\&= T_1(j) = p_4\left(1-p_3\right)^j + (1-p_4)\sum_{l=0}^{j}\binom{j}{l}\frac{(-p_3)^{j-l}}{\rho_s(j-l)+1}\end{aligned} \qquad \text{(B.6)}$$

where $p_4 = \exp\left(-\Omega_4^{-1}\frac{\sigma^2}{P_p}\rho_p\right)$.

Next, since $\gamma_{t2} > \gamma_{2p} > \gamma_{t1}$ under $\mathbb{C}_1$, we have

$$\Pr\left\{|\mathcal{S}| = j \;\middle|\; \mathbb{C}_1\right\} = \int_{\gamma_{t1}}^{\gamma_{t2}}\binom{M-f}{j} p_5^j(1-p_5)^{M-f-j} p_{\gamma_{2p}}(\gamma_{2p} \mid \mathbb{C}_1)d\gamma_{2p} \qquad \text{(B.7)}$$

where

$$p_5 = \Pr\left\{\gamma_{2i} < \frac{I_p}{P_s} \mid i \in \mathcal{M} \setminus \mathcal{F}, \mathbb{C}_1\right\},$$

and $p_{\gamma_{2p}}(\gamma_{2p} \mid \mathbb{C}_1)$ denotes the p.d.f. of γ_{2p} conditioned on $\mathbb{C}_1$.

Since $\gamma_{2i} > \gamma_{t1}$, $\forall i \in \mathcal{F}$, the p.d.f. for γ_{2i}, $i \in \mathcal{F}$ can be easily derived and given by the truncated exponential distribution,

$$p_{\gamma_{2i}|i\in\mathcal{F}}(\gamma_{2i}) = p_2^{-1}\Omega_2^{-1}\exp\left(-\Omega_2^{-1}\gamma_{2i}\right), \qquad \gamma_{2i} > \gamma_{t1}. \tag{B.8}$$

Noting that $p = \arg\max_{i\in\mathcal{F}} [\gamma_{2i}]$, from order statistics we have

$$\begin{aligned} & p_{\gamma_{2p}}\left(\gamma_{2p} \;\middle|\; |\mathcal{F}| = f, |\mathcal{D}| = k\right) \\ &= f[1 - p_2^{-1}\exp(-\Omega_2^{-1}\gamma_{2p})]^{f-1} p_2^{-1}\Omega_2^{-1}\exp\left(-\Omega_2^{-1}\gamma_{2p}\right), \qquad \gamma_{2p} > \gamma_{t1}, \end{aligned} \tag{B.9}$$

and thus

$$\begin{aligned} & p_{\gamma_{2p}}\left(\gamma_{2p} \mid \mathbb{C}_1\right) = p_{\gamma_{2p}}\left(\gamma_{2p} \;\middle|\; \gamma_{2p} < \gamma_{t2}, |\mathcal{F}| = f, |\mathcal{D}| = k\right) \\ = \;& c_1 f[1 - p_2^{-1}\exp(-\Omega_2^{-1}\gamma_{2p})]^{f-1} p_2^{-1}\Omega_2^{-1}\exp\left(-\Omega_2^{-1}\gamma_{2p}\right), \qquad \gamma_{t2} > \gamma_{2p} > \gamma_{t1}, \end{aligned} \tag{B.10}$$

where $c_1 = \left[1 - p_2^{-1}\exp\left(\Omega_2^{-1}\gamma_{t2}\right)\right]^{-f}$.

Furthermore, note that $\mathcal{M} \setminus \mathcal{F} = (\mathcal{D} \setminus \mathcal{F}) \bigcup \overline{\mathcal{D}}$ and $(\mathcal{D} \setminus \mathcal{F}) \cap \overline{\mathcal{D}} = \emptyset$, where $\overline{\mathcal{D}}$ is the complement set of $\mathcal{D}$. Thus

$$\begin{aligned} p_5 \;=\; & \Pr\left\{\gamma_{2i} < \frac{I_p}{P_s} \;\middle|\; i \in \mathcal{D} \setminus \mathcal{F}, \mathbb{C}_1\right\} \Pr\left\{i \in \mathcal{D} \setminus \mathcal{F} \;\middle|\; i \in \mathcal{M} \setminus \mathcal{F}, \mathbb{C}_1\right\} \\ + \;& \Pr\left\{\gamma_{2i} < \frac{I_p}{P_s} \;\middle|\; i \in \overline{\mathcal{D}}, \mathbb{C}_1\right\} \Pr\left\{i \in \overline{\mathcal{D}} \;\middle|\; i \in \mathcal{M} \setminus \mathcal{F}, \mathbb{C}_1\right\}. \end{aligned} \tag{B.11}$$

Since $\gamma_{2i} < \gamma_{t1}$, $\forall i \in \mathcal{D} \setminus \mathcal{F}$, the p.d.f. of γ_{2i}, $i \in \mathcal{D} \setminus \mathcal{F}$ is given by

$$p_{\gamma_{2i}|i\in\mathcal{D}\setminus\mathcal{F}}(\gamma_{2i}) = \frac{\Omega_2^{-1}\exp(-\Omega_2^{-1}\gamma_{2i})}{1 - \exp(-\Omega_2^{-1}\gamma_{t1})}, \qquad 0 < \gamma_{2i} < \gamma_{t1}. \tag{B.12}$$

Therefore we have

$$\Pr\left\{\gamma_{2i} < \frac{I_p}{P_s} \;\middle|\; i \in \mathcal{D} \setminus \mathcal{F}, \mathbb{C}_1\right\} = \frac{1 - c_2 \exp\left(-\Omega_2^{-1}\frac{\gamma_{2p}}{\rho_p}\right)}{1 - \exp(-\Omega_2^{-1}\gamma_{t1})}, \tag{B.13}$$

where $c_2 = \exp\left(\Omega_2^{-1}\frac{\sigma^2}{P_s}\right)$.

Similarly, since γ_{2i}, $\forall i \in \overline{\mathcal{D}}$ has a p.d.f. given by

$$p_{\gamma_{2i}|i\in\overline{\mathcal{D}}}(\gamma_{2i}) = \Omega_2^{-1}\exp\left(-\Omega_2^{-1}\gamma_{2i}\right), \qquad \gamma_{2i} > 0, \tag{B.14}$$

we can derive

$$\Pr\left\{\gamma_{2i} < \frac{I_p}{P_s} \;\middle|\; i \in \overline{\mathcal{D}}, \mathbb{C}_1\right\} = 1 - c_2 \exp\left(-\Omega_2^{-1}\frac{\gamma_{2p}}{\rho_p}\right). \tag{B.15}$$

We also note that

$$\Pr\left\{i \in \mathcal{D} \setminus \mathcal{F} \;\middle|\; i \in \mathcal{M} \setminus \mathcal{F}, \mathbb{C}_1\right\} = \begin{cases} \frac{k-f}{M-f} & f \neq M \\ 0 & f = M \end{cases} \tag{B.16}$$

and

$$\Pr\left\{i \in \overline{\mathcal{D}} \;\middle|\; i \in \mathcal{M} \setminus \mathcal{F}, \mathbb{C}_1\right\} = \begin{cases} \frac{M-k}{M-f} & f \neq M \\ 0 & f = M \end{cases}. \tag{B.17}$$

Substituting (B.13), (B.15), (B.16), and (B.17) into (B.11), we can obtain

$$p_5 \;=\; c_3\left[1 - c_2 \exp\left(-\Omega_2^{-1}\frac{\gamma_{2p}}{\rho_p}\right)\right] \tag{B.18}$$

where

$$c_3 = \begin{cases} \frac{k-f}{(M-f)\left[1-\exp\left(-\Omega_2^{-1}\gamma_{t1}\right)\right]} + \frac{M-k}{M-f} & f \neq M \\ 0 & f = M \end{cases}. \tag{B.19}$$

Substituting (B.10) and (B.18) into (B.7), we can obtain

$$\Pr\left\{|\mathcal{S}| = j \;\middle|\; \mathbb{C}_1\right\} = T_2(j)$$

$$= \binom{M-f}{j} \sum_{n=0}^{M-f-j} \sum_{w=0}^{M-f-n} \sum_{t=0}^{f-1} \binom{M-f-j}{n} \binom{M-f-n}{w} \binom{f-1}{t}$$
$$\cdot(-1)^{f+j+w+t+1} c_1 c_2^{M-f-n-w} c_3^{M-f-n} f p_2^{t-f} \frac{\exp\left(-\Omega_2^{-1} v_1 \gamma_{t1}\right) - \exp\left(-\Omega_2^{-1} v_1 \gamma_{t2}\right)}{v_1} \tag{B.20}$$

where $v_1 = \frac{M-f-n-w}{\rho_p} + f - t$. Substituting (B.6) and (B.20) into (B.2), a closed-form expression for $\Pr\left\{R_{3s} < R_{st} \mid \mathbb{C}_1\right\}$ is given by

$$\Pr\left\{R_{3s} < R_{st} \mid \mathbb{C}_1\right\} = \sum_{j=0}^{M-f} T_1(j) T_2(j). \tag{B.21}$$

This completes the derivation required under $\mathbb{C}_1$.

Under $\mathbb{C}_2$, we have $\gamma_{t1} = \frac{\sigma^2}{P_s}\rho_p \leq \frac{\gamma_{2p}}{\rho_p} - \frac{\sigma^2}{P_s} = \frac{I_p}{P_s}$. Since $\gamma_{2i} < \gamma_{t1}$, $\forall i \in \mathcal{D} \setminus \mathcal{F}$, it is clear that $\gamma_{2i} < \frac{I_p}{P_s}$, $\forall i \in \mathcal{D} \setminus \mathcal{F}$, i.e. $P_s\gamma_{2i} < I_p$, $\forall i \in \mathcal{D} \setminus \mathcal{F}$ and thus $\mathcal{S} \cap (\mathcal{D} \setminus \mathcal{F}) = \mathcal{D} \setminus \mathcal{F}$. In other words, all ST_i in $\mathcal{D} \setminus \mathcal{F}$ are able to satisfy the interference constraint and thus are eligible for secondary spectrum access. Therefore, we have $(k-f) \leq |\mathcal{S}| \leq (M-1)$ under $\mathbb{C}_2$, and

$$\Pr\left\{R_{3s} < R_{st} \mid \mathbb{C}_2\right\} = \sum_{z=k-f}^{M-1} \Pr\left\{R_{3s} < R_{st} \mid |\mathcal{S}| = z, \mathbb{C}_2\right\} \Pr\left\{|\mathcal{S}| = z \mid \mathbb{C}_2\right\}. \tag{B.22}$$

Using the same derivation as in (B.3), we obtain

$$\begin{aligned} &\Pr\left\{R_{3s} < R_{st} \mid |\mathcal{S}| = z, \mathbb{C}_2\right\} = T_3(z) \\ &= p_4 \left(1-p_3\right)^z + \left(1-p_4\right) \sum_{l=0}^{z} \binom{j}{l} \frac{(-p_3)^{z-l}}{\rho_s(z-l)+1}. \end{aligned} \tag{B.23}$$

Furthermore, since $\gamma_{2p} \geq \gamma_{t2}$ under $\mathbb{C}_2$, we have

$$\begin{aligned} \Pr\left\{|\mathcal{S}| = z \mid \mathbb{C}_2\right\} \;=\; & \int_{\gamma_{t2}}^{\infty} \binom{(M-k)+(f-1)}{z-(k-f)} p_6^{z-(k-f)} (1-p_6)^{(M-k+f-1)-(z-(k-f))} \\ & \cdot p_{\gamma_{2p}}(\gamma_{2p} \mid \mathbb{C}_2) d\gamma_{2p}, \end{aligned} \tag{B.24}$$

where

$$p_6 = \Pr\left\{\gamma_{2i} < \frac{I_p}{P_s} \;\middle|\; i \in (\mathcal{F}\setminus\{p\})\bigcup\overline{\mathcal{D}}, \mathbb{C}_2\right\},$$

and $p_{\gamma_{2p}}(\gamma_{2p} \mid \mathbb{C}_2)$ denotes the p.d.f. of γ_{2p} conditioned on $\mathbb{C}_2$ and is given by

$$p_{\gamma_{2p}}(\gamma_{2p} \mid \mathbb{C}_2) = c_4 f[1-p_2^{-1}\exp(-\Omega_2^{-1}\gamma_{2p})]^{f-1}p_2^{-1}\Omega_2^{-1}\exp\left(-\Omega_2^{-1}\gamma_{2p}\right), \quad \gamma_{2p} \geq \gamma_{t2} \tag{B.25}$$

where $c_4 = \left[1-\left[1-p_2^{-1}\exp(-\Omega_2^{-1}\gamma_{t2})\right]^f\right]^{-1}$.

Follow the same derivation as in (B.18), it is easy to show that

$$p_6 = \begin{cases} \frac{f-1}{M-k+f-1}\frac{\exp\left(-\Omega_2^{-1}\gamma_{t1}\right)-c_2\exp\left(-\Omega_2^{-1}\frac{\gamma_{2p}}{\rho_p}\right)}{\exp\left(-\Omega_2^{-1}\gamma_{t1}\right)-\exp\left(-\Omega_2^{-1}\gamma_{2p}\right)} + \frac{(M-k)\left[1-c_2\exp\left(-\Omega_2^{-1}\frac{\gamma_{2p}}{\rho_p}\right)\right]}{M-k+f-1} \\ 0 \end{cases}. \tag{B.26}$$

where the first and second terms correspond to the cases where $M-k+f-1 \neq 0$ and $M-k+f-1=0$, respectively.

For mathematical tractability, we drop the term $\exp\left(-\Omega_2^{-1}\gamma_{2p}\right)$ in (B.26) and obtain a lower bound for p_6 given by

$$p_6 \geq \begin{cases} 1-c_5\exp\left(-\Omega_2^{-1}\frac{\gamma_{2p}}{\rho_p}\right) & M-k+f-1 \neq 0 \\ 0 & M-k+f-1=0 \end{cases}, \tag{B.27}$$

where $c_5 = \frac{c_2(f-1)}{(M-k+f-1)\exp(-\Omega_2^{-1}\gamma_{t2})} + \frac{c_2(M-k)}{M-k+f-1}$. It is clear that this lower bound is tight when $\exp\left(-\Omega_2^{-1}\gamma_{2p}\right)$ is small or equivalently γ_{2p} is large. Furthermore, since $\gamma_{2p} \geq \gamma_{t2} = \frac{\sigma^2}{P_s}\rho_p(\rho_p+1)$ under $\mathbb{C}_2$, we will obtain a tighter lower bound for p_6 when P_s is small and/or R_{pt} is large.

Note that a smaller p_6 indicates a smaller possibility that ST_i, $i \in (\mathcal{F}\setminus\{p\})\bigcup\overline{\mathcal{D}}$ is eligible for secondary spectrum access, and hence leads to a smaller $|\mathcal{S}| = z$. Furthermore, it can be easily shown that $\Pr\left\{R_{3s} < R_{st} \;\middle|\; |\mathcal{S}| = z, \mathbb{C}_2\right\}$ in (B.23) is a decreasing function with increasing z. Thus by using the lower bound for p_6 in (B.27), we can obtain an upper bound for $\Pr\left\{R_{3s} < R_{st} \;\middle|\; \mathbb{C}_2\right\}$. Following the

same derivations as in (B.21), the upper bound is given by

$$\Pr\left\{R_{3s} < R_{st} \;\middle|\; \mathbb{C}_2\right\} \leq \sum_{z=k-f}^{M-1} T_3(z)T_4(z) \tag{B.28}$$

where $T_4(z)$ is obtained by substituting (B.27) and (B.25) into (B.24) such that

$$\begin{aligned} T_4(z) = & \begin{pmatrix} g \\ z-k+f \end{pmatrix} \sum_{q=0}^{M-z-1} \sum_{u=0}^{g-q} \sum_{t=0}^{f-1} \begin{pmatrix} M-z-1 \\ q \end{pmatrix} \begin{pmatrix} g-q \\ u \end{pmatrix} \begin{pmatrix} f-1 \\ t \end{pmatrix} \\ & \cdot(-1)^{k+z+u+t+1} c_4 c_5^{g-q-u} f p_2^{t-f} \frac{\exp\left(-\Omega_2^{-1} v_2 \gamma_{t2}\right)}{v_2}, \end{aligned} \tag{B.29}$$

$g = M-k+f-1$, and $v_2 = \frac{g-q-u}{\rho_p} + f - t$. Furthermore, it can be easily derived from (B.9) that

$$\Pr\left\{\gamma_{2p} < \gamma_{t2} \;\middle|\; |\mathcal{F}| = f, |\mathcal{D}| = k\right\} = \left[1 - p_2^{-1} \exp\left(-\Omega_2^{-1}\gamma_{t2}\right)\right]^f = c_1^{-1} \tag{B.30}$$

and

$$\Pr\left\{\gamma_{2p} \geq \gamma_{t2} \;\middle|\; |\mathcal{F}| = f, |\mathcal{D}| = k\right\} = 1 - c_1^{-1}. \tag{B.31}$$

Substituting (B.21), (B.28), (B.30), and (B.31) into (B.1), we obtain

$$\begin{aligned} &\Pr\left\{R_{3s} < R_{st} \;\middle|\; |\mathcal{F}| = f, |\mathcal{D}| = k\right\} \leq P_{\text{out}}^{s,ub}(f,k) \\ &= c_1^{-1} \sum_{j=0}^{M-f} T_1(j)T_2(j) + \left(1 - c_1^{-1}\right) \sum_{z=k-f}^{M-1} T_3(z)T_4(z). \end{aligned} \tag{B.32}$$

Appendix C

List of Publications

Journal Papers

- Y. Han, S. H. Ting, and Y. L. Guan, "High rate open-loop MIMO multi-user downlink transmission scheme based on blind precoding quasi-orthogonal space time block code," *IET Communications*, vol. 3, no. 11, pp. 1757-1768, Nov. 2009.

- Y. Han, A. Pandharipande, and S. H. Ting, "Cooperative decode-and-forward relaying for secondary spectrum access," *IEEE Transactions on Wireless Communications*, vol. 8, no. 10, pp. 4945-4950, Oct. 2009.

- Y. Han, S. H. Ting, C. K. Ho, W. H. Chin, "Performance bounds for two-way amplify-and-forward relaying," *IEEE Transactions on Wireless Communications*, vol. 8, no. 1, pp. 432-439, Jan. 2009.

- Y. Han, S. H. Ting, and A. Pandharipande, "Spectrally efficient sensing protocol in cognitive relay systems," to appear in *IET Communications*, 2010.

- Y. Han, S. H. Ting, and A. Pandharipande, "Cooperative spectrum sharing protocol with secondary user selection," *IEEE Transactions on Wireless Communications*, vol. 9, no. 9, pp. 2914-2923, Sept. 2010.

- Y. Han, S. H. Ting, and A. Pandharipande, "Cooperative spectrum sharing protocol with selective relaying system," submitted to *IEEE Transactions on Communications*, 2010.

- Q. Li, S. H. Ting, A. Pandharipande, and Y. Han, "Adaptive two-way relaying and outage analysis," *IEEE Transactions on Wireless Communications*, vol. 8, no. 6, pp. 3288-3299, June 2009.

Conference Papers

- Y. Han, S. H. Ting, Y. L. Guan, "A high rate open-loop MIMO multi-user downlink transmission system," in *Proceedings of 6th International Conference on Information, Communications and Signal Processing*, Singapore, pp. 1-5, Dec. 2007.

- Y. Han, S. H. Ting, C. K. Ho, W. H. Chin, "High rate two-way amplify-and-forward half-duplex relaying with OSTBC," in *Proceedings of IEEE Vehicular Technology Conference 2008 Spring* Singapore, pp. 2426-2430, May 2008.

- Y. Han, S. H. Ting, C. K. Ho, W. H. Chin, "Moments of harmonic mean and rate analysis for two-way amplify-and-forward relaying," in *Proceedings of IEEE International Conference on Communications, Workshop on Cooperative Communications and Networking, Theory, Practice, and Applications*, Beijing, PRC China, pp. 365-369, May 2008.

- Q. Li, S. H. Ting, A. Pandharipande, and Y. Han, "Outage analysis for adaptive two-way relaying," in *Proceedings of IEEE PIMRC 2008*, Cannes, France, pp. 1-5, Sep. 2008

- A. Pandharipande,Y. Han, Y. Wang, "Sensing and communication protocols in cognitive sensor relay networks," in *Proceedings of 2008 IEEE Sensors*, Rome, Italy, pp. 617-620, Oct. 2008.

- Y. Han, A. Pandharipande, S. H. Ting, "Spectrally efficient sensing protocol for cognitive relay systems," in *Proceedings of 1st International Conference on COMmunication Systems and NETworkS (COMSNETS), WIreless Systems: Advanced Research and Development (WISARD)*, Bangalore, India, pp. 1-6, Jan. 2009.

- Y. Han, A. Pandharipande, and S. H. Ting, "Cooperative spectrum sharing via controlled amplify-and-forward relaying," in *Proceedings of IEEE PIMRC 2008*, Cannes, France, pp.1-5, Sep. 2008.

- Y. Han, S. H. Ting, and A. Pandharipande, "Cooperative spectrum sharing with distributed secondary user selection," in *Proceedings of IEEE ICC 2010*, Cap Town, South Africa, pp. 1-5, May 2010.

- Y. Han, S. H. Ting, and A. Pandharipande, "Cooperative Spectrum Sharing with Relay Selection," to appear in *Proceedings of IEEE ICCS 2010*, Singapore, Nov. 2010.

Patents

- Y. Han and A. Pandharipande, "Cooperative spectrum sharing systems," patent pending, 81361778EP01, May 2008.

- Y. Han, A. Pandharipande, and Y. Wang, "Sensing and communication protocols for shared spectrum usage," patent pending, PCT/IB2009/053091, July 2009.

Bibliography

[1] National Telecommunications and Information Administration (NTIA), "FCC Frequency Allocation Chart," 2003. Available at: http://www.ntia.doc.gov/osmhome/allochrt.pdf.

[2] A. Sendonaris, E. Erkip, and B. Aazhang, "User cooperation diversity-Part I: System description," *IEEE Transactions on Communications,* vol. 51, no. 11, pp. 1927–1938, Nov. 2003.

[3] J. N. Laneman, D. N. C. Tse, and G. W. Wornell, "Cooperative diversity in wireless networks: efficient protocols and outage behavior," *IEEE Transactions on Information Theory*, vol. 50, no. 10, pp. 3062-3080, Dec. 2004.

[4] G. J. Foschini and M. J. Gans,"On limits of wireless communications in fading environment when using multiple antennas," *IEEE Wireless Personal Communications,* vol. 6, pp. 311–335, March 1998.

[5] L. Zheng and D. N. C. Tse, "Diversity and multiplexing: A fundamental tradeoff in multiple antenna channels," *IEEE Transactions on Information Theory,* vol. 49, no. 5, pp. 1073–1096, May 2003.

[6] E. Telatar, "Capacity of multi-antenna Gaussian channels," *European Transactions on Telecommunications,* Vol. 10, no. 6, pp. 585–595, Nov./Dec. 1999.

[7] IEEE Standard for Local and Metropolitan Area Networks Part 16, IEEE Std. IEEE 802.16-2004, 2004.

[8] IEEE Standard for Local and Metropolitan Area Networks Part 16, IEEE Std. 802.16e-2005, 2005.

[9] M. E. Sahin and H. Arslan, "MIMO-OFDMA measurements; Reception, testing, and evaluation of WiMAX MIMO signals with a single channel receiver," *IEEE Transactions on Instrumentation and Measurement*, vol. 58, no. 3, pp. 713-721, March 2009.

[10] E. Meulen, "Three-terminal communication channels," *Advances in Applied Probability,* vol. 3, no. 1, pp. 120-154, Spring 1971.

[11] T. Cover and El-Gamal, "Capacity theorems for the relay channels," *IEEE Transactions on Information Theory,* vol. 25, no. 5, pp. 572-584, Sep. 1979.

[12] T. E. Hunter, S. Sanayei, A. Nosratinia, "Outage analysis of coded cooperation," *IEEE Transactions on Information Theory,* vol. 52, no. 2, pp. 375–391, Feb. 2006.

[13] M. O. Hasna and M.-S. Alouini,"Outage probability of multihop transmission over Nakagami fading channels," *IEEE Communications Letters,* vol. 7, no. 5, pp. 216-218, May 2003.

[14] P. A. Anghel and M. Kaveh, "Exact symbol error probability of a cooperative network in a Rayleigh-fading environment," *IEEE Transactions on Wireless Communications,* vol. 3, no. 5, pp. 1416-1421, Sep. 2004.

[15] J. N. Laneman, "Cooperative diversity in wireless networks: algorithms and architectures," Ph.D. dissertation, Massachusetts Institute of Technology, Sep. 2002.

[16] J. N. Laneman, G. W. Wornell, "Distributed space-time coded protocols for exploiting cooperative diversity in wireless networks," *IEEE Global Telecommunications Conference 2002,* vol. 1, vol. 1, pp. 77–81, Nov. 2002.

[17] Y. Jing and B. Hassibi "Distributed space-time coding in wireless relay networks," *IEEE Transactions on Wireless Communications*, vol. 5, no. 12, pp. 3524 - 3536 , Dec. 2006.

[18] Y. Jing, H. Jafarkhani, "Using orthogonal and quasi-orthogonal designs in wireless relay networks," *IEEE Transactions on Information Theory,* vol. 53, no. 11, pp. 4106–4118, Nov. 2007.

[19] S. Wei, D. L. Goeckel, and M. Valenti, "Asynchronous cooperative diversity," *IEEE Transactions on Wireless Communications,* vol. 5, no. 6, pp. 1547C1557, Jun. 2006.

[20] X. Guo and X.-G. Xia, "Distributed linear convolutive space-time codes for asynchronous cooperative communication networks," *IEEE Transactions on Wireless Communications*, vol. 7, no. 5, pp. 1857C1861, May 2008.

[21] A. K. Sadek, Z. Han, and K. J. R. Liu, "A distributed relay-assignment algorithm for cooperative communications in wireless networks," in *Proceedings of ICC,* Turkey, June 2006.

[22] Z. Lin, E. Erkip, and A. Stefanov, "Cooperative regions and partner choice in coded cooperative systems," *IEEE Transactions on Communications,* vol. 54, pp. 1323-1334, July 2006.

[23] Y. Jing and H. Jafarkhani, "Single and multiple relay selection schemes and their achievable diversity orders," *IEEE Transactions on Wireless Communications,* vol. 8, no. 3, pp. 1414-1423, March 2009.

[24] A. Bletsas, A. Khisti, D. P. Reed, and A. Lippman: "A simple cooperative diversity method based on network path selection," *IEEE Journal on Selected Areas in Communications*, vol. 24, no. 3, pp. 659-672, March 2006.

[25] B. Rankov and A. Wittneben, "Spectral efficient protocols for half-duplex fading relay channels," *IEEE Journal on Selected Areas in Communications*, vol. 25, no. 2, pp. 379-389, Feb. 2007.

[26] J. N. Laneman, D. N. Tse, and G. W. Wornell, "Cooperative diversity in wireless networks: efficient protocols and outage behavior," *IEEE Transactions on Information Theory*, vol. 50, no. 12, pp. 3062-3080, Dec. 2004.

[27] P. Larsson and N. Johansson, "Interference cancellation in wireless relaying networks," United States Patent no. 7.336.930, Apr. 2004.

[28] C. E. Shanon, "Two-way communication channels," *in Proc. 4th Berkeley Symp. Math. Statist and Prob.,* vol. 1, pp. 611-644, 1961.

[29] Y. Wu, P. A. Chou and S. -Y. Kung "Information exchange in wireless networks with network coding and physical-layer broadcast," in *Proceedings of CISS*, USA, March 2005.

[30] P. Larsson, N. Johansson and K. -E. Sunell "Coded bi-directional relaying," in *Proceedings of VTC*, Australia, pp. 851-855, May 2006.

[31] S. J. Kim, P. Mitran and V. Tarokh "Performance bounds for bi-directional coded cooperation protocols," *IEEE Transactions on Information Theory,* vol. 54, no. 11, pp. 5235-5241, Nov. 2008.

[32] P. Popovski and H. Yomo "Wireless network coding by amplify-and-forward for bi-directional traffic flows," *IEEE Communications Letters,* vol. 11, no. 1, pp. 16-18, Jan. 2007.

[33] G. Staple and K. Werbach, "The end of spectrum scarcity," *IEEE Spectrum*, vol. 41, no. 3, pp. 48-52, March 2004.

[34] M. McHenry, "Frequency agile spectrum access technologies," *Proc. FCC Workshop on Cognitive Radio,* May 2003.

[35] R. I. C. Chiang, G. B. Rowe, and K. W. Sowerby, "A quantitative analysis of spectral occupancy measurements for cognitive radio," *IEEE Vehicular Technology Conference*, pp. 3016-3020, Apr. 2007.

[36] D. A. Roberson, C. S. Hood, J. L. LoCicero, and J. T. MacDonald, "Spectral occupancy and interference studies in support of cognitive radio technology deployment," *IEEE Workshop on Networking Technologies for Software Defined Radio Networks*, pp. 26-35, Sep. 2006.

[37] C. Stevenson, G. Chouinard, Z. Lei, W. Hu, S. Shellhammer, and W. Caldwell, "IEEE 802.22: The first cognitive radio wireless regional area network standard," *IEEE Communications Magazine*, vol. 47, no. 1, pp. 130-138, Jan. 2009.

[38] C. Cordeiro, K. Challapali, and D. Birru, "IEEE 802.22: an introduction to the first wireless standard based on cognitive radios," *IEEE Journal of Communications,* vol. 1, no. 1, pp. 38-47, Apr. 2006.

[39] J. Mitola, "Cognitive Radio: an integrated agent architecture for aoftware defined radio", Ph.D. Thesis. KTH, Stockholm, Sweden, Dec. 2000.

[40] J. Mitola and G. Q. Maguire, Jr., "Cognitive radio: making software radios more personal," *IEEE Personal Communications,* vol. 6, no. 4, pp. 13-18, Aug 1999.

[41] FCC, "FCC 03-322", Dec. 2003. Available at: http://fjallfoss.fcc.gov/edocs_public/attachmatch/FCC-03-322A1.pdf.

[42] S. Haykin, "Cognitive radio: brain-empowered wireless communications," *IEEE Journal on Selected Areas in Communications*, vol. 23, no. 2, pp. 201-220, Feb. 2005.

[43] N. Devroye, P. Mitran, and V. Tarokh, "Achievable rates in cognitive radio channels," *IEEE Transactions on Information Theory*, vol. 52, pp. 1813-1827, May 2006.

[44] S. Srinivasa and S. A. Jafar, "Cognitive radios for dynamic spectrum access - the throughput potential of cognitive radio: a theoretical perspective," *IEEE Communication Magazine*, vol. 45, pp. 73-79, May 2007.

[45] A. Goldsmith, S. A. Jafar, I. Maric, and S. Srinivasa, "Breaking spectrum gridlock with cognitive radios: an information theoretic perspective," *Proceedings of the IEEE*, vol. 97, pp. 894-914, May 2009.

[46] M. Gastpar, "On capacity under receive and spatial spectrum-sharing constraints," *IEEE Transactions on Information Theory,* vol. 53, pp. 471-487, Feb. 2007.

[47] A. Ghasemi and E. S. Sousa, "Capacity of fading channels under spectrum-sharing constraints," in *Proceedings of ICC*, Turkey, pp. 4373-4378, June 2006.

[48] H. Suraweera, J. Gao, P. Smith, M. Shafi, and M. Faulkner, "Channel capacity limits of cognitive radio in asymmetric fading environments" in *Proceedings of ICC*, China, pp. 4048-4053, May 2008.

[49] W. Zhang and U. Mitra, "A spectrum-shaping perspective on cognitive radio: Uncoded primary transmission case," in *Proceedings of ISIT*, Canada, pp. 1338-1342, Jul. 2008.

[50] R. Zhang and Y.-C. Liang, "Exploiting multi-antennas for opportunistic spectrum sharing in cognitive radio networks," *IEEE Journal of Selected Topics in Signal Processing,* vol. 2, pp. 88-102, Feb. 2008.

[51] H. Gu and C. Yang, "Power and Admission Control for UWB Cognitive Radio Networks," in *Proceedings of ICC*, China, pp. 4933-4937 May 2008.

[52] T. Yucek and H. Arslan, "A survey of spectrum sensing algorithms for cognitive radio applications," *IEEE Communications Surveys & Tutorials*, vol. 11, no. 1, pp. 116-130, First Quarter 2009.

[53] S. D. Jones, E. Jung, X. Liu, N. Merheb, and I.-J. Wang, "Characterization of spectrum activities in the U.S. public safety band for opportunistic spectrum access," in *Proceedings of DySBAN*, Ireland, pp. 137-146, Apr. 2007.

[54] S. Y. Lee; E. C. Kim, S. Park, J. Y. Kim, "Effective spectrum sensing with antenna diversity for cognitive radio systems," in *Proceedings of ISCIT*, Korea, pp. 1073-1077, Sep. 2009.

[55] H.-S. Chen, W. Gao, and D.G. Daut, "Spectrum sensing for OFDM systems employing pilot tones," *IEEE Transactions on Wireless Communications,* vol. 8, no. 12, pp. 5862-5870, Dec. 2009.

[56] H. Urkowitz, "Energy detection of unknown deterministic signals," *Proceedings of the IEEE*, vol. 55, pp. 523-531, Apr. 1967.

[57] A. Ghasemi and E. S. Sousa, "Collaborative spectrum sensing for opportunistic access in fading environments," in *Proceedings of DySPAN*, USA, pp. 131-136, Nov. 2005.

[58] S. M. Mishra, A. Sahai, and R. W. Brodersen, "Cooperative sensing among cognitive radios," in *Proceedings of ICC*, Korea, pp. 1658-1663, June 2006.

[59] J. Unnikrishnan and V. V. Veeravalli, "Cooperative sensing for primary detection in cognitive radio," *IEEE Journal of Selected Topics in Signal Processing*, vol. 2, no. 1, pp. 18-27, Feb. 2008.

[60] Y. Han, S. H. Ting, C. K. Ho, W. H. Chin, "Moments of harmonic mean and rate analysis for two-way amplify-and-forward relaying," in *Proceedings of IEEE International Conference on Communications, Workshop on Cooperative Communications and Networking, Theory, Practice, and Applications, Beijing, PRC China*, May 2008.

[61] Y. Han, S. H. Ting, C. K. Ho, and W. H. Chin "High rate two-way amplify-and-forward half-duplx relaying with OSTBC," in *Proceedings of VTC 2008 Spring*, Singapore, pp. 2426- 2430, May 2008, .

[62] Y. Han, S. H. Ting, C. K. Ho, W. H. Chin, "Performance bounds for two-way amplify-and-forward relaying," *IEEE Transactions on Wireless Communications*, vol. 8, no. 1, pp. 432-439, Jan. 2009.

[63] Y. Han, A. Pandharipande, Y. Wang, and S. H. Ting, "Spectrally efficient sensing protocol for cognitive relay systems," in *Proceedings of First International Conference on Communication Systems and Networks*, India, pp.1-6, Jan. 2009.

[64] Y. Han, S. H. Ting, and A. Pandharipande, "Spectrally efficient sensing protocol in cognitive relay systems," to appear in *IET Communications*, 2010.

[65] Y. Han, A. Pandharipande, and S. H. Ting, "Cooperative spectrum sharing via controlled amplify-and-forward relaying," in *Proceedings of PIMRC*, France, pp.1-5, Sep. 2008.

[66] Y. Han, A. Pandharipande, and S. H. Ting, "Cooperative decode-and-forward relaying for secondary spectrum access," *IEEE Transactions on Wireless Communications*, vol. 8, no. 10, pp. 4945-4950, Oct. 2009.

[67] Y. Han, S. H. Ting, and A. Pandharipande, "Cooperative Spectrum Sharing with Distributed Secondary User Selection," in *Proceedings of ICC 2010*, Cape Town, South Africa, pp.1-5, May 2010.

[68] Y. Han, S. H. Ting, and A. Pandharipande, "Cooperative spectrum sharing protocol with secondary user selection" *IEEE Transactions on Wireless Communications*, vol. 9, no. 9, pp. 2914-2923, Sept. 2010.

[69] R. Pabst, B. H. Walke, D. C. Schultz, P. Herhold, H. Yanikomeroglu, S. Mukherjee, H. Viswanathan, M. Lott, W. Zirwas, M. Dohler, H. Aghvami, D. D. Falconer, and G. P. Fettweis, "Relay-based deployment concepts for wireless and mobile broadband radio," *IEEE Communications Magazine,* vol. 42, no. 9, pp. 80-89, Sep. 2004.

[70] A. Sendonaris, "Advanced Techniques for Next-generation Wireless Systems," Ph.D. dissertation, Rice University, Aug. 1999.

[71] T. M. Cover and A. El Gamal, "Capacity theorems for the relay channel," *IEEE Transactions on Information Theory,* vol. 25, no. 5, pp. 572-584, Sep. 1979.

[72] M. O. Hasna and M. S. Alouini, "Performance anaylsis of two-hop relayed transmission over Rayleigh fading channels," in *Proceedings of VTC 2002 Fall,* Canada, pp. 1992-1996, Sep. 2002.

[73] M. O. Hasna and M. S. Alouini, "Harmonic mean and end-to-end performance of transmission systems with relays," *IEEE Transactions on Communications,* vol. 52, no. 1, pp. 130-135, Jan. 2004.

[74] S. M. Alamouti, "A simple transmit diversity technique for wireless communications," *IEEE Journal on Selected Areas in Communications*, vol. 16, no. 8, pp. 1451-1458, Oct. 1998.

[75] I. S. Gradshteyn and I. M. Ryzhik, *Tables of Integrals, Series, and Products,* Academic, 5th Edition, 1994.

[76] A. Papoulis and S. U. Pillai, *Probability, Random Variables and Stochastic Processes,* McGraw-Hill, 4th Edtion, 2002.

[77] J. F. Monahan, *Numerical Methods of Statistics,* Cambridge University Press, 1st Edtion, 2001.

[78] V. Tarokh, N. Seshadri, and A. R. Calderbank "Space-time codes for high rate wireless communication: performance analysis and code construction," *IEEE Transactions on Information Theory*, vol. 44, no. 2, pp. 744-765, Mar. 1998.

[79] Federal Communications Commission - First Report and Order and Further Notice of Proposed Rulemaking, "Unlicensed operation in the TV broadcast bands," *FCC 06-156*, Oct. 2006.

[80] D. Cabric, S. M. Mishra, and R. W. Brodersen, "Implementation issues in spectrum sensing for cognitive radios," *Asilomar Conference on Signals, Systems and Computers*, pp 772-776, Nov 2004.

[81] D. Cabric, I. D. O'Donnell, M. S.-W. Chen and R. W. Brodersen, "Spectrum sharing radios," *IEEE Circuits and Systems Magazine*, pp. 30-45, 2006.

[82] O. Ileri, and N. B. Mandayam,"Dynamic spectrum access models: toward an engineering perspective in the spectrum debate," *IEEE Communications Magazine*, vol. 46, pp. 153-160 2008.

[83] Y.-C. Liang, Y. Zeng, E. C. Y. Peh, A. T. Hoang, " Sensing-throughput tradeoff for cognitive radio networks," *IEEE Transactions on Wireless Communications*, vol. 7, no. 4, pp. 1326-1337, Apr. 2008.

[84] G. Kramer, I. Maric, and R. D. Yates, *Cooperative Communications*, Foundations and Trends in Networking, NOW Publishers, 2006.

[85] K. R. Chowdhury and I. F. Akyildiz, "Cognitive wireless mesh networks with dynamic spectrum access," *IEEE Journal on Selected Areas in Communications*, vol. 26, no. 1, pp. 168-181, Jan. 2008.

[86] A. Pandharipande and C. K. Ho, "Stochastic spectrum pool reassignment for cognitive relay systems," *IEEE Wireless Communications and Networking Conference*, pp. 588-592, May 2008.

[87] F. F. Digham, M.-S. Alouini, and M. K. Simon, "On the energy detection of unknown signals over fading channels," *IEEE Transactions on Communications*, vol. 55, no. 1, pp. 21-24, Jan. 2007.

[88] G. Ganesan and Y. (G.) Li, "Cooperative spectrum sensing in cognitive radio - Part I: Two user networks," *IEEE Transactions on Wireless Communications*, vol. 6, no. 6, pp. 2204-2213, June 2007.

[89] G. Ganesan and Y. (G.) Li, "Spatiotemporal sensing in cognitive radio networks ," *IEEE Journal on Selected Areas in Communications*, pp. 5-12, vol. 26, no. 1, Jan. 2008.

[90] G. Farhadi and N. Beaulieu, "On the ergodic capacity of wireless relaying systems over Rayleigh fading channels," *IEEE Transactions on Wireless Communications,* vol. 7, no. 11, pp. 4462-4467, Nov. 2008.

[91] D. Niyato, E. Hossain, and Zhu Han, "Dynamic spectrum access in IEEE 802.22- based cognitive wireless networks: a game theoretic model for competitive spectrum bidding and pricing," *IEEE Wireless Communications*, vol. 16, no. 2, pp. 16-23, Apr. 2009.

[92] Y. Xing, R. Chandramouli, and C. Cordeiro, "Price dynamics in competitive agile spectrum access markets" *IEEE Journal on Selected Areas in Communications*, vol. 25, no. 3, pp. 613-621, Apr. 2007.

[93] S. M. Kay, *Fundamentals of Statistical Signal Processing, Volume 2: Detection Theory*, Prentice Hall PTR, 1st Edition 1998.

[94] A. T. Hoang, Y.-C. Liang, D. T. C. Wong, Y. Zeng, R. Zhang, "Opportunistic spectrum access for energy-constrained cognitive radios," *IEEE Transactions on Wireless Communications*, vol. 8, pp.1206-1211, March 2009.

[95] A. Ghasemi and E. S. Sousa, "Fundamental limits of spectrum-sharing in fading environments," *IEEE Transactions on Wireless Communication*, vol. 6, pp. 649-658, Feb. 2007.

[96] X. Kang, Y.-C. Liang, A. Nallanathan, H. K. Garg, and R. Zhang, "Optimal power allocation for fading channels in cognitive radio networks: ergodic capacity and outage capacity," *IEEE Transactions on Wireless Communication*, vol. 8, pp. 940-950, Feb. 2009.

[97] O. Simeone, I. Stanojev, S. Savazzi, Y. Bar-Ness, U. Spagnolini, and R. Pickholtz, "Spectrum leasing to cooperating secondary ad hoc networks," *IEEE Journal on Selected Areas in Communications*, vol. 26, no. 1, pp. 203-213, Jan. 2008.

[98] A. Jovicic and P. Viswanath, "Cognitive radio: an information-theoretic perspective," *IEEE Transactions on Information Theory*, vol. 55, no. 9, pp. 3945-3958, Sep. 2009.

[99] Federal Communications Commission - Second Report and Order and Memorandum Opinion and Order, "Unlicensed operation in the TV broadcast bands," *FCC 08–20*, 2008.

[100] Office of Communications (OFCOM), "Spectrum Framework Overview," 2005.

[101] Z. Beyaztas, A. Pandharipande and D. Gesbert, "Optimum power allocation in a hierarchical spectrum sharing scheme," in *Proceedings of ICC*, China, pp. 97-101, May 2008.

[102] Y. Chen, G. Yu, Z. Zhang, and H-H. Chen, P. Qiu, "On cognitive radio networks with opportunistic power control strategies in fading channels," *IEEE Transactions on Wireless Communications*, vol. 7, no. 7, pp. 2752-2761, July 2008.

[103] M. Zorzi and R. R. Rao, "Geographic random forwarding (GeRaF) for ad hoc and sensor networks: multihop performance," *IEEE Transactions on Mobile Computing*, vol. 2, no.4, pp. 337-348, Oct.-Dec. 2003.

[104] K. Woradit, T. Q. S. Quek, W. Suwansantisuk, M.Z. Win, L. Wuttisittikulkij, and H. Wymeersch, "Outage Behavior of Selective Relaying Schemes," *IEEE Transactions on Wireless Communications*, vol. 8, no. 8, pp. 3890–3895, Aug. 2009.